Acta Universitatis Agriculturae Sueciae

Doctoral Thesis No. 2025:22
Faculty of Natural Resources and Agricultural Sciences

Development of innovative treatment techniques for infrastructure contaminated with per- and polyfluoroalkyl substances

Björn Bonnet

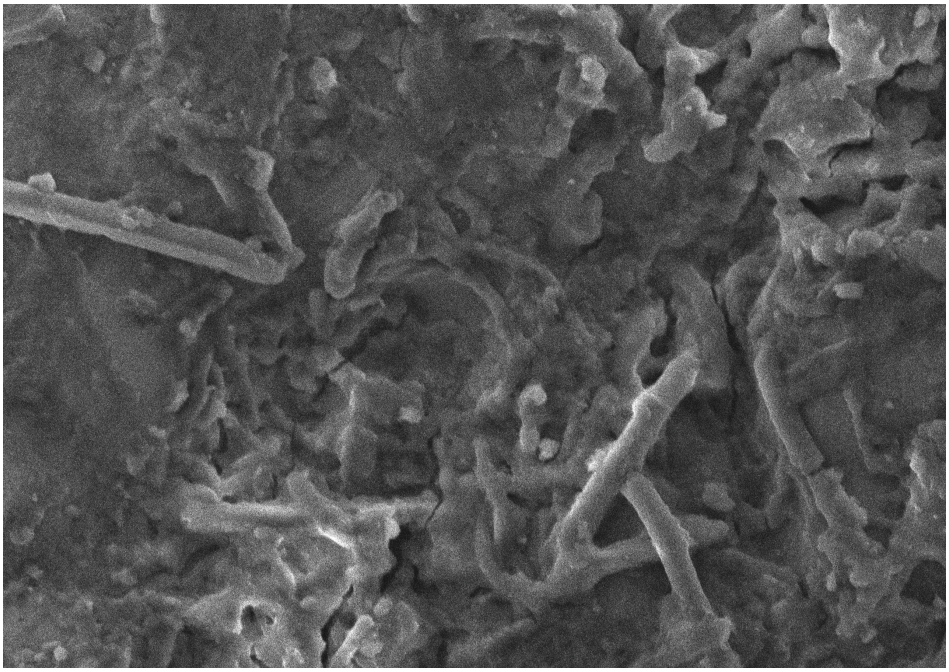

Development of innovative treatment techniques for infrastructure contaminated with per- and polyfluoroalkyl substances

Björn Bonnet
Faculty of Natural Resources and Agricultural Sciences
Department of Aquatic Sciences and Assessment
Uppsala

SLU
SWEDISH UNIVERSITY OF AGRICULTURAL SCIENCES

DOCTORAL THESIS
Uppsala 2025

Acta Universitatis Agriculturae Sueciae
2025:22

Cover: Image of AFFF-impacted stainless steel pipe by scanning electron microscopy. (produced by G. Seisenbaeva and B. Bonnet)

ISSN 1652-6880
ISBN (print version) 978-91-8046-457-4
ISBN (electronic version) 978-91-8046-507-6
https://doi.org/10.54612/a.7ap0tq7hvg

Swedish University of Agricultural Sciences, Department of Aquatic Sciences and Assessment, Uppsala, Sweden
Print: SLU Grafisk service, Uppsala 2025

Development of innovative treatment techniques for infrastructure contaminated with per- and polyfluoroalkyl substances

Abstract

Per- and polyfluoroalkyl substances (PFAS) are of growing concern due to their persistence, mobility, and toxicity. A major contamination source is aqueous film-forming foam (AFFF) used in firefighting, impacting both infrastructure and soil. This thesis explores methods for decontamination of fire suppression systems and PFAS immobilization in soil.

Laboratory-scale decontamination of AFFF-contaminated stainless-steel pipes showed that butyl carbitol-based solutions removed more PFAS than tap water, with higher temperature enhancing removal. However, surface analysis using time-of-flight elastic recoil detection revealed residual fluorine, posing a risk of PFAS rebound.

In another experiment, a swab sampling method was developed. It was then successfully applied on AFFF-contaminated pipe surfaces to determine total PFAS concentrations.

In laboratory-scale leaching tests of PFAS-contaminated soil, the performance of cement with and without additional activated carbon (AC)-based sorbents was assessed in stabilization and solidification trials. Addition of cement showed higher PFAS leaching (µg/kg) than unsolidified soil. In contrast, the addition of AC-sorbent achieved immobilization efficiencies of >99% for most PFAS compounds. Temporal changes in Kd-values and mass flux rates suggest a transition to diffusion-controlled release mechanisms over time.

In field-deployed lysimeter experiments, PFAS immobilization using waste-derived biochars and AC-based sorbents under natural, variably saturated conditions resulted in >99% PFAS reduction in leachate for long-chain PFAS and 79-99% reduction for short-chain PFAS. A 1-D transport model suggests substantial PFAS retention at the air-water interface.

Keywords: PFAS, decontamination, foam transition, surface analysis, time-of-flight elastic recoil detection, supramolecular assemblies, stabilisation and solidification, lysimeters, variably saturated conditions

Utveckling av innovativa behandlingstekniker för infrastruktur som förorenats med per- och polyfluorerade alkylsubstanser

Sammanfattning

Per- och polyfluorerade alkylsubstanser (PFAS) är ett växande problem på grund av deras persistens, mobilitet och toxicitet. En viktig föroreningskälla är vattenhaltigt filmbildande skum (AFFF) som används vid brandbekämpning och som påverkar både infrastruktur och mark. Denna avhandling utforskar metoder för sanering av brandsläckningssystem och immobilisering av PFAS i jord.

Sanering av AFFF-förorenade rör av rostfritt stål i laboratorieskala visade att butylkarbitolbaserade lösningar avlägsnade mer PFAS än kranvatten, och att högre temperatur förbättrade avlägsnandet. Ytanalys med ”time-of-flight elastic recoil detection” avslöjade dock kvarvarande fluor, vilket utgör en risk för spridning av PFAS till omgivande miljö.

I ett annat experiment utvecklades en provtagningsmetod med gaskompresser gjorda av polyester. Metoden användes sedan framgångsrikt på AFFF-kontaminerade rörytor för att bestämma de totala PFAS-koncentrationerna.

I laktester i laboratorieskala av PFAS-förorenad jord bedömdes prestandan hos cement med och utan aktivt kol (AC)-baserade sorbenter i stabiliserings- och solidifieringsförsök. Tillsats av cement visade högre läckage av PFAS (µg/kg) än för ej solidifierad jord. Tillsats av AC-sorbenter resulterade i immobiliseringseffektiviteter på >99% för de flesta PFAS-föreningarna. Förändringar av K_d-värden och massflödeshastigheter över tid tyder på en övergång till diffusionsstyrda frisättningsmekanismer över tid.

I fältförsök med lysimetrar resulterade immobilisering av PFAS med hjälp av biokol från olika typer av avfall och AC-baserade sorbenter under naturliga, varierande mättade förhållanden i >99% PFAS-reduktion i lakvatten för långkedjiga PFAS och 79-99% reduktion för kortkedjiga PFAS. En 1D-transportmodell tyder på att PFAS kvarhålls i betydande omfattning vid luft-vattengränssnittet.

Nyckelord: PFAS, dekontaminering, skumövergång, ytanalys, time-of-flight elastisk rekyldetektering, supramolekylära sammansättningar, stabilisering och stelning, lysimetrar, variabelt mättade förhållanden

Dedication

To Sitka!

Contents

List of publications

This thesis is based on the work contained in the following papers, referred to by Roman numerals in the text:

I. Bonnet, B., Sharpe M.K., Seisenbaeva G., Yeung L.W.Y., Ross, I. & Ahrens, L. (2025). Decontamination and Surface Analysis of PFAS-contaminated Fire suppression System Pipes: Effects of Cleaning Agents and Temperature. *Environmental Science & Technology*, 59, 2222-2232.

II. Bonnet, B., Sharpe M.K., Williams, G., Ross, I., Ahrens, L. (2025). Development of a Novel Swab Sampling Methodology to Determine the Total PFAS Concentration on AFFF Contaminated Fire Suppression System Pipes. (manuscript).

III. Bonnet, B., McDonough, J., Wikner, P., Wall, E., Berggren-Kleja, D., Ahrens, L. (2025). Comparison of Different Laboratory-Scale Leaching Tests for Stabilization and/or Solidification of Soil Contaminated with PFASs. (manuscript).

IV. Hubert, M., Bonnet, B., Hale, S., Sörmo, E., Cornelissen, G., Ahrens, L., Arp, H.P.H. (2025). Modelling the Impact of Biochar and Sorbent Amendments on Seasonal and Long-Term PFAS Transport Behaviour Through Unsaturated Soil Lysimeters. Journal of hazardous materials. (under review)

The contribution of Björn Bonnet to the papers included in this thesis was as follows:

I. Planned the study with the co-authors and had the main responsibility for research questions, networking, study designs, laboratory experiments, data analysis, synthesis, writing, submission and funding acquisition for ToF-ERD analysis

II. Planned the study with the co-authors and had the main responsibility for research questions, networking, study designs, laboratory experiments, data analysis, synthesis, writing, submission and funding acquisition for ToF-ERD analysis

III. Planned the study with the co-authors and had the main responsibility for research questions, networking, study designs, laboratory experiments, data analysis, synthesis, writing and submission

IV. Planned the study with the co-authors and had the shared responsibility together with Michel Hubert for research questions, networking, study designs, laboratory experiments, data analysis, synthesis and writing.

Abbreviations

11CL-PF3OUdS	11-chloro-eicosafluoro-3-oxaundecane-1-sulfonic acid
4:2 FTSA	4:2 Fluorotelomer sulfonic acid
6:2 FTSA	6:2 Fluorotelomer sulfonic acid
8:2 FTSA	8:2 Fluorotelomer sulfonic acid
9Cl-PF3ONS	9-chloro-hexadecafluoro-3-oxanonane sulfonate
AC	Activated carbon
AFFF	Aqueous-film-forming foam
ARFF	Aircraft rescue and firefighting
BC-SL	Sewege sludge-derive biochar
BC-WT	Waste timber-derived biochar
C	Carbon
CAC	Colloidal activated carbon
CIC	Combustion-ion-chromatography
CMC	Critical micelle concentration
dw	dry weight
ECF	Electrochemical fluorination
Et-FOSAA	N-ethyl-perfluorooctane sulfonamido acetic acid
F	Fluorine
F3	Fluorine-free firefighting foams
F-chain	Fluorinated alkyl chain
Fe	Iron
FOSA	perfluorooctane sulfonamide
FT	Fluorotelomerization
GAC	Granular activated carbon
H-chain	Hydrocarbon chain

HFPO-Da	Hexafluoropropylene oxide dimer acid
HRMS	High-resolution mass spectrometry
$K_2S_2O_8$	Potassium persulfate
K_d	Soil-water sorption coefficients
L/S	Liquid-to-solid
LEAF	Leaching Environmental Assessment Framework
LOD	Limit of detection
LOQ	Limit of quantification
Me-FOSAA	N-methyl-perfluorooctane sulfonamido acetic acid
mM	millimolar
NaOH	Sodium hydroxide
NaDONA	4,8-dioxa-3G-perfluorononaoic acid
OH	Hydroxide
PAC	Powdered activated carbon
PC	Portland Cement
PFDoDA	Perfluorododecanoic acid
PFAAs	Perfluoroalkyl acids
PFAS	Per- and polyfluoroalkyl substances
PFBA	Perfluorobutanoic acid
PFBS	perfluorobutanesulfonic acid
PFDA	perfluorodecanoic acid
PFDS	perfluorodecanesulfonic acid
PFECHS	perfluoroethyl-cyclohexane sulfonate
PFHpA	perfluorohepanoic acid
PFHpS	perfluorohepanesulfonic acid
PFHxA	perfluorohexanoic acid
PFHxS	perfluorohexanesulfonic acid

PFNA	perfluorononanoic acid
PFNS	perfluorononanesulfonic acid
PFOA	perfluorooctanoic acid
PFOS	Perfluorooctanesulfonic acid
PFOSF	Perfluorooctanesulfonyl fluoride
PFPeA	perfluoropentanoic acid
PFPeS	perfluorohepanesulfonic acid
PFSAs	Perfluoroalkyl sulfonates
PFTeDA	perfluorotetradecanoic acid
PFTriDa	perfluorotridecanoic acid
PFUnDA	perfluoroundecanoic acid
POPs	Persistent organic pollutants
REACH	Regulation concerning the Registration, Evaluation, Authorisation and Restriction of Chemicals
S/S	Solidification and stabilization
SEM	Scanning electron microscopy
TF	Total fluorine
T_K	Krafft point
TFU	Thin film units
ToF-ERD	Time-of-flight elastic recoil detection
TOP	Total oxidizable precursors
UPLC-MS/MS	Ultra-performance liquid chromatography – tandem mass spectrometry
US EPA	United Stated Environmental Protection Agency
wt	weight

1. Introduction

Per- and polyfluoroalkyl substances (PFASs) are a group of man-made chemicals. Due to their unique physical-chemical properties most PFASs are extremely persistent. PFASs obtain their properties due to their stable covalent polar bonds between carbon and fluorine, resulting in hydrophobic as well as lipophobic character[1]. In principle, PFASs are characterized by their alkyl chains of different lengths, where the hydrogen atoms are either completely or partially substituted by fluorine, as well as differently charged functional head-groups[2]. PFAS mass-production started in the 1930s[3] and they are applied in numerous industrial and consumer products such as surfactants, coatings for paper[4] and textiles[5], cookware and food-packaging[6], semiconductor production[7], and aqueous-film-forming foam (AFFF) application[1, 8]. Within the last decades, PFASs were found in ubiquitously in environmental matrices, such as soil[9], groundwater[10], landfill leachate[11], sewage sludge[12], wastewater[13], sediment[14], wildlife[15, 16] as well as in humans[17]. PFASs are linked to cause adverse health effects in humans, such as cancer[18], thyroid toxicity, and altered immune response[19] and affect e.g., freshwater organisms[20]. Recently, research has recognized ultra-short-chain PFAS as a growing issue[21].

Some PFASs were regulated, e.g. perfluorooctanesulfonic acid (PFOS) and perfluorooctanesulfonyl fluoride (PFOSF) were added to the list of persistent organic pollutants (POPs) by the Stockholm Convention in 2009. To date, more single PFAS and their use have been restricted and regulated[22] and recently, the largest ever substance ban has been proposed by 5 EU member states aiming to restrict PFASs under REACH[23].

One major source of PFASs entering the environment are releases of AFFF from extinguishing fires of e.g., highly flammable hydrocarbons[8, 10, 24-26]. AFFFs contain a wide range of PFASs, but the composition often remains unclear. It has been found that analyses for targeted PFASs do not account for all organic fluorine present in AFFFs and environmental samples[27]. Hence, numerous studies identified mixtures of PFASs including legacy PFASs, such as PFOS, but also precursor-PFASs of zwitterionic, cationic and anionic character in AFFF formulations and AFFF-impacted sites, such as soils and groundwater[26, 28-30]. For limitation of existing and prevention of further contamination, remediation strategies must be developed.

Since PFAS legislations are becoming stricter regarding restriction of PFAS, industries have started to shift towards application of PFAS-free foam alternatives (F3 foams) in their fire-suppression systems. Simply changing to F3 foam will likely be insufficient with respect to preventing further PFASs release from fire-suppression systems, since PFASs adsorb to walls within storage containers and sprinkler system pipes and will potentially leach out over time. Therefore, enhancing the understanding of how the physicochemical properties of PFAS impact their adsorption behavior is crucial for developing more effective decontamination strategies.

2. Objective

The overall aim of this PhD research was to investigate and evaluate different approaches to mitigate AFFF-impacted infrastructure. It investigated how to prevent further PFAS spread from contaminated AFFF-impacted fire suppression systems, as well as how to remediate existing soils contaminated with historically used PFAS-containing AFFFs.

Specific objectives of the work described in Papers I-IV were to:

- Assess the effects of different cleaning agents and temperature on the decontamination of AFFF-impacted sprinkler system pipes (Paper I)

- Develop a methodology to assess the total PFAS mass present on AFFF-impacted sprinkler system pipes (Paper II)

- Evaluate different laboratory-scale leaching tests and the effect of solidification and stabilization to soil contaminated with PFASs (Paper III)

- Compare the performance of novel waste-derived biochars as materials for PFAS in the unsaturated zone (Paper IV)

3. Background

3.1 The basic properties of fluorinated surfactants

PFAS - a group of chemicals that has been making negative headlines for quite some time. They are ubiquitous in the environment[31, 32], extremely persistent[33, 34], challenging to remediate[35-38], and harmful to health[18, 19, 39, 40]. Yet, despite these concerns, PFAS are found in countless applications and products[41], "seemingly irreplaceable" – which they are not[42]. But what gives them such extraordinary properties - both beneficial and problematic? The answer lies in the bond between carbon (C) and fluorine (F) and the way fluorinated alkyl chains (F-chains) are structured.

F-chains exhibit exceptional properties that set them apart from other organic compounds. The C-F bond is among the strongest in organic chemistry[43], requiring significant energy to break. Additionally, F is the most electronegative element, strongly attracting electrons, creating a densely packed, repelling electron cloud that shields the C backbone[44]. As a result, fluorinated alkyl chains are highly resistant to thermal, physical, chemical, and biological degradation[45].

The strong electron-withdrawing effect of F also reduces the ability of electrons to interact with external electric fields, leading to low polarizability and a high ionization potential. Consequently, fluorinated chains exhibit weak intermolecular forces, such as van der Waals interactions[46].

In comparison to hydrocarbon-chains (H-chains), fluorocarbon-chains (F-chains) possess a larger van der Waals radius[47] and a greater cross-sectional area[48-50]. This structural difference results in a helical conformation, rather than the planar structure seen in hydrocarbon chains[49, 51]. This torsional potential makes fluorinated chains significantly more rigid than their hydrocarbon counterparts[52]. Furthermore, the larger molecular volume and surface area, combined with their low polarizability, contribute to the superior hydrophobic and lipophobic properties of F-chains[46, 48, 53]

When an F-chain, which is both hydrophobic and lipophobic, is combined with a hydrophilic head group, it creates an extremely surface-active molecule. Many PFAS incorporate both properties and can therefore be classified as surfactants.

When PFAS surfactants are introduced into an aqueous solution, they do not solely exist as monomers but can self-assemble into larger structures. The specific form in which surfactant molecules exist - whether as monomers, micelles, or aggregates - is influenced by two key factors: surfactant concentration and system temperature[54]. The conditions under which different molecular species form, are illustrated in the surfactant phase behavior diagram (Figure 1). The most critical transition point in this system is the Krafft-point (T_K). T_K is the temperature at which a surfactant's solubility becomes equal to its critical micelle concentration (CMC)[54, 55].

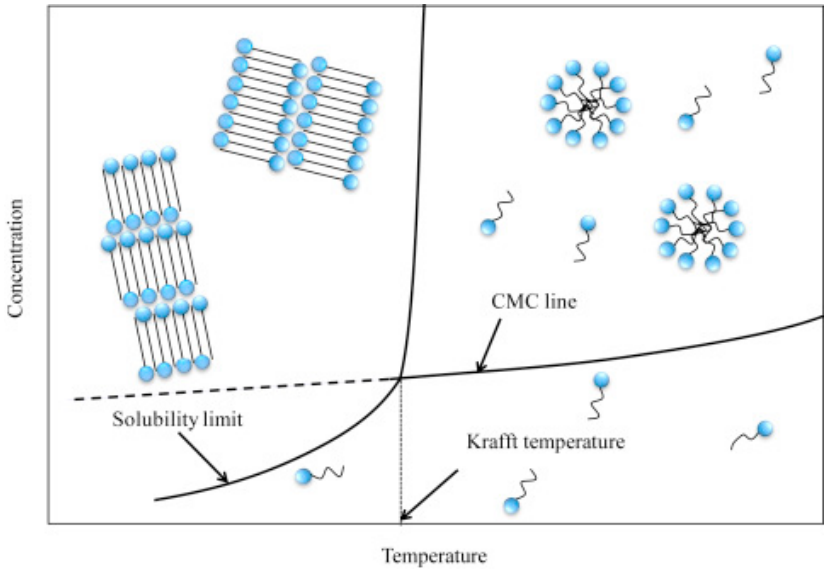

Figure 1: Surfactant solubility diagram[56]

If the temperature is below T_K and the surfactant concentration is sufficiently high, the surfactant precipitates as a crystalline phase, forming bilayers or lamellar structures. When the system temperature exceeds T_K and the surfactant concentration is above the CMC, the surfactant molecules self-assemble into micelles, whereas if the concentration is below the CMC, the surfactant exists as monomers in solution[54].

Due to the rigidity and low conformational flexibility of F-chains, PFAS are less likely to form spherical micelles. Instead, they preferentially arrange into cylindrical micelles, bilayer vesicles, or lamellar structures[54, 57]. Furthermore, PFAS have a substantially lower CMC than hydrocarbon surfactants[58], making them significantly more efficient.

Because of their strong hydrophobic and lipophobic nature, PFAS exhibit a strong tendency to assemble at interfaces such as the air-water interface[45, 59-61] or the liquid-solid interface[62, 63]. At the air-water interface, the fluorinated tail avoids direct contact with water, with the hydrophobic tail being expelled from the bulk phase, while the hydrophilic headgroup remains in solution. This effect occurs because it is energetically more favorable for a PFAS molecule to migrate to the surface than for a water molecule[54], thereby reducing the surface tension of water.

The ability of PFAS to lower surface tension is so strong that it remains effective in both aqueous and hydrocarbon liquids[64], making them far more efficient surfactants than hydrocarbon-based alternatives. The surface tension-lowering capability, combined with their weak intermolecular forces, enhances fluidity and spreadability[44, 59, 65]. These properties are essential in applications such as AFFF, where stability, rapid spreading and film formation are crucial for fire suppression.

3.2 Fundamentals of firefighting foams

Firefighting foams can be classified in different ways, either based on their chemical composition or on their expansion ratio[66]. Based on their chemical composition, foams are divided into synthetic or protein-based foams[66, 67]. In this work, the focus is put on synthetic foams, in particular AFFF for employment on Class B (flammable liquids or gasses) fires. The basic working principle of AFFF is the proportioning of AFFF concentrate with water which, through agitation, will generate a foam that is spread across the fire surface. The foam is basically a dispersion of gas bubbles and the constituents of AFFF concentrate that are briefly outlined in the following section[66-68].

3.2.1 Composition of AFFF

Typical constituents of AFFF concentrates are hydrocarbon surfactants, PFAS, organic solvents, and other additives such as foam stabilizers, anti-freeze agents, corrosion inhibitors, pH buffers and biocides. The role of the first three will be outlined briefly [67-69].

Hydrocarbon surfactants

Hydrogen surfactants of varying charge and chain length are added to AFFF concentrates. They serve as foaming agents facilitating foam generation.

They also improve the drainage control of the foam, enhancing the foam stability. In combination with fluorosurfactants they provide even superior surface activity[67, 68]. They also reduce the interfacial tension between water and the fuel surface, enhancing the interaction between water and fuel, thereby suppressing vapor formation and reducing the risk of reignition of the fire[54, 67, 68].

PFAS

Due to their physicochemical properties, PFAS very effectively decrease the surface tension of an aqueous foam solution below that of a hydrocarbon fuel. As a result, the foams' ability to spread on the fuel is accelerated forming a thin but stable film on top of the fuel surface[54]. Due to their thermal stability, they are vital for rapid fire extinguishment[67, 68, 70].

Organic solvents

Organic solvents serve multiple purposes in AFFF concentrates. Besides their function as foam stabilizers, due to formation of smaller bubble size, and their role as anti-freeze agents, they help to solubilize the different ingredients of AFFF. They prevent phase separation between hydrogen surfactants and fluorosurfactants and maintain consistency in performance and shelf-life. One commonly used solvent in AFFF concentrates is diethylene glycol monobutyl ether (CAS no. 112-34-5) also known as butyl carbitol[67, 68].

3.2.2 AFFF – complex mixtures of PFAS

A comprehensive characterization of PFAS compounds in AFFF formulations is a complex task that goes beyond the scope of this thesis. However, outlining the key aspects of PFAS composition in AFFF is essential, as it plays a crucial role in interpreting the analysis results.

AFFF production started in the 1960s[69] by a process called electrochemical fluorination (ECF)[2, 71]. AFFF-containing compounds produced by ECF were predominantly linear and branched perfluoroalkyl sulfonates (PFSAs) with PFOS as the most dominant compound [2, 54]. Another production process called fluorotelomerization (FT) became the dominant production process for AFFF after the manufacturer 3M ceased their ECF production for AFFF in 2002 [54, 72]. FT-based AFFFs contain a wide(r) range of polyfluorinated compounds, of which the precise molecular structure is often proprietary. Great efforts have been made in scientific studies and

reports to identify polyfluorinated compounds in AFFF[26, 28, 30, 73, 74]. Important classes that were identified are, for instance, fluorotelomer sulfonamide amines and betaines, fluorotelomer thioether (amido) sulfonic acids and fluorotelomer betains of 4 – 10 carbon chains [28, 73]. Dozens of compounds of anionic, cationic, non-ionic and zwitterionic character belonging to the classes mentioned above and others have been identified in AFFF formulations and in environmental matrices, such as soil and groundwater [26, 28, 30, 73, 74]. Due to polyfluorinated PFAS being affected by degradation such as aerobic [75, 76] and anaerobic [77], hydrolysis [78], photolysis [79] or microbial degradation [80], several unstable intermediates can be formed and found, before they are transformed to their stable endpoints: perfluoroalkyl acids (PFAAs)[21, 81].

Identification of polyfluorinated precursors is usually performed by high-resolution mass spectrometry (HRMS); however, quantification of these compounds is difficult due to lack of analytical standards. Knowledge about their presence has made scientists aware of the issue that a targeted analysis for the legacy PFAAs may not account for a substantial fraction of the PFAS that are present in AFFF contaminated matrices. To meet this challenge an additional analytical technique was developed – the total oxidizable precursor (TOP) assay.

3.3 Analytical challenges – The total oxidizable precursor assay

The TOP assay is an analytical procedure which was originally proposed by Houtz and Sedlak[82]. It was developed to convert unknown polyfluoroalkyl precursor PFASs to stable PFAAs by a hydroxyl radical driven oxidation under alkaline (pH>12) conditions. In the original method, the sample is exposed to a solution of 60 millimolar (mM) potassium persulfate ($K_2S_2O_8$) and 150 mM sodium hydroxide (NaOH). Under heat activation to 85°C sulphate radicals ($SO_4^{-}\cdot$) are formed which further react with hydroxide (OH^-) to produce hydroxyl radicals ($\cdot OH$). During oxidation, CH- and CC-bonds of polyfluoroalkyl precursors are attacked by $\cdot OH$ radicals, leading to a stepwise conversion of polyfluorinated PFAS precursors to stable PFAAs. The stable PFAAs products can then be detected by Ultra-performance liquid chromatography – tandem mass spectrometry (UPLC-MS/MS) and comparison of the sample before and after oxidation allows to estimate the contribution of unknown precursor PFAS in the sample.

A few challenges must be considered, since it is possible to both "undercook" or "overcook". The former case refers to the possibility to not fully convert all polyfluoroalkyl precursors during the oxidation process due to presence of matrix constituents, such as dissolved organic matter or constituents of AFFF and reduced metals[83], which may scavenge the *·OH* radicals and leading to incomplete oxidation of precursor PFAS. Detection of target-precursors e.g., 6:2 FTSA or FOSA, in the sample after TOP assay would be a sign of incomplete oxidation. By addition of an oxidation standard before oxidation, the completeness of the oxidation can be checked. Furthermore, pre-oxidation of the sample with e.g., hydrogen peroxide [84, 85] (H_2O_2) could remove possible interferences before starting the TOP assay.

Indication of "overcooking" would be if losses of PFCAs after TOP assay are observed. This will happen if the pH drops below 3.5, because of acidic species generation e.g., due to presence of organic compounds [86]. Sufficient buffering by NaOH and pH measurement after TOP assay are crucial factors.

Inclusion of ultra-short chain PFASs into the analytical suite is important, too, with respect to closing the fluorine mass balance [83, 87].

3.4 Treatment of PFAS-contaminated fire suppression infrastructure

Due to growing environmental and human health concerns associated with PFAS, the use of AFFF has been increasingly restricted [88-93], compelling the industry to transition toward F3 foam. However, fire suppression infrastructure, including stationary fire suppression sprinkler systems and mobile aircraft rescue and firefighting (ARFF) vehicles, has been exposed to AFFF over multiple decades, leading to the accumulation of PFAS on inner surfaces of these systems. Merely substituting AFFF with F3 foams presents the risk of surface-bound PFAS desorbing into the F3 foam, potentially contaminating it beyond acceptable thresholds [94]. Consequently, thorough decontamination of fire suppression systems is essential before the implementation of F3 foams [95, 96].

A common decontamination strategy involves repeated rinsing of affected systems using a range of cleaning solutions, from water to proprietary chemical agents [97-100]. The efficacy of decontamination in such trials is typically assessed by comparing PFAS concentrations in the liquid phase of the initial flush to those in the final flush. However, this approach does not account for residual surface-bound PFAS, which may remain

adsorbed to infrastructure materials. Several studies have documented a phenomenon known as the rebound effect, characterized by a secondary increase in PFAS concentrations in the liquid phase following an initial decline [96, 100]. This effect has been observed in both AFFF-impacted sprinkler systems and other PFAS-contaminated surfaces [101], highlighting the limitations of relying solely on decreasing liquid-phase PFAS concentrations as an indicator of successful decontamination.

To ensure effective decontamination, it is essential to incorporate surface analytical techniques capable of quantitatively assessing PFAS accumulation on AFFF-exposed infrastructure. Additionally, determining the total PFAS mass present on surfaces is critical for evaluating removal efficiencies in decontamination trials and for developing more reliable remediation strategies.

3.5 Approaches for remediation of PFAS-contaminated soil

3.5.1 The challenge – from laboratory-scale to field-scale

Although treatment of AFFF-impacted soil is being done in full-scale projects, there is no defined textbook approach that is applicable in all cases or scenarios. Soil treatment may require handling large amounts of soil and resources. Hence, before full-scale application is being conducted it is necessary to perform tests to verify and ensure successful treatment. The first steps are generally being taken on a much smaller scale in the laboratory.

Numerous test procedures are available e.g., the Leaching Environmental Assessment Framework (LEAF) by the US EPA. The challenge lies within selecting the appropriate test and transferring laboratory-scale results to full-scale application [102].

While tests in the laboratory take place under controlled conditions, they may be limited to fewer parameters as the ones being encountered in the field. The real case scenario can never completely be captured in a laboratory-scale setup.

The extent of the contamination as well as the factors controlling it are always site specific. Besides the PFAS concentrations and composition itself, the most relevant physical and chemical factors determining sorption and desorption processes in soil are soil type, soil texture, mineral composition,

presence of organic material, permeability, hydraulic conductivity, groundwater depth and flow, pH, ionic strength and the presence of co-contaminants [103-108]. Furthermore, climate conditions and seasonal variability must be considered as well.

In addition to playing a role in the assessment of the contamination, these factors are also relevant for determining the most suitable remediation action. For successful remediation, the remediation strategy, applied technology and remediation depth must be adjusted to site-specific conditions. Specifically, for sorbent-based technologies, the dose of sorbent is a crucial parameter that requires optimization.

3.5.2 Immobilization of PFAS in soil

In principle, immobilization of PFASs is achieved by addition of a sorbent and mixing it into contaminated soil. The sorbent adsorbs PFASs and reduces the concentration in pore water, thereby preventing leaching into groundwater. This technique is referred to as stabilization [109]. If cement is additionally used for solidification, the technical term 'solidification and stabilization' (S/S) is used, since cement is effectively solidifying the soil matrix [110]. Different sorbents have been tested for their immobilization potential, both at laboratory and field scale [110].

Most effective sorbents are based on activated carbon (AC), such as powdered activated carbon (PAC) and granular activated carbon (GAC) [111]. Commercially available products include Rembind®, a mixture of AC, aluminum hydroxide and kaolinite clay, and PlumeStop®, a colloidal activated carbon (CAC) with extremely fine particle size (1–2 μm) [104]. Several studies used laboratory-scale batch tests to verify treatment efficiency. In a study by Kupryianchyk et al.[112], three AFFF-impacted soils with different texture (organic rich forest soil, peat and sand) from Norway were treated with 4wt% (dry weight basis) AC. Batch desorption experiments over 14 days showed immobilization efficiencies for PFOA, PFOS and PFHxS of >99%. Another study from Norway by Hale et al[9] investigated PFASs immobilization of an AFFF-impacted sandy soil mixed with 3 wt% AC in batch desorption experiments over 8 days, and reported a removal efficiency for PFOS of 99%. In both studies, AC outcompeted alternative sorbents like biochar and montmorillonite.

Sörengård et al. performed a solidification and stabilization experiment including PAC and Rembind® as sorbents on a PFASs-spiked loamy sand on laboratory-scale [113]. Sorbents were added at 2 wt % and equilibrated for 24

hours. PAC and Rembind® showed 70% and 94% removal efficiency, respectively, for 13 out of 14 added PFASs and 99.9% removal efficiency for C8 and longer chained PFASs. Further sorbent materials, such as chitosan, bentonite, zeolite, and calcium chloride were tested and shown to be less effective sorbents. Sörengård et al.[110] also performed a pilot scale solidification and stabilization study on an AFFF-impacted soil. They investigated long-term efficiency with rainfall simulations over 7 years. Their experiments showed >97% PFASs immobilization for the four most dominant PFASs (PFHxA, PFOA, PFHxS and PFOS) but only 3% for short-chain PFPeA. Their treatment also showed good long-term stabilization efficiency, indicating increased PFASs sorption over time. Comparison of pilot scale to laboratory scale tests showed higher PFASs sorption in the pilot scale experiments.

Overall, laboratory and pilot scale experiments showed successful PFASs immobilization. One of the most important factors determining successful immobilization in the field is dependent on efficient mixing of contaminated soil and sorbent. In principle, there are two available options for incorporating the sorbent into the soil. Mixing could either happen in-situ, with specially designed rigs e.g., for dry soil mixing[114] and wet soil mixing[115]. These techniques are commonly used in geotechnical engineering to enhance soil stability and load capacity [116]. Hereby, circular columns are created by mixing sorbent into the soil down to a predetermined depth. For successful PFASs immobilization, it is required that columns overlap and, depending on target depth and area, wear of machinery and time, precise feasibility estimations are necessary.

The other option to mix binding agents into soils is *ex-situ* mixing, which is a three-stage process. In the first stage, contaminated soil is excavated and temporarily stored elsewhere. In the second stage, contaminated soil is mixed with sorbent e.g., by loaders or excavators using specially designed shovels or soil mixing facilities. The third stage is backfilling the now stabilized contaminated soil to the source zone [109]. These techniques have been applied at full-scale, but (to the authors' knowledge) not accompanied by peer-reviewed studies.

Unlike dry sorbents, such as GAC or PAC, CAC has an extremely small particle size and can therefore be injected directly into the soil. CAC is readily available for soil remediation purposes. Niarchos et al. (2022) [104] tested CAC in dynamic column experiments. They showed eight times higher ∑PFASs retardation in CAC treated soil with respect to the untreated

reference soil. Mass balance calculations yielded in 37% ∑PFASs retention in treated soil after approximately 600 pore volumes, achieving a 99.7% higher PFASs retention rate than the untreated reference soil. Disadvantages experienced during the column experiments were redistribution of CAC out from the columns of about 20% of the initially applied CAC and competition effects of longer chain PFASs replacing shorter chains PFASs.

Niarchos et al. also tested the application of CAC at full-scale on a firefighting training site in Arboga, Sweden [104]. CAC was injected as a barrier into the soil to intercept PFASs within the groundwater flow downstream of the PFASs contaminated area. Initial results of CAC indicated a 76% reduction of summed concentrations of eleven PFASs regulated in Swedish drinking water quality standards ($\sum_{11}$PFASs), with higher removal rates for long-chain PFASs, such as PFOS and PFOA. However, six months after injection, a rebound of PFASs in groundwater was measured and treatment efficiency dropped to 52% for $\sum_{11}$PFASs. The rebound effect can generally be described as delayed release of PFASs after initial sorption. The PFASs plume was found to bypass the barrier, presumably due to presence of high conductivity zones alternating with seasonal changes of groundwater flow directions and the CAC application itself as reasons for PFASs rebound. This study showed the importance of proper hydro(geo)logical site assessment and conceptual site models before full-scale implementation of the treatment.

Since PFAAs are neither removed nor destroyed in immobilization treatment, assurance of treatment longevity is crucial. Kabiri and McLaughlin [117, 118] investigated the long-term performance of Rembind® in modified repetitive soil extraction tests and column leaching experiments. To evaluate the long-term efficiency, 32 pore volumes were passed through the columns over 7 days. Their results showed 92 to 99.9 % immobilization efficiency compared to the untreated reference soil. They also showed unaltered immobilization performance in the presence of competing anions, as well as in scenarios with extreme conditions, such as temperatures (45 °C and -15 °C), ionic strengths (0-17 dS/m), and pH (2-12). Bräuning et al.[119] tested the longevity of Rembind® by reassessment of soil three years after initial mixing of soil and Rembind® and also found good long-term immobilization performance. The soil was stored in closed vessels, but not airtight, outdoors. Batch desorption experiments showed minor shifts towards higher concentration of short-chain PFAAs and lower concentrations of long-chain PFAAs in the leachate of the aged soil.

For S/S treatment, Sörengård et al. observed an increase in soil-water sorption coefficients (K_d) with time in simulated 7 years of precipitation[110]. They found these results for both the untreated reference soil and the S/S treated soil, with the K_d values for the S/S treated soil being significantly higher. As explanation for their findings, they hypothesized that the exchangeable fraction of PFASs leached first, leading to lower K_d values in the beginning of the experiment. They also compared PFAS concentration from laboratory scale leaching tests (batch and monolithic) to their pilot scale leaching tests and found that laboratory scale tests yielded 1-2 order of magnitude higher concentration in the leachate.

Bierbaum et al.[102] assessed PFASs immobilization in three different leaching tests. First, they applied a batch test with repeated sampling, referred to as an infinite sink test. Additionally, they prepared saturated column tests and variably saturated laboratory lysimeters. As sorbents, they used AC-based materials and a cement and bentonite mixture. Batch tests were run for 180 days and columns and lysimeters for approximately 30 months. They found immobilization efficiencies of >95% in the batch tests for treatment with AC-based products and 73% for cement and bentonite treatment for ∑PFASs. Column experiments showed reduced ∑PFASs concentration in leachate by approximately a factor 100 for the AC-based products. For cement and bentonite treatment, only long-chain PFASs were immobilized, whereas the highly alkaline conditions in the treated soil caused an increased leaching of short-chain PFASs compared to the untreated reference soil. In both the column and lysimeter experiments with treated soil, they found delayed breakthrough of short-chain PFASs after initial low concentrations in leachate. Breakthrough in the lysimeters happened with a stronger delay than in saturated columns, due to stronger interactions of PFASs at the air-water interface[120]. Comparison of batch tests to column tests revealed stronger desorption for batch tests. This section summarizes various approaches for remediation options of PFAS contaminated soils and outlines some of the site specific key challenges associated with it.

4. Material and Methods

4.1 PFAS targeted analysis

The targeted method used in Paper I, III and IV included 29 PFAS: PFBA, PFPeA, PFHxA, PFHpA, PFOA, PFNA, PFDA, PFUnDA, PFDoDA, PFTriDa, PFTeDA, PFBS, PFPeS, PFHxS, PFHpS, PFOS, PFNS, PFDS,4:2 FTSA, 6:2 FTSA and 8:2 FTSA Me-FOSAA, Et-FOSAA, FOSA, 9Cl-PF3ONS, 11CL-PF3OUdS, HFPO-Da, NaDONA and PFECHS. Twenty mass-labelled internal standards (IS) were used, $^{13}C_4$-PFBA, $^{13}C_5$-PFPeA, $^{13}C_5$-PFHxA, $^{13}C_4$-PFHpA, $^{13}C_8$-PFOA, $^{13}C_9$-PFNA, $^{13}C_6$-PFDA, $^{13}C_7$-PFUnDA, $^{13}C_3$-PFDoDA, $^{13}C_2$-PFTeDA, $^{13}C_3$-PFBS, $^{13}C_3$-PFHxS, $^{13}C_8$-PFOS, $^{13}C_2$-4:2 FTSA, $^{13}C_2$-6:2 FTSA, $^{13}C_2$-8:2 FTSA, $^{13}C_8$-FOSA, D_3-MeFOSAA, and D_5-EtFOSA (MPFAC-24ES, Wellington Laboratories, USA), and $^{13}C_3$-HFPO-DA.

All sample extracts were run on a SCIEX Triple Quad 3500 UPLC-MS/MS system. The detailed method is published in Smith et al. 2022[121].

4.2 Chemicals and other materials

Butyl carbitol (CAS number: 112-34-5) was purchased from Merck, Germany. GAC (Filtrasorb® 400) and PAC (Pulsorb® WP235) were provided by Chemviron, Sweden. Rembind® was provided by Envytech, Sweden. The biochar materials in paper IV were produced from wood waste (BC-WT) and sewage sludge (BC-SL) by pyrolysis[122-124].

4.3 Extraction methods

Different sample preparation approaches were applied for the water samples analysed in different studies. For samples with high expected PFAS concentration (paper I), samples were prepared in direct injection mode in 50%/50% aqueous phase/methanol (including 5 ng of each IS). For samples with low expected PFAS concentration (paper III and IV), solid phase extraction (SPE) was used. Samples were spiked 5 ng of each IS before filtration (paper III), or before SPE, if no filtration step was done (paper IV)[110]. SPE cartridges were Oasis® WAX cartridges (6mL, 150 mg, 30 µm, Waters, Ireland). Samples were concentrated under a gentle nitrogen stream to 0.1 - 1 mL.

Soil samples (paper III and IV) were extracted by solid-liquid extraction [125, 126]. Freeze-dried soil (0.1 g) was spiked with 5 ng of each IS and extracted in methanol, after soaking in 100 mM sodium hydroxide in 80%/20% methanol/MilliQ, in two rounds. After equilibration, extracts were concentrated under nitrogen followed by a clean-up step using ENVI-Carb (Sigma-Aldrich, USA).

Cotton swabs used in paper II were extracted by ALS UK for 18 PFAS including: PFBA, PFPeA, PFHxA PFHpA PFOA PFNA PFDA PFUnDA, PFDoDA, PFTriDA, PFBS, PFPeS PFHxS, PFHpS, linear and branched PFOS, 6:2 FTSA and FOSA. A sequential basic-acidic extraction based on Nickerson et al.[127] was applied on the swabs.

4.4 Total (organic) fluorine methods

4.4.1 Total oxidizable precursor assay

In paper I, TOP assays were run for all samples from the first time interval of the soaking experiment to account for the contribution of precursor PFAS. TOP assays were successfully run for samples containing TAP and MeOH (after evaporation to dryness).

In paper II, TOP assays were performed on extracts from cotton swabs.

4.4.2 Total fluorine analysis

Total fluorine (TF) analysis was performed in paper I, because oxidation of PFAS during TOP assay for samples containing butyl carbitol was inhibited due to the presence of butyl carbitol. Samples for all treatment solutions of the most contaminated pipe section in the first time interval (12 hours) were selected. TF analysis was performed directly on the cleaning solutions by combustion-ion-chromatography (CIC).

4.5 Quality assurance and quality control

Quality assurance and quality control samples were prepared in all experimental setups and sample extractions in form of blanks containing only solvent and no sample matrix for every batch. Analysis was done on duplicate (batch tests, paper III) or triplicate (soaking experiment, paper I). For semi-dynamic leaching tests (paper III) and lysimeter columns (paper

IV) only single setups were run due to lack of material (monoliths) and scale of the experiment (lysimeters). Due to high frequency analysis of lysimeter leachate, individual time points were analysed in singlicate. Limits of detection (LOD) and limits of quantification (LOQ) were estimated by the average blank concentration plus three time the standard deviation for LOD, and ten times the standard deviation for LOQ. If compounds were not detected within the blanks, the lowest point of the calibration curve with a signal-to-noise ratio >3 was used. IS recoveries were calculated based on the IS area in the sample compared to the IS area of the calibration curve.

4.6 Experimental techniques for investigation of AFFF-impacted sprinkler system pipes

4.6.1 Scanning electron microscopy

Scanning electron microscopy (SEM) was used as a pre-evaluation step for identification of AFFF-impacted stainless steel pipes (paper I). This was done to have visual confirmation of contaminated pipe sections used for further investigations. Images of AFFF-impacted pipe sections were compared to pristine stainless steel.

4.6.2 Time-of-flight elastic recoil detection

Time-of-flight elastic recoil detection (ToF-ERD) is an advanced ion beam analysis which is used to determine the elemental composition and depth profiling of materials [128, 129]. A high-energy (16 MEV) ion beam ($^{127}I^{8+}$) is directed at the sample. The ions interact with the atoms on the investigated sample, causing elastic recoil. Recoiled atoms travel towards a detector. On their way towards the detector, they pass two timing points between which their velocity (time-of-flight) is measured. Thereafter, the atoms enter the gas ionization chamber, for their energy measurement. With both parameters, atoms can be distinguished by their atomic mass. Thereby, ToF-ERD measurements provide quantitative elemental compositions in atomic % (at%) of the investigated surface as well as sensitive depth profiling in thin film units (TFU), an aerial unit of 10^{15} atoms per cm^2, even for light elements such as hydrogen. ToF-ERD was used to quantify fluorine atoms present on AFFF-impacted sprinkler system pipes. Measurements were taken before treatment, after each consecutive treatment interval, after treatment and after swab sampling (explained below), to follow up on removal progress.

4.6.3 Soaking experiment of AFFF-impacted pipe sections

To test different cleaning solutions with respect to their performance in removing PFAS assemblies from AFFF-impacted sprinkler system pipe sections, pipe sections were soaked in the respective solutions (paper I). Tested solutions were tap water, methanol and a 10- and 20-weight% solution of butyl carbitol. All solutions were tested at room temperature, 40°C and 70°C for a total of 8 days. The treatment solutions were exchanged after 24, 48, and 72 hours. PFAS concentration was measured in all soaking solutions and after every time interval.

4.6.4 Swab sampling

The swab sampling method was employed to quantify the total fluorine mass present on sprinkler system pipe sections impacted by AFFF (paper II). The procedure involved systematically swiping a cotton swab across the entire surface of the affected pipe sections in a predefined pattern[130]. Initially, a cotton gauze swab was soaked in basic methanol and applied to the surface for five minutes to facilitate PFAS extraction. This was followed by a second round, where a fresh cotton swab was soaked in acidic methanol and applied using the same method, ensuring thorough collection of fluorinated residues. Pipe sections on which the swab sampling was performed were from the same pipe that was used for the soaking experiment.

4.7 Experimental techniques for investigation of contaminated soils

4.7.1 Laboratory-scale leaching tests

Batch-tests

In batch tests in paper III and IV, contaminated soil, optionally mixed with sorbent, was mixed with water at a defined liquid-to-solid (L/S) ratio. The mixture was agitated, usually by shaking on an end-over-end shaker for 24 h (paper III) or 10 days (paper IV). The partitioning of PFAS between the solid and the liquid phase was assumed to be in chemical equilibrium after this period.

In paper III, different doses (1%, 3% and 5%) of Rembind® were mixed into field-contaminated soil to determine the stabilization properties of the different doses. Furthermore, addition of 10% PC and 5% of either

Rembind®, GAC or PAC was evaluated. Solidified soil material was crushed to a particle size <2mm on which the batch tests were performed. In paper IV, batch tests were performed on soil spiked with PFAS. 1% doses of either Rembind® or PAC were tested against 1% and 4% of either a SL-BC or a WT-BC.

Soil-water-partitioning coefficients (K_d-values) were determined in both studies to assess the treatments' PFAS stabilization efficiency. In paper IV, the K_d-values were used to calibrate the model.

Semi-dynamic leaching tests

In paper III, diffusive transport conditions of both granular soil material and solidified (monoliths) soil material, were performed in semi-dynamic leaching tests based on US EPA Method 1315. For granular soil material, approximately 700-750 g of wet untreated reference soil (soil-only control) and soil mixed with different doses of Rembind® (1%, 3% and 5%) were compacted into a 1 L PP vessel. 600 mL of MilliQ water were filled on top. Monolithic samples of reference soil solidified with 10% PC (PC-only control) and samples containing soil, 10% PC and 5% of either Rembind®, GAC or PAC were prepared according to Swedish standard procedure SGF 2:2000. After 28-30 days of curation, monoliths were exposed to 900 mL of MilliQ water in a 1L PP-vessel. The liquid phase was exchanged after 2 hours, 1 day, 2 days, 14 days, 28 days, 49 days, 70 days and 91 days. The PFAS concentration in the liquid phase was measured for each time point.

4.7.2 Field-deployed lysimeters

Field-deployed lysimeter experiments were performed using large scale soil columns (height: 120 cm; diameter 30 cm) (paper IV). Lysimeters were packed with soil spiked with PFAS to determine the leaching behaviour in the unsaturated zone. Besides unamended lysimeters, six lysimeters were amended with PFAS stabilizing sorbent. Doses of 1% of Rembind®, PAC, WT-BC and SL-BC and 4% of WT-BC and SL-BC were mixed into the soil after spiking. Lysimeters were set up in the outdoor lysimeter station at SLU in Uppsala for 1 year and were exposed to atmospheric condition throughout the entire experimental time. Rainwater leachate was collected once per week (when available) and was analysed for PFAS concentration. After 1 year, the lysimeters were sliced up into 5 sections of 20 cm each. Soil samples were taken from each section and analysed for PFAS in triplicate.

5. Results and Discussion

5.1 Decontamination of AFFF-impacted sprinkler system pipes (paper I)

In the decontamination trials of AFFF-impacted sprinkler system pipes the effectiveness of cleaning solutions generally ranked in the order of tap water < 10 wt% butyl carbitol < MeOH < 20 wt% butyl carbitol. Elevated temperature increased desorption of PFAS in the order of room temperature < 40°C < 70°C.

Butyl carbitol proved to be an effective solvent for PFAS. At 20 wt% in aqueous solution, it outperformed pure methanol. Due to butyl carbitols' molecular properties, it can lower the CMC [131-133] of a surfactant and reduce micelle sizes [134, 135], both essential factors for dissolving PFAS that have aggregated on surfaces. In all treatments, most PFAS (68%±22%) were removed during the initial soaking interval of 12 hours.

Targeted analysis before TOP assay identified PFOS as the most abundant single compound, with 76 ±22 wt% over all measurements, which is an indicator for the pipes being impacted by PFOS-containing AFFF manufactured by ECF[73]. Targeted analysis after TOP assay and TF analysis showed a 2 – 4-fold and 2 – 8-fold increase in fluorine equivalent, respectively, indicating the presence of polyfluoroalkyl precursors and possibly ultra-short chain PFAS.

Surface analysis by ToF-ERD showed between 3.4 to 8 at.% F on untreated AFFF-impacted pipe sections. F content could be reduced to 1.1 at.% with the most effective treatment: BC20 at 70°C. Decreased concentrations of carbon (C) and increased concentration of iron (Fe) further indicated the successful removal of the AFFF-associated PFAS layer, exposing the surface of the pipe section. Depth profile comparison toward pristine stainless steel showed that the pipe section after treatment with 20 wt% butyl carbitol at 70°C was not completely free of F, but that a substantial portion had been removed.

The highly precise quantitative ToF-ERD measurements, allowed us to estimate a number of at least 70.6 PFOS molecules/nm² to be present on the untreated AFFF-impacted pipe sections. This surface density indicates a three-dimensional arrangement of PFOS molecules beyond a monolayer. The measurement depth was confined to 1500 TFU, although the AFFF-associated layer extends beyond this depth. The number of molecules/nm²

was therefore likely to be even larger than the 70.6 molecule/nm² estimated above.

5.2 Determination of the total PFAS mass present on AFFF-impacted sprinkler system pipes (paper II)

The extraction of cotton swabs yielded a ∑PFAS concentration of 60±11 µg/cm² before TOP assay and 88±10 µg/cm² after TOP assay. 97% of ∑PFAS were removed with the 1st swab (basic methanol). PFOS was the most dominant compound at 93 wt%.

A 95%±1.5% and 74%±5.3% decrease of F and C, respectively, were measured by ToF-ERD, indicating removal of fluorinated carbons from the pipe surfaces. >500% increase of Fe and depth profiling confirm that the pipe surface is no longer covered and that the PFAS-associated layer has been removed successfully. It is suggested that residual F is inaccessible for the swab sampling method, by F being situated in holes and fissures within the stainless-steel surface.

The results obtained from the swab sampling methodology could serve as a reference point when decontamination procedures are performed, by comparing ∑PFAS concentrations in cleaning solutions to the ∑PFAS concentrations in swab samples.

5.3 Stabilization and solidification of a contaminated source zone (paper III)

In both applied laboratory-scale tests, addition of sorbent reduced the ∑PFAS concentration by at least 98% with respect to the untreated reference soil in granular or solidified soil.

In batch tests on granular soil material, amendment with 1% Rembind® stabilized short-chain PFCA compounds PFBA and PFPeA least efficiently, at around <10% and 55% stabilization compared to the reference soil, respectively. In the solidified reference soil including only cement, short-chain compounds PFBA, PFPeA and PFHxA (24% - 33%) and PFBS and PFPeS (28% and 52%) were less efficiently stabilized than PFOS (~90%).

In semi-dynamic leaching tests for granular material, the accumulated leaching of the untreated reference soil PFAS was reduced by 98% for amendment with 1% and 3% Rembind® and by 99% for 5% Rembind®. Solidification by 10% Portland Cement and 5% of either Rembind®, GAC or

PAC reduced leaching by >99%, showing only marginal differences between the different sorbents.

When comparing samples where the only difference was the addition of cement, those containing cement exhibited a 1.3 to 9-fold greater increase in PFAS leaching.

Comparison of K_d-values obtained in batch tests and semi-dynamic leaching tests showed that equilibrium conditions between the solid and the liquid phase were approached in semi-dynamic leaching tests sometime between 28 to 49 days. Before and after, the difference between K_d-values in semi-dynamic leaching tests and batch tests became increasingly large.

Slower release of PFAS in later time intervals is supported by observed declining release rates in the later time intervals. This supports a transition from leaching of readily available PFAS to a slower diffusion-controlled process as time increases.

5.4 Stabilization of PFAS contaminated soil in the unsaturated zone using waste-derived biochars (paper IV)

In the lysimeter study, commercial sorbents Rembind® and PAC were most efficient in reducing PFAS concentration. Even with respect to short-chain compounds PFBA, PFHxA and PFBS, they showed a >99% reduction in leachate concentration.

Biochar amendments of 1% and 4% BC-SL and 4% BC-WT reduced leachate concentrations for all PFSAs and long-chain PFCAs by >99% and for short-chain PFCAs by >95%. 1% BC-WT showed lower PFAS retentions regarding short-chain PFSAs and short-chain PFCAs with 83% and 96% respectively.

Superior sorption capacities of commercial sorbents are related to higher pore size surface areas of commercial binders compared to biochar materials. Differences in pore size are likely the reason for BC-SL showing better sorption capacities than BC-WT, due to pores of BC-SL being predominantly present between 3 and 35 nm, giving enough space for PFAS molecules to diffuse into.

Long-term modelling showed that BC-SL 4% enabled stabilization of 68% for short-chain PFCAs after 100 years, which is slightly lower than Rembind® at 81%. Long-chain PFCAs and PFOS were stabilized by >99%.

BC-WT 1% showed the lowest long-term stabilization efficiency, of around 10%-15% for short-chain PFAAs and 77% for long-chain PFCAs.

6. Conclusions and Future work

The aim of this theses was to identify and explore techniques for decontamination of PFAS-impacted fire suppression systems and for PFAS-contaminated soils. Brief answers to the research questions described in chapter 2 are given below.

- Assessment of the effects of different cleaning agents and temperature on the decontamination of AFFF-impacted sprinkler system pipes showed that solutions containing butyl carbitol and elevated temperatures enabled effective removal of PFAS and reduced rebound effects. Furthermore, it showed that investigations of surface bound PFAS are important and that decreasing concentrations in liquid phase is no credible way to determine successful decontamination.

- Swab sampling has proven to be an effective tool for determination of the PFAS mass present on AFFF-impacted sprinkler system pipes. It was shown that a large PFAS mass is present in surface bound form.

- The evaluation of stabilization and solidification treatment on PFAS-contaminated soil showed that solidification without additional sorbent is less effective than when sorbents are included. Furthermore, leaching rates decreased with increasing experimental time indicating diffusion-controlled leaching mechanism as experiments progressed.

- Novel waste-derived biochar materials as sorbents for PFAS in the unsaturated zone showed to be effective sorbents for PFAS, with sludge-derived biochar being more promising than wood-derived biochar. Modelling showed that promising long-term stabilization efficiencies and that variably saturated conditions had a substantial impact on PFAS release/retention.

Future work

The research presented in this thesis on the decontamination of AFFF-impacted fire suppression infrastructure provides valuable insights applicable to large-scale decontamination trials. As legislation surrounding the remediation of AFFF-impacted infrastructure advances, the need for effective decontamination solutions becomes increasingly critical to meet legally binding targets. The findings presented here will benefit all stakeholders involved in the decontamination process, including problem owners, consultants, and industry representatives.

While there is a significant step from laboratory-scale experiments to full-scale application, this work serves as a foundation for developing more effective decontamination strategies, aiming to minimize the challenges associated with the decontamination process. Further research is warranted, particularly in optimizing cleaning solutions. Aqueous solutions containing butyl carbitol provide a promising starting point, but additional adjustments to pH and ionic strength could enhance their efficiency.

Moreover, gaining a deeper understanding of the surface assembly processes of fluorinated surfactants is essential. Investigating the formation of stable fluorinated surfactant structures may lead to more effective removal strategies. A broader understanding of their physicochemical properties could also benefit other areas of research in the ongoing challenge of PFAS remediation in the environment.

The immobilization of PFAS-contaminated soil using activated carbon (AC)-based sorbents is an established field with full-scale applications worldwide. The leaching tests conducted in this study contribute to assessing the long-term efficiency of PFAS immobilization, a crucial factor in evaluating the success of even well-established methods. Additionally, the lysimeter study highlights the challenges of immobilization under natural, variably saturated conditions, offering a realistic representation of field scenarios. Future studies should consider longer monitoring periods and increased pore volume exchange combined with installation of measurement probes such as suction lysimeters for measurements of pore water content and sampling during flushing events to further refine our understanding.

Regarding biochars, results indicate that they hold high potential as a sustainable alternative for PFAS immobilization. Further research into

production optimization and large-scale application would be highly beneficial.

To improve analytical accuracy, it is crucial to incorporate techniques beyond targeted analysis, especially for AFFF-impacted samples. The presence of unknown precursors and ultra-short-chain PFAS can be significant and must not be overlooked. Advanced analytical methods, such as TOP assay integration in LC analyses, semi-quantitative HRMS, and total organic fluorine analysis via CIC, are essential for closing the fluorine mass balance. Research laboratories must prioritize the implementation of these methodologies into routine analysis, with academia taking the lead in setting new standards for PFAS research.

References

1. Lemal, D. M., Perspective on fluorocarbon chemistry. *The Journal of organic chemistry* **2004,** *69* (1), 1-11.
2. Buck, R. C.; Franklin, J.; Berger, U.; Conder, J. M.; Cousins, I. T.; De Voogt, P.; Jensen, A. A.; Kannan, K.; Mabury, S. A.; van Leeuwen, S. P., Perfluoroalkyl and polyfluoroalkyl substances in the environment: terminology, classification, and origins. *Integrated environmental assessment and management* **2011,** *7* (4), 513-541.
3. Hendricks, J. O., Industrial fluorochemicals. *Industrial & Engineering Chemistry* **1953,** *45* (1), 99-105.
4. Langberg, H. A.; Arp, H. P. H.; Breedveld, G. D.; Slinde, G. A.; Høiseter, Å.; Grønning, H. M.; Jartun, M.; Rundberget, T.; Jenssen, B. M.; Hale, S. E., Paper product production identified as the main source of per-and polyfluoroalkyl substances (PFAS) in a Norwegian lake: Source and historic emission tracking. *Environmental Pollution* **2021,** *273*, 116259.
5. Lang, J. R.; Allred, B. M.; Field, J. A.; Levis, J. W.; Barlaz, M. A., National estimate of per-and polyfluoroalkyl substance (PFAS) release to US municipal landfill leachate. *Environmental science & technology* **2017,** *51* (4), 2197-2205.
6. Trier, X.; Granby, K.; Christensen, J. H., Polyfluorinated surfactants (PFS) in paper and board coatings for food packaging. *Environmental Science and Pollution Research* **2011,** *18*, 1108-1120.
7. Lin, A. Y.-C.; Panchangam, S. C.; Lo, C.-C., The impact of semiconductor, electronics and optoelectronic industries on downstream perfluorinated chemical contamination in Taiwanese rivers. *Environmental Pollution* **2009,** *157* (4), 1365-1372.
8. Moody, C. A.; Field, J. A., Determination of perfluorocarboxylates in groundwater impacted by fire-fighting activity. *Environmental science & technology* **1999,** *33* (16), 2800-2806.
9. Hale, S. E.; Arp, H. P. H.; Slinde, G. A.; Wade, E. J.; Bjørseth, K.; Breedveld, G. D.; Straith, B. F.; Moe, K. G.; Jartun, M.; Høisæter, Å., Sorbent amendment as a remediation strategy to reduce PFAS mobility and leaching in a contaminated sandy soil from a Norwegian firefighting training facility. *Chemosphere* **2017,** *171*, 9-18.
10. Høisæter, Å.; Pfaff, A.; Breedveld, G. D., Leaching and transport of PFAS from aqueous film-forming foam (AFFF) in the unsaturated soil at a firefighting training facility under cold climatic conditions. *Journal of contaminant hydrology* **2019,** *222*, 112-122.
11. Benskin, J. P.; Li, B.; Ikonomou, M. G.; Grace, J. R.; Li, L. Y., Per-and polyfluoroalkyl substances in landfill leachate: patterns, time trends, and sources. *Environmental science & technology* **2012,** *46* (21), 11532-11540.
12. Yan, H.; Zhang, C.-J.; Zhou, Q.; Chen, L.; Meng, X.-Z., Short-and long-chain perfluorinated acids in sewage sludge from Shanghai, China. *Chemosphere* **2012,** *88* (11), 1300-1305.

13. Gallen, C.; Eaglesham, G.; Drage, D.; Nguyen, T. H.; Mueller, J., A mass estimate of perfluoroalkyl substance (PFAS) release from Australian wastewater treatment plants. *Chemosphere* **2018,** *208*, 975-983.
14. White, N. D.; Balthis, L.; Kannan, K.; De Silva, A. O.; Wu, Q.; French, K. M.; Daugomah, J.; Spencer, C.; Fair, P. A., Elevated levels of perfluoroalkyl substances in estuarine sediments of Charleston, SC. *Science of the Total Environment* **2015,** *521*, 79-89.
15. Martin, J. W.; Mabury, S. A.; Solomon, K. R.; Muir, D. C., Bioconcentration and tissue distribution of perfluorinated acids in rainbow trout (Oncorhynchus mykiss). *Environmental Toxicology and Chemistry: An International Journal* **2003,** *22* (1), 196-204.
16. Kelly, B. C.; Ikonomou, M. G.; Blair, J. D.; Surridge, B.; Hoover, D.; Grace, R.; Gobas, F. A., Perfluoroalkyl contaminants in an Arctic marine food web: trophic magnification and wildlife exposure. *Environmental science & technology* **2009,** *43* (11), 4037-4043.
17. Worley, R. R.; Moore, S. M.; Tierney, B. C.; Ye, X.; Calafat, A. M.; Campbell, S.; Woudneh, M. B.; Fisher, J., Per-and polyfluoroalkyl substances in human serum and urine samples from a residentially exposed community. *Environment international* **2017,** *106*, 135-143.
18. Boyd, R. I.; Ahmad, S.; Singh, R.; Fazal, Z.; Prins, G. S.; Madak Erdogan, Z.; Irudayaraj, J.; Spinella, M. J., Toward a mechanistic understanding of poly-and perfluoroalkylated substances and cancer. *Cancers* **2022,** *14* (12), 2919.
19. Fenton, S. E.; Ducatman, A.; Boobis, A.; DeWitt, J. C.; Lau, C.; Ng, C.; Smith, J. S.; Roberts, S. M., Per-and polyfluoroalkyl substance toxicity and human health review: Current state of knowledge and strategies for informing future research. *Environmental toxicology and chemistry* **2021,** *40* (3), 606-630.
20. Wang, L.; Yang, T.; Liu, X.; Liu, J.; Liu, W., Critical evaluation and meta-analysis of ecotoxicological data on per-and polyfluoroalkyl substances (PFAS) in freshwater species. *Environmental Science & Technology* **2024,** *58* (40), 17555-17566.
21. Arp, H. P. H.; Gredelj, A.; Glüge, J.; Scheringer, M.; Cousins, I. T., The global threat from the irreversible accumulation of trifluoroacetic acid (TFA). *Environmental Science & Technology* **2024,** *58* (45), 19925-19935.
22. Gobelius, L.; Hedlund, J.; Dürig, W.; Troger, R.; Lilja, K.; Wiberg, K.; Ahrens, L., Per-and polyfluoroalkyl substances in Swedish groundwater and surface water: implications for environmental quality standards and drinking water guidelines. *Environmental science & technology* **2018,** *52* (7), 4340-4349.
23. ECHA ECHA receives PFASs restriction proposal from five national authorities https://echa.europa.eu/-/echa-receives-pfass-restriction-proposal-from-five-national-authorities (accessed 9 March 2023).
24. Guelfo, J. L.; Wunsch, A.; McCray, J.; Stults, J. F.; Higgins, C. P., Subsurface transport potential of perfluoroalkyl acids (PFAAs): Column experiments and modeling. *Journal of Contaminant Hydrology* **2020,** *233*, 103661.

25. Houtz, E. F.; Higgins, C. P.; Field, J. A.; Sedlak, D. L., Persistence of perfluoroalkyl acid precursors in AFFF-impacted groundwater and soil. *Environmental science & technology* **2013,** *47* (15), 8187-8195.
26. Baduel, C.; Mueller, J. F.; Rotander, A.; Corfield, J.; Gomez-Ramos, M.-J., Discovery of novel per-and polyfluoroalkyl substances (PFASs) at a fire fighting training ground and preliminary investigation of their fate and mobility. *Chemosphere* **2017,** *185*, 1030-1038.
27. Weiner, B.; Yeung, L. W.; Marchington, E. B.; D'Agostino, L. A.; Mabury, S. A., Organic fluorine content in aqueous film forming foams (AFFFs) and biodegradation of the foam component 6: 2 fluorotelomermercaptoalkylamido sulfonate (6: 2 FTSAS). *Environmental Chemistry* **2013,** *10* (6), 486-493.
28. Place, B. J.; Field, J. A., Identification of novel fluorochemicals in aqueous film-forming foams used by the US military. *Environmental science & technology* **2012,** *46* (13), 7120-7127.
29. D'Agostino, L. A.; Mabury, S. A., Identification of novel fluorinated surfactants in aqueous film forming foams and commercial surfactant concentrates. *Environmental science & technology* **2014,** *48* (1), 121-129.
30. Barzen-Hanson, K. A.; Roberts, S. C.; Choyke, S.; Oetjen, K.; McAlees, A.; Riddell, N.; McCrindle, R.; Ferguson, P. L.; Higgins, C. P.; Field, J. A., Discovery of 40 classes of per-and polyfluoroalkyl substances in historical aqueous film-forming foams (AFFFs) and AFFF-impacted groundwater. *Environmental science & technology* **2017,** *51* (4), 2047-2057.
31. Toskos, T.; Panagiotakis, I.; Dermatas, D., Per-and polyfluoroalkyl substances–Challenges associated with a family of ubiquitous emergent contaminants. SAGE Publications Sage UK: London, England: 2019; Vol. 37, pp 449-451.
32. Buttle, E.; Sharp, E. L.; Fisher, K., Managing ubiquitous 'forever chemicals': More-than-human possibilities for the problem of PFAS. *New Zealand Geographer* **2023,** *79* (2), 97-106.
33. Brunn, H.; Arnold, G.; Körner, W.; Rippen, G.; Steinhäuser, K. G.; Valentin, I., PFAS: forever chemicals—persistent, bioaccumulative and mobile. Reviewing the status and the need for their phase out and remediation of contaminated sites. *Environmental Sciences Europe* **2023,** *35* (1), 1-50.
34. Cousins, I. T.; DeWitt, J. C.; Glüge, J.; Goldenman, G.; Herzke, D.; Lohmann, R.; Ng, C. A.; Scheringer, M.; Wang, Z., The high persistence of PFAS is sufficient for their management as a chemical class. *Environmental Science: Processes & Impacts* **2020,** *22* (12), 2307-2312.
35. Wanninayake, D. M., Comparison of currently available PFAS remediation technologies in water: A review. *Journal of Environmental Management* **2021,** *283*, 111977.
36. Leung, S. C. E.; Wanninayake, D.; Chen, D.; Nguyen, N.-T.; Li, Q., Physicochemical properties and interactions of perfluoroalkyl substances (PFAS)-Challenges and opportunities in sensing and remediation. *Science of The Total Environment* **2023,** *905*, 166764.

37. Travar, I.; Uwayezu, J. N.; Kumpiene, J.; Yeung, L. W., Challenges in the PFAS remediation of soil and landfill leachate: a review. *Advances in Environmental and Engineering Research* **2021,** *2* (2), 1-40.
38. Darlington, R.; Barth, E.; McKernan, J., The challenges of PFAS remediation. *The Military Engineer* **2018,** *110* (712), 58.
39. Mamsen, L. S.; Björvang, R. D.; Mucs, D.; Vinnars, M.-T.; Papadogiannakis, N.; Lindh, C. H.; Andersen, C. Y.; Damdimopoulou, P., Concentrations of perfluoroalkyl substances (PFASs) in human embryonic and fetal organs from first, second, and third trimester pregnancies. *Environment international* **2019,** *124*, 482-492.
40. Sunderland, E. M.; Hu, X. C.; Dassuncao, C.; Tokranov, A. K.; Wagner, C. C.; Allen, J. G., A review of the pathways of human exposure to poly-and perfluoroalkyl substances (PFASs) and present understanding of health effects. *Journal of exposure science & environmental epidemiology* **2019,** *29* (2), 131-147.
41. Glüge, J.; Scheringer, M.; Cousins, I. T.; DeWitt, J. C.; Goldenman, G.; Herzke, D.; Lohmann, R.; Ng, C. A.; Trier, X.; Wang, Z., An overview of the uses of per-and polyfluoroalkyl substances (PFAS). *Environmental Science: Processes & Impacts* **2020,** *22* (12), 2345-2373.
42. Figuière, R.; Miaz, L. T.; Savvidou, E.; Cousins, I. T., An Overview of Potential Alternatives for the Multiple Uses of Per-and Polyfluoroalkyl Substances. *Environmental Science & Technology* **2025**.
43. Banks, R. E.; Smart, B. E.; Tatlow, J., *Organofluorine chemistry: principles and commercial applications*. Springer Science & Business Media: 2013.
44. Riess, J. G., Highly fluorinated systems for oxygen transport, diagnosis and drug delivery. *Colloids and Surfaces A: Physicochemical and Engineering Aspects* **1994,** *84* (1), 33-48.
45. Gladysz, J. A.; Curran, D. P.; Horváth, I. T., *Handbook of fluorous chemistry*. John Wiley & Sons: 2006.
46. Smart, B. E., Characteristics of CF systems. In *Organofluorine Chemistry: Principles and commercial applications*, Springer: 1994; pp 57-88.
47. Bondi, A. v., van der Waals Volumes and Radii. *The Journal of physical chemistry* **1964,** *68* (3), 441-451.
48. Eicke, H.-F., *Modern trends of colloid science in chemistry and biology*. Springer: 1985.
49. Riess, J. G., Highly fluorinated amphiphilic molecules and self-assemblies with biomedical potential. *Current opinion in colloid & interface science* **2009,** *14* (5), 294-304.
50. Krafft, M. P.; Riess, J. G., Selected physicochemical aspects of poly-and perfluoroalkylated substances relevant to performance, environment and sustainability—Part one. *Chemosphere* **2015,** *129*, 4-19.
51. Erkoç, Ş.; Erkoç, F., Structural and electronic properties of PFOS and LiPFOS. *Journal of Molecular Structure: THEOCHEM* **2001,** *549* (3), 289-293.

52. Röthlisberger, U.; Laasonen, K.; Klein, M. L.; Sprik, M., The torsional potential of perfluoro n-alkanes: a density functional study. *The Journal of chemical physics* **1996,** *104* (10), 3692-3700.
53. Krafft, M. P.; Riess, J. G., Chemistry, Physical Chemistry, and Uses of Molecular Fluorocarbon− Hydrocarbon Diblocks, Triblocks, and Related Compounds□ Unique "Apolar" Components for Self-Assembled Colloid and Interface Engineering. *Chemical reviews* **2009,** *109* (5), 1714-1792.
54. Kissa, E., *Fluorinated surfactants and repellents*. CRC Press: 2001; Vol. 97.
55. Chang, Q., *Colloid and interface chemistry for water quality control*. Academic Press: 2016.
56. Iwata, T., Lamellar gel network. *Cosmetic Science and Technology: Theoretical Principles and Applications* **2017**, 415-447.
57. Ramanathan, M.; Shrestha, L. K.; Mori, T.; Ji, Q.; Hill, J. P.; Ariga, K., Amphiphile nanoarchitectonics: from basic physical chemistry to advanced applications. *Physical Chemistry Chemical Physics* **2013,** *15* (26), 10580-10611.
58. Tiddy, G. J. In *Concentrated surfactant systems*, Modern Trends of Colloid Science in Chemistry and Biology: International Symposium on Colloid & Surface Science, 1984 held from, October 17–18, 1984 at Interlaken, Switzerland, Springer: 1985; pp 148-183.
59. Krafft, M.; Riess, J., Highly fluorinated amphiphiles and colloidal systems, and their applications in the biomedical field. A contribution. *Biochimie* **1998,** *80* (5-6), 489-514.
60. Riess, J. G., Fluorous micro-and nanophases with a biomedical perspective. *Tetrahedron* **2002,** *58* (20), 4113-4131.
61. Lemay, A. C.; Bourg, I. C., Interactions between Per-and Polyfluoroalkyl Substances (PFAS) at the Water‑Air Interface. *Environmental Science & Technology* **2025**.
62. Ferrari, M., Self-Assembly of Surfactants at Solid Surfaces. *Supramolecular Chemistry: From Molecules to Nanomaterials* **2012**.
63. Paria, S.; Khilar, K. C., A review on experimental studies of surfactant adsorption at the hydrophilic solid–water interface. *Advances in colloid and interface science* **2004,** *110* (3), 75-95.
64. Handa, T.; Mukerjee, P., Surface tensions of nonideal mixtures of fluorocarbons and hydrocarbons and their interfacial tensions against water. *The Journal of Physical Chemistry* **1981,** *85* (25), 3916-3920.
65. Reed, T., Fluorine chemistry. *JH Simons, ed* **1964,** *5*.
66. Rakowska, J. In *Best practices for selection and application of firefighting foam*, MATEC Web of Conferences, EDP Sciences: 2018; p 00014.
67. Malik, P.; Nandini, D.; Tripathi, B. P., Firefighting aqueous film forming foam composition, properties and toxicity: a review. *Environmental Chemistry Letters* **2024**, 1-21.
68. Peshoria, S.; Nandini, D., Understanding Aqueous Film-forming Foam Components. In *Perfluoroalkyl Substances*, Améduri, B., Ed. The Royal Society of Chemistry: 2022; pp 357 - 387.

69. Moody, C. A.; Field, J. A., Perfluorinated surfactants and the environmental implications of their use in fire-fighting foams. *Environmental science & technology* **2000,** *34* (18), 3864-3870.
70. Peshoria, S.; Nandini, D.; Tanwar, R.; Narang, R., Short-chain and long-chain fluorosurfactants in firefighting foam: a review. *Environmental Chemistry Letters* **2020,** *18*, 1277-1300.
71. Simons, J. H., Electrochemical process of making fluorine-containing carbon compounds. Google Patents: 1950.
72. Lewandowski, G.; Meissner, E.; Milchert, E., Special applications of fluorinated organic compounds. *Journal of hazardous materials* **2006,** *136* (3), 385-391.
73. Field, J.; Sedlak, D., SERDP Project ER-2128 Final Report - Characterization of the Fate and Biotransformation of Fluorochemicals in AFFF-Contaminated Groundwater at Fire/Crash Testing Military Sites. **2017**.
74. Backe, W. J.; Day, T. C.; Field, J. A., Zwitterionic, cationic, and anionic fluorinated chemicals in aqueous film forming foam formulations and groundwater from US military bases by nonaqueous large-volume injection HPLC-MS/MS. *Environmental science & technology* **2013,** *47* (10), 5226-5234.
75. Liu, M.; Munoz, G.; Vo Duy, S.; Sauvé, S.; Liu, J., Stability of nitrogen-containing polyfluoroalkyl substances in aerobic soils. *Environmental Science & Technology* **2021,** *55* (8), 4698-4708.
76. Mejia-Avendaño, S.; Vo Duy, S.; Sauvé, S.; Liu, J., Generation of perfluoroalkyl acids from aerobic biotransformation of quaternary ammonium polyfluoroalkyl surfactants. *Environmental science & technology* **2016,** *50* (18), 9923-9932.
77. Zhang, S.; Lu, X.; Wang, N.; Buck, R. C., Biotransformation potential of 6: 2 fluorotelomer sulfonate (6: 2 FTSA) in aerobic and anaerobic sediment. *Chemosphere* **2016,** *154*, 224-230.
78. Washington, J. W.; Jenkins, T. M., Abiotic hydrolysis of fluorotelomer-based polymers as a source of perfluorocarboxylates at the global scale. *Environmental science & technology* **2015,** *49* (24), 14129-14135.
79. Liu, F.; Guan, X.; Xiao, F., Photodegradation of per-and polyfluoroalkyl substances in water: A review of fundamentals and applications. *Journal of Hazardous Materials* **2022,** *439*, 129580.
80. Liu, J.; Avendaño, S. M., Microbial degradation of polyfluoroalkyl chemicals in the environment: a review. *Environment international* **2013,** *61*, 98-114.
81. Lange, F. T.; Freeling, F.; Göckener, B., Persulfate based total oxidizable precursor (TOP) assay approaches for advanced PFAS assessment in the environment– a review. *Trends in Environmental Analytical Chemistry* **2024**, e00242.
82. Houtz, E. F.; Sedlak, D. L., Oxidative conversion as a means of detecting precursors to perfluoroalkyl acids in urban runoff. *Environmental science & technology* **2012,** *46* (17), 9342-9349.
83. Tsou, K.; Antell, E.; Duan, Y.; Olivares, C. I.; Yi, S.; Alvarez-Cohen, L.; Sedlak, D. L., Improved total oxidizable precursor assay for quantifying polyfluorinated compounds amenable to oxidative conversion to perfluoroalkyl carboxylic acids. *ACS ES&T Water* **2023,** *3* (9), 2996-3003.

84. Hutchinson, S.; Rieck, T.; Wu, X., Advanced PFAS precursor digestion methods for biosolids. *Environmental Chemistry* **2020,** *17* (8), 558-567.
85. Patch, D.; O'Connor, N.; Ahmed, E.; Houtz, E.; Bentel, M.; Ross, I.; Scott, J.; Koch, I.; Weber, K., Advancing PFAS characterization: Development and optimization of a UV-H2O2-TOP assay for improved PFCA chain length preservation and organic matter tolerance. *Science of The Total Environment* **2024**, 174079.
86. Bruton, T. A.; Sedlak, D. L., Treatment of aqueous film-forming foam by heat-activated persulfate under conditions representative of in situ chemical oxidation. *Environmental Science & Technology* **2017,** *51* (23), 13878-13885.
87. Patch, D.; O'Connor, N.; Vereecken, T.; Murphy, D.; Munoz, G.; Ross, I.; Glover, C.; Scott, J.; Koch, I.; Sauvé, S., Advancing PFAS characterization: Enhancing the total oxidizable precursor assay with improved sample processing and UV activation. *Science of The Total Environment* **2024,** *909*, 168145.
88. Commission Delegated Regulation (EU) 2020/784. Amending Annex I to Regulation (EU) 2019/1021 of the European Parliament and of the Council as regards the listing of perfluorooctanoic acid (PFOA), ots salts and PFOA-related compounds. 2020. In *Official Journal of the European Union* European Union pp 1 - 3.
89. Commission Regulation (EU) 2021/1297. Amending Annex XVII to Regulation (EC) No 1907/2006 of the European Parliament and of the Council as regards perfluorocarboxylic acids containing 9 to 14 carbon atoms in the chain (C9-C14 PFCAs), and their salts and C9-C14 PFCA-related substances. 2021. In *Official Journal of the European Union*, European Union pp 29 - 32.
90. Congress, National Defense Authorization Act for Fiscal Year 2020. 2020.
91. IPEN, POPRC-14. White paper, Fluorine-free firefighting foams (3F) - Viable alternatives to fluorinated aqueous film-forming foams (AFFF). **2018**.
92. IPEN, Stockholm Convention COP-9 White Paper. The Global PFAS Problem: Fluorine-Free Alternatives As Solutions. **2019**.
93. Commission Regulation (EU) 2017/1000. Amending Annex XVII to Regulation (EC) No 1907/2006 of the European Parliament and of the Council concerning the Registration, Evaluation, Authorisation and Restriction of Chemicals (REACH) as regards perfluorooctanoic acid (PFOA), its salts and PFOA-related substances. 2017. In *Official Journal of the European Union* European Union.
94. Ross, I., Is it as simple as "Foam out / Foam in?". *The Catalyst* **2020,** *Q2 Supplement*, 1 - 15.
95. Nguyen, D.; Bellona, C.; Lau, A.; Stults, J.; Andrews, H.; Jones, D.; Megson, D.; Ross, I., Practical Limits of Current Technologies in Removing Per-and Polyfluoroalkyl Substances from Fire Suppression Systems. *Available at SSRN 4944573*.
96. Dahlbom, S.; Bjarnemark, F.; Nguyen, B.; Petronis, S.; Mallin, T., Analysis of per-and polyfluoroalkyl substances (PFAS) extraction from contaminated firefighting materials: Effects of cleaning agent, temperature, and chain-length dependencies. *Emerging Contaminants* **2024,** *10* (3), 100335.

97. Cornelsen, M.; Weber, R.; Panglisch, S., Minimizing the environmental impact of PFAS by using specialized coagulants for the treatment of PFAS polluted waters and for the decontamination of firefighting equipment. *Emerging Contaminants* **2021,** *7*, 63-76.
98. Lang, J. R.; McDonough, J.; Guillette, T.; Storch, P.; Anderson, J.; Liles, D.; Prigge, R.; Miles, J. A.; Divine, C., Characterization of per-and polyfluoroalkyl substances on fire suppression system piping and optimization of removal methods. *Chemosphere* **2022,** *308*, 136254.
99. AECOM *AFFF Fire Truck and Foam Unit Decontamination Summary Report. Prepared for and published by Connecticut Department of Energy and Environmental Protection.* ; 2022.
100. Arcadis *Trailer Demonstration Project Summary Report.* ; 2022.
101. Vo, P. H.; Key, T. A.; Le, T. H.; McDonough, J. T.; Porman, S.; Fiorenza, S.; Nguyen, H. T.; Dao, V. T.; Mueller, J. F.; Thai, P. K., Evaluation of sealants to mitigate the release of per-and polyfluoroalkyl substances (PFAS) from AFFF-impacted concrete: Characterization and forecasting. *Water Research X* **2023,** *20*, 100195.
102. Bierbaum, T.; Klaas, N.; Braun, J.; Nürenberg, G.; Lange, F. T.; Haslauer, C., Immobilization of per-and polyfluoroalkyl substances (PFAS): comparison of leaching behavior by three different leaching tests. *Science of The Total Environment* **2023,** *876*, 162588.
103. Milinovic, J.; Lacorte, S.; Vidal, M.; Rigol, A., Sorption behaviour of perfluoroalkyl substances in soils. *Science of the Total Environment* **2015,** *511*, 63-71.
104. Niarchos, G.; Ahrens, L.; Kleja, D. B.; Leonard, G.; Forde, J.; Bergman, J.; Ribeli, E.; Schütz, M.; Fagerlund, F., In-situ application of colloidal activated carbon for PFAS-contaminated soil and groundwater: A Swedish case study. *Remediation Journal* **2022**.
105. Nguyen, T. M. H.; Bräunig, J.; Thompson, K.; Thompson, J.; Kabiri, S.; Navarro, D. A.; Kookana, R. S.; Grimison, C.; Barnes, C. M.; Higgins, C. P., Influences of chemical properties, soil properties, and solution pH on soil–water partitioning coefficients of per-and polyfluoroalkyl substances (PFASs). *Environmental science & technology* **2020,** *54* (24), 15883-15892.
106. Liu, Y.; Qi, F.; Fang, C.; Naidu, R.; Duan, L.; Dharmarajan, R.; Annamalai, P., The effects of soil properties and co-contaminants on sorption of perfluorooctane sulfonate (PFOS) in contrasting soils. *Environmental Technology & Innovation* **2020,** *19*, 100965.
107. Liao, S.; Arshadi, M.; Woodcock, M. J.; Saleeba, Z. S.; Pinchbeck, D.; Liu, C.; Cápiro, N. L.; Abriola, L. M.; Pennell, K. D., Influence of Residual Nonaqueous-Phase Liquids (NAPLs) on the Transport and Retention of Perfluoroalkyl Substances. *Environmental Science & Technology* **2022,** *56* (12), 7976-7985.
108. Brusseau, M. L., Assessing the potential contributions of additional retention processes to PFAS retardation in the subsurface. *Science of the Total Environment* **2018,** *613*, 176-185.

109. Ross, I.; McDonough, J.; Miles, J.; Storch, P.; Thelakkat Kochunarayanan, P.; Kalve, E.; Hurst, J.; S. Dasgupta, S.; Burdick, J., A review of emerging technologies for remediation of PFASs. *Remediation Journal* **2018,** *28* (2), 101-126.
110. Sörengård, M.; Gago-Ferrero, P.; Kleja, D. B.; Ahrens, L., Laboratory-scale and pilot-scale stabilization and solidification (S/S) remediation of soil contaminated with per-and polyfluoroalkyl substances (PFASs). *Journal of Hazardous Materials* **2021,** *402*, 123453.
111. Sörengård, M.; Östblom, E.; Köhler, S.; Ahrens, L., Adsorption behavior of per-and polyfluoralkyl substances (PFASs) to 44 inorganic and organic sorbents and use of dyes as proxies for PFAS sorption. *Journal of Environmental Chemical Engineering* **2020,** *8* (3), 103744.
112. Kupryianchyk, D.; Hale, S. E.; Breedveld, G. D.; Cornelissen, G., Treatment of sites contaminated with perfluorinated compounds using biochar amendment. *Chemosphere* **2016,** *142*, 35-40.
113. Sörengård, M.; Kleja, D. B.; Ahrens, L., Stabilization and solidification remediation of soil contaminated with poly-and perfluoroalkyl substances (PFASs). *Journal of hazardous materials* **2019,** *367*, 639-646.
114. Keller, G. E. Dry Soil Mixing. https://www.keller-na.com/expertise/techniques/dry-soil-mixing.
115. Keller, G. E. Wet Soil Mixing https://www.keller-na.com/expertise/techniques/wet-soil-mixing (accessed 14.04.2023).
116. Li, S.; Kirstein, A.; Gurpersaud, N.; Liu, J. In *Experimental investigation of cement mixing to improve Champlain Sea clay*, GeoVancouver 2016 CGS Annual Conference, Vancouver, Canada, 2016.
117. Kabiri, S.; McLaughlin, M. J., Durability of sorption of per-and polyfluorinated alkyl substances in soils immobilized using common adsorbents: 2. Effects of repeated leaching, temperature extremes, ionic strength and competing ions. *Science of The Total Environment* **2021,** *766*, 144718.
118. Kabiri, S.; Centner, M.; McLaughlin, M. J., Durability of sorption of per-and polyfluorinated alkyl substances in soils immobilised using common adsorbents: 1. Effects of perturbations in pH. *Science of the Total Environment* **2021,** *766*, 144857.
119. Bräunig, J.; Baduel, C.; Barnes, C. M.; Mueller, J. F., Sorbent assisted immobilisation of perfluoroalkyl acids in soils–effect on leaching and bioavailability. *Journal of Hazardous Materials* **2021,** *412*, 125171.
120. Brusseau, M.; Guo, B., PFAS concentrations in soil versus soil porewater: Mass distributions and the impact of adsorption at air-water interfaces. *Chemosphere* **2022,** *302*, 134938.
121. Smith, S. J.; Wiberg, K.; McCleaf, P.; Ahrens, L., Pilot-scale continuous foam fractionation for the removal of per-and polyfluoroalkyl substances (PFAS) from landfill leachate. *ACS Es&t Water* **2022,** *2* (5), 841-851.
122. Sørmo, E.; Castro, G.; Hubert, M.; Licul-Kucera, V.; Quintanilla, M.; Asimakopoulos, A. G.; Cornelissen, G.; Arp, H. P. H., The decomposition and emission factors of a wide range of PFAS in diverse, contaminated organic waste

fractions undergoing dry pyrolysis. *Journal of Hazardous Materials* **2023,** *454*, 131447.
123. Sørmo, E.; Silvani, L.; Thune, G.; Gerber, H.; Schmidt, H. P.; Smebye, A. B.; Cornelissen, G., Waste timber pyrolysis in a medium-scale unit: Emission budgets and biochar quality. *Science of the Total Environment* **2020,** *718*, 137335.
124. Krahn, K. M.; Cornelissen, G.; Castro, G.; Arp, H. P. H.; Asimakopoulos, A. G.; Wolf, R.; Holmstad, R.; Zimmerman, A. R.; Sørmo, E., Sewage sludge biochars as effective PFAS-sorbents. *Journal of Hazardous Materials* **2023,** *445*, 130449.
125. Sörengård, M.; Kikuchi, J.; Wiberg, K.; Ahrens, L., Spatial distribution and load of per-and polyfluoroalkyl substances (PFAS) in background soils in Sweden. *Chemosphere* **2022,** *295*, 133944.
126. Ahrens, L.; Felizeter, S.; Sturm, R.; Xie, Z.; Ebinghaus, R., Polyfluorinated compounds in waste water treatment plant effluents and surface waters along the River Elbe, Germany. *Marine pollution bulletin* **2009,** *58* (9), 1326-1333.
127. Nickerson, A.; Maizel, A. C.; Kulkarni, P. R.; Adamson, D. T.; Kornuc, J. J.; Higgins, C. P., Enhanced extraction of AFFF-associated PFASs from source zone soils. *Environmental science & technology* **2020,** *54* (8), 4952-4962.
128. Shi, Y.; Wright, M.; Sharpe, M. K.; McAleese, C. D.; Polzin, J.-I.; Niu, X.; Zhao, Z.; Morris, S. M.; Bonilla, R. S., Characterization of solar cell passivating contacts using time-of-flight elastic recoil detection analysis. *Applied Physics Letters* **2023,** *123* (26).
129. Julin, J.; Sajavaara, T., Conceptual study of a heavy-ion-ERDA spectrometer for energies below 6 MeV. *Nuclear Instruments and Methods in Physics Research Section B: Beam Interactions with Materials and Atoms* **2017,** *406*, 61-65.
130. Environmental Protection (Water) Policy 2009 - Monitoring and Sampling Manual Physical and chemical assessment. 2018. Queensland Government.
131. Ooshika, Y., A theory of critical micelle concentration of colloidal electrolyte solutions. *Journal of Colloid Science* **1954,** *9* (3), 254-262.
132. Nakayama, H.; Shinoda, K.; Hutchinson, E., The effect of added alcohols on the solubility and the Krafft point of sodium dodecyl sulfate. *The Journal of Physical Chemistry* **1966,** *70* (11), 3502-3504.
133. Shinoda, K., The effect of alcohols on the critical micelle concentrations of fatty acid soaps and the critical micelle concentration of soap mixtures. *The Journal of Physical Chemistry* **1954,** *58* (12), 1136-1141.
134. Dong, D.; Kancharla, S.; Hooper, J.; Tsianou, M.; Bedrov, D.; Alexandridis, P., Controlling the self-assembly of perfluorinated surfactants in aqueous environments. *Physical Chemistry Chemical Physics* **2021,** *23* (16), 10029-10039.
135. Giles, S. L.; Snow, A. W.; Hinnant, K. M.; Ananth, R., Modulation of fluorocarbon surfactant diffusion with diethylene glycol butyl ether for improved foam characteristics and fire suppression. *Colloids and Surfaces A: Physicochemical and Engineering Aspects* **2019,** *579*, 123660.

Popular science summary

Per- and polyfluoroalkyl substances (PFAS), often called “forever chemicals,” have been widely used in firefighting foams, waterproof coatings, consumer goods and industrial products. Unfortunately, these chemicals do not break down easily in the environment and can contaminate firefighting infrastructure, soil, and water. Since some PFAS are toxic and highly mobile, finding ways to remove them from fire suppression systems and prevent their spread from contaminated soils is a major challenge.

Fire suppression systems, like sprinkler pipes, can retain a large mass of PFAS, leading to ongoing contamination. In laboratory-scale tests carried out at 70°C, a water solution containing 20% butyl carbitol (a cleaner solvent) removed 2 to 8 times more PFAS than hot tap water alone, and up to 20 times more than cold tap water. However, even after cleaning, traces of PFAS remained on the pipe surfaces, meaning that these pipes may still pose a contamination risk.

Another approach involved swabbing the contaminated pipe surfaces with a two-step basic-acidic extraction procedure. This method successfully extracted 88±10 µg/cm² of PFAS, and surface analysis confirmed that 95% of fluorine residues were removed.

When PFAS have entered soil, it can leach into groundwater from where the contamination is spread. A key strategy to prevent this is to immobilize PFAS by mixing the soil with stabilizing agents. Lab experiments showed that using cement alone actually increased PFAS leaching by 2 to 3.5 times compared to untreated soil. However, adding just 1% of Rembind®, a specially designed sorbent, reduced PFAS leaching by over 98%, making it a much more effective solution.

To test how well these immobilization methods work outside the controlled laboratory environment, large-scale soil columns - lysimeters - were installed in the field to simulate natural conditions. Biochar and activated carbon-based sorbents were tested under variably saturated conditions, achieving >99% PFAS stabilization for long-chain compounds and 79-99% reduction for short-chain PFAS. A model predicted that 30-65% of PFAS gets trapped at the air-water interface, and that biochar made from sludge can immobilize PFOS for at least 100 years.

While these results show promise, PFAS contamination remains a serious and complex problem. More research is needed to optimize cleaning

solutions, ensure long-term soil stabilization, to further deepen the understanding of PFAS in the environment. By developing effective decontamination and immobilization strategies, we can reduce the spread of PFAS and protect human and ecosystem exposure for future generations.

Populärvetenskaplig sammanfattning

Per- och polyfluorerade alkylsubstanser (PFAS), ofta kallade ”evighetskemikalier”, har använts i stor utsträckning i brandsläckningsskum, vattentäta beläggningar, konsumentvaror och industriprodukter. Tyvärr bryts dessa kemikalier inte ned så lätt i miljön och kan förorena infrastruktur som använts för brandsläckning, mark och vatten. Eftersom vissa PFAS är giftiga och mycket lättrörliga är det en stor utmaning att hitta sätt att avlägsna dem från brandsläckningssystem och förhindra att de sprids från förorenad mark.

Brandbekämpningssystem, t.ex. sprinklerrör, kan innehålla stora mängder PFAS, vilket leder till fortsatt förorening. I tester i laboratorieskala utförda vid 70°C med en vattenlösning som innehöll 20% butylkarbitol (lösningsmedel som bl.a. används för olika typer av rengöring) avlägsnades 2 till 8 gånger mer PFAS än enbart varmt kranvatten, och upp till 20 gånger mer än kallt kranvatten. Men även efter rengöringen fanns det spår av PFAS kvar på rörytorna, vilket innebär att dessa rör fortfarande kan utgöra en föroreningsrisk.

Ett annat tillvägagångssätt var att svabba de förorenade rörytorna med en tvåstegs syra-bas-extraktion. Denna metod kunde extrahera 88±10 μg/cm² PFAS, och en ytanalys bekräftade att 95% av fluorföroreningarna hade avlägsnats.

När PFAS har trängt ner i marken kan det läcka ut i grundvattnet varifrån föroreningen sprids. En viktig strategi för att förhindra detta är att immobilisera (binda fast) PFAS genom att blanda jorden med stabiliseringsmedel. Laboratorieförsök visade att tillsats av cement ökade PFAS-utlakningen med 2 till 3,5 gånger jämfört med obehandlad jord. Genom att tillsätta cement tillsammans med 1% av Rembind®, en specialdesignad sorbent, minskades dock PFAS-utlakningen med över 98%, vilket gör det till en mycket mer effektiv lösning.

För att testa hur väl dessa immobiliseringsmetoder fungerar utanför den kontrollerade laboratoriemiljön installerades storskaliga jordkolonner - lysimetrar – i fält för att simulera naturliga, mer storskaliga förhållanden. Sorbenter baserade på biokol och aktivt kol testades under varierande nederbördsförhållanden och uppnådde >99% PFAS-stabilisering för långkedjiga föreningar och 79-99% reduktion för kortkedjiga PFAS. En prediktionsmodell förutspådde att 30-65% av PFAS fastnar vid luft-

vattengränssnittet, och att biokol tillverkat av slam kan immobilisera PFOS i minst 100 år.

Även om dessa resultat är lovande är PFAS-föroreningar fortfarande ett allvarligt och komplext problem. Mer forskning behövs för att optimera rengöringslösningar, säkerställa långsiktig markstabilisering och ytterligare fördjupa förståelsen av PFAS i miljön. Genom att utveckla effektiva saneringss- och immobiliseringsstrategier kan vi minska spridningen av PFAS och skydda människor och ekosystem från framtida exponering.

Acknowledgements

I would like to express my deepest gratitude to all those who supported and contributed to this PhD journey.

Thank you …

Lutz Ahrens, for giving me the opportunity to undertake this PhD. **Karin Wiberg**, for being there when I needed you the most. **Dan Berggren-Kleja**, for guiding me onto the right track for Paper III. **Gulaim Seisenbaeva**, for the SEM analysis. **Leo**, for the TF analysis. **Foon**, for being such a credible researcher. **Ove**, for being the greatest mentor. Thank you for the endless discussions about analytical work, for respectfully listening when things didn't go as planned, and for always sharing your wisdom. **Ian Ross**, for your invaluable contribution to this work. You were not only a tremendous source of information but also an inspiration and motivation. You truly elevated this work to another level! **Matthew Sharpe**, for introducing me to the fascinating world of particle accelerators. **Geraint Williams**, for the swab extractions. **Jeff McDonough**, for your helpful insights on Paper III. **Erik Wall** and **Svante Skårpas** for providing samples for my experiments. **Per Wikner** and **Kalman Gergely**, for your support with sample preparation. The **late lunch crew** - **Chen**, **Uzair**, **Javad**, **Raj**, and **Harold** - for our unconventional lunch hours. **Patrick**, for the hot-pot. My office mates **Khadija**, **Oscar**, and **Svante**, for enduring my endless calls with collaborators. **Kong**, for your support with the Kappa guidelines. **Valentina**, for sharing your Sciex expertise. **George** for always sharing fume hoods. **My colleagues from the floor above** - **Ashkan**, **Chibbzz**, **Iva**, **Lindsay**, **Mari**, and **Max** - for welcoming the "downstairs stranger" into your group. **Henrik**, for your LC support. **Marcus**, for double-checking even the most basic chemical calculations. **Andreas**, for your help with all the administrative tasks. **Fiskis&Svettis** for creating such an amazing "playground" right next to my "living room". The **PERFORCE3 ESR**s, for being an incredible group of PhDs to share this experience with. **Lisa** and **Gabriel**, for building the most amazing sauna. **Dimitrije**, for the Parliament Breaks. **Sepp**, for the time in Susbo.

Alex and **Ortrud**, for the BBQs, skiing trips, and your infectious passion for outdoor activities. **Paul**, for your unwavering support, especially during the final days of Kappa writing. **Michel**, for your company during the lysimeter project. **Sanne**, for your reminders of deadlines, for booking transportation and accommodation at just the right times, for speaking up when needed, and for reading my Kappa and providing real, valuable feedback. **Marc**, for helping me build my home for the months ahead. **Verena** and **Gabriel**, for making sure I found time to do what I truly enjoy. **Sharon**, for introducing me to the best party in the world. **Heiko** - I find it difficult to put into words what I'd like to say here. Even scratching the surface of my gratitude would *"exceed the scope of this"*. I am truly fortunate to have a friend like you. **Spezi -** the amber nectar, the elixir of life!

Finally, to **my parents**, **Inga** and **Peter**, for their lifelong support and for encouraging me to embark on adventures like this one.

Thank you all for being part of this journey.

I

Environmental Science & Technology

pubs.acs.org/est

Article

Decontamination and Surface Analysis of PFAS-Contaminated Fire Suppression System Pipes: Effects of Cleaning Agents and Temperature

Björn Bonnet,* Matthew K. Sharpe, Gulaim Seisenbaeva, Leo W. Y. Yeung, Ian Ross, and Lutz Ahrens

Cite This: *Environ. Sci. Technol.* 2025, 59, 2222−2232

Read Online

ACCESS | Metrics & More | Article Recommendations | Supporting Information

ABSTRACT: Per- and polyfluoroalkyl substances (PFAS)-containing firefighting foam have been used in stationary fire suppression systems for several decades. However, there is a lack of research on how to decontaminate PFAS-contaminated infrastructure and evaluate treatment efficiency. This study assessed the removal of PFAS from stainless steel pipe surfaces using different cleaning agents (tap water, methanol, and aqueous solutions containing 10 and 20 wt % of butyl carbitol (BC)) at different temperatures (20 °C, 40 °C, and 70 °C). The content of the remaining fluorine (F)-containing compounds on the pipe surfaces was evaluated for the first time using time-of-flight elastic recoil detection (ToF-ERD). The results showed that a 20% BC aqueous solution heated to 70 °C removed up to 40 $\mu g/cm^2$ ∑PFAS from surfaces via soaking (targeted analysis). Treatment with 20% BC was 2- to 8-fold more effective than tap water at 70 °C and 10- to 20-fold more effective than tap water at 20 °C. Total fluorine analysis determined by combustion ion chromatography showed a 2- to 8-fold higher F-equivalent compared to targeted analysis in the cleaning solution after treatment, indicating the presence of a significant amount of polyfluoroalkyl PFAS. Surface analysis with ToF-ERD confirmed partial F removal from pipe surfaces throughout consecutive soaking intervals, with residual F remaining on pipe surfaces after treatment, leaving the risk of PFAS rebound into F-free firefighting foams. Furthermore, supramolecular assemblies of PFAS with at least 70 PFOS molecules/nm^2 were identified by ToF-ERD on pipe interior surfaces.

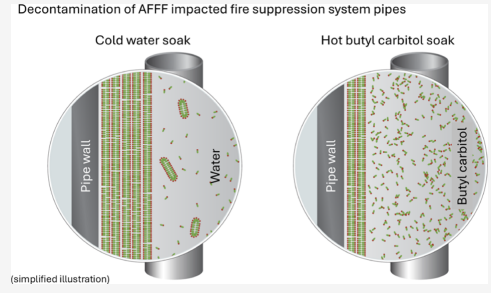

KEYWORDS: *Per- and polyfluoroalkyl substances, AFFF, foam transition, desorption, rebound effect, surfactant-surface interactions, supramolecular assemblies, butyl carbitol*

INTRODUCTION

Per- and polyfluoroalkyl substances (PFAS) are a group of synthetic chemicals that have some unique physical-chemical properties, such as chemical and thermal stability, resulting in extreme environmental persistence.[1−4] This has led to ubiquitous detection in different environmental matrices[5−12] and adverse health effects due to human exposure.[13] In general, PFAS are characterized by containing perfluorinated carbons,[14] which may form perfluoroalkyl chains of different lengths and may contain differing polar functional groups.[15] PFAS mass production started in the 1930s[16] and was subsequently applied in numerous industrial and consumer products,[17−20] and fluorinated firefighting foams, such as fluoroprotein foams and aqueous film-forming foams (AFFFs).[1,21−25] Different AFFF products contain a wide range of PFAS, such as legacy PFAS like perfluorooctanesulfonic acid (PFOS), perfluorooctanoic acid (PFOA), and novel polyfluoroalkyl precursors which may be zwitterionic, cationic, and anionic.[26−30]

Releases of fluorinated foams for extinguishment of Class B flammable liquid fires at airports, oil refineries, military bases, and during practice use at fire-training facilities are a major source of PFAS entering the environment.[6,21,22,28,29,31,32] AFFF is also applied in stationary sprinkler systems, which consist of storage tanks for AFFF concentrate, foam proportioners, vast pipe networks, and sprinkler heads.[33] Recurring release of fluorinated firefighting foams in suppression system testing or accidental discharge can lead to contamination of fire suppression infrastructure with PFAS.

Due to increasingly stringent regulatory guidelines being enacted, fluorinated firefighting foams are progressively being replaced with fluorine-free foams (FFF, which we refer to as F3 foams).[34−39] The European Union (EU) published a

Received: September 6, 2024
Revised: January 10, 2025
Accepted: January 13, 2025
Published: January 23, 2025

https://doi.org/10.1021/acs.est.4c09474
Environ. Sci. Technol. 2025, 59, 2222−2232

regulation that will come into full force on 4th July, 2025, banning "C_8" foams with regulatory limits of 25 μg/L for PFOA and 1,000 μg/L for PFOA precursors[34] and "C_9−C_{14}" foams, with regulatory thresholds for $\sum C_9$−C_{14} perfluorocarboxylic acids (PFCAs) at 25 μg/L and 260 μg/L for C_9−C_{14} PFCA precursors.[40] However, these guideline values are likely to be breached even by using F3 foam with old infrastructure, since PFAS may have adsorbed to the inner surfaces of the fire suppression infrastructure[33] and will potentially leach out and get into F3 foams. PFAS concentrations of up to 1.6 g/L have been observed in F3 foams without sufficient decontamination of fire suppression systems.[41]

Decontamination procedures and techniques on fire suppression infrastructure (e.g., pipework, steel and synthetic storage tanks, hoses) have been reported in peer-reviewed literature,[33,42,43] nonpeer- reviewed literature, technical reports,[44−47] and webinars.[48] Multiple cleaning agents, such as tap water (TAP), TAP-solvent mixtures with other additives, glycols, and proprietary commercially available products, were tested for their potential PFAS removal from contaminated infrastructure. In general, PFAS removal was higher for solvent- or glycol-based solutions and proprietary products as compared to TAP.[42−48] Adjustment of pH and increased temperature also showed positive effects on PFAS removal.[43] When removing PFAS from the walls of fire suppression system infrastructure, one issue encountered is described as the rebound effect.[43,47] This phenomenon refers to the observed increase in PFAS concentrations in cleaning agents, TAP, or F3 foam after an initial PFAS reduction during reagent flushes used for decontamination. This rebound effect demonstrates that a significant mass of residual PFAS remains associated with the interior surfaces of fire suppression infrastructure and that a retention mechanism that promotes surface storage of PFAS must exist. The formation of supramolecular structures formed by amphiphilic PFAS (fluorosurfactants) has been described in several articles in physical chemistry journals, which describe their self-organization into multilayered membranes with enhanced stability.[49,50] Removal of these structures is essential to confirm successful decontamination and minimize PFAS rebound before switching to F3 foams. To date, little is known about the effectiveness of cleaning agents with respect to the remaining PFAS mass on sprinkler system pipes after treatment.

Despite previous advances in the decontamination of fire suppression infrastructure, there are limitations associated with the techniques outlined above. For example, the use of proprietary cleaning agents is limited by a lack of discussion and understanding of the mechanism regarding the solvation of PFAS assemblies. Furthermore, chemical analysis of PFAS concentration in liquid cleaning agents used for decontamination does not consider the residual mass of PFAS that may remain on the pipework surfaces, resulting in insufficient evidence to confirm effective decontamination. Therefore, credible chemical analytical methods are required to assess the PFAS concentrations on the inner surfaces of fire suppression systems for coverage of PFAS.

In this study, we aim to investigate the effectiveness of butyl carbitol (BC) (CAS number: 112−34−5, Merck, Germany), commonly used as an effective stabilizing solvent for PFAS[23,25] in AFFF formulations, at concentrations of 10 and 20 mass% (m.%) in aqueous solution. The performance of BC was compared to that of TAP and methanol (MeOH) in removing adsorbed PFAS from AFFF-contaminated sprinkler system pipes. We also assessed the effect of temperature elevations in incubation experiments at 20 °C, 40 °C, and 70 °C. Furthermore, we conducted a quantitative analysis of the surfaces and approximately the upper 200 nm of AFFF-impacted stainless steel pipes, assessing their elemental concentration before, during, and after treatment by using time-of-flight elastic recoil detection (ToF-ERD) to identify any remaining PFAS mass on the pipe surfaces.

MATERIAL AND METHODS

Selection of AFFF-Contaminated Pipe Sections. The pipe sections used in this experiment were decommissioned stainless steel (316L) fire suppression system pipes from a large industrial production site in Uppsala, Sweden. The fire suppression system comprises a vast network across the entire company premises. Decommissioning took place in multiple sections, but there is no record of where the pipes are from in the system. The pipe diameter range (3.9−5.7 cm) supports the conclusion that they were positioned on the foam side rather than the AFFF concentrate side of the fire suppression system. The pipes were in use with PFAS-containing AFFF for two to three decades. The usage of four different AFFF concentrates, produced by electrochemical fluorination (ECF) and fluorotelomer (FT)-based products, has been documented. Furthermore, several releases of AFFF in different parts of the fire suppression system have occurred and might have contributed to different PFAS loadings in both concentration and composition. After ultrasonication-supported extraction using MeOH of nine pipe sections (A−J), three pipe sections with the highest PFAS levels were selected for further experiments (F, H, and I). The three pipe sections were characterized using scanning electron microscopy (SEM) (for details see Text S1, Figure S1, and Table S1).

Experimental Design—Soaking Experiment. In the soaking experiment, pipe sections were incubated in 500 and 1000 mL polypropylene (PP) containers filled with four different cleaning solutions separately, and they were tested at three different temperatures (room temperature (20 °C), 40°C, and 70 °C) (Figure 1). The four different cleaning solutions were: (i) pure TAP, (ii) TAP containing 10 mass% BC (BC10), (iii) TAP containing 20 mass% BC (BC20), and

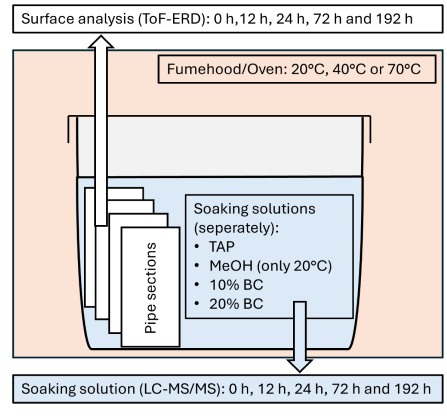

Figure 1. Illustration of the experimental design of the cleaning solution soaking experiment.

https://doi.org/10.1021/acs.est.4c09474
Environ. Sci. Technol. 2025, 59, 2222−2232

(iv) pure MeOH (LiChrosolv, hypergrade for LC-MS, Merck, Germany). MeOH was only used at 20 °C. For this, pipes were cut into similarly sized quarters using a metal bandsaw (Meec Tools, Metal bandsaw 230 V, 1100 W) and angle grinder (Makita, DGA521, 18 V). Due to different dimensions in length (60 cm −100 cm) and diameter (3.9 cm −5.7 cm) of the initial pipe, the pipe sections used for the soaking experiment differed in size (38−68 cm^2) and, therefore, in AFFF-contaminated area as well (Text S2 and Table S2). Importantly, only pipe sections of the same initial pipe were put together in a PP container. Pipe sections of each pipe were prepared for different combinations of treatment solution and temperature scenarios, representing experimental triplicates (Table S2). After 12 h of the experiment, the pipe sections were removed from the container and put into another container filled with a fresh soaking solution of the same kind, volume, and temperature. This exchange was repeated at 24 and 72 h after the start of the experiment. After 8 days of soaking, the experiment was stopped by removing all pipe sections from their containers. This yielded a total of five time points (0 h, 12 h, 24 h, 72 h, and 192 h) for each pipe section, soaking solution, and temperature. PFAS concentration was determined in the aqueous solution for each time point separately. A rebound experiment was performed after the 8-day soaking experiment. Pipe sections H and I were air-dried and put into 1 L polyethylene freezer zip bags, and stored in darkness for 4 months at 20 °C. Subsequently, the pipe sections were individually incubated in TAP for 7 days at 20 °C, and TAP was analyzed for PFAS.

PFAS Target Analysis. A total of 24 PFAS (Text S3) were analyzed, including 11 C_3−C_{13} PFCAs (PFBA, PFPeA, PFHxA, PFHpA, PFOA, PFNA, PFDA, PFUnDA, PFDoDA, PFTriDa, PFTeDA), seven C_4−C_{10} PFSAs (PFBS, PFPeS, PFHxS, PFHpS, PFOS, PFNS, PFDS), three FT-sulfonates (4:2 FTSA, 6:2 FTSA, and 8:2 FTSA), *N*-methyl- and ethyl-perfluorooctane sulfonamido acetic acid (Me-FOSAA, Et-FOSAA), and perfluorooctane sulfonamide (FOSA). Nineteen mass-labeled internal standards (IS) were used (Wellington Laboratories MPFAC-24 mixture), including, $^{13}C_4$−PFBA, $^{13}C_5$−PFPeA, $^{13}C_5$−PFHxA, $^{13}C_4$−PFHpA, $^{13}C_8$−PFOA, $^{13}C_9$−PFNA, $^{13}C_6$−PFDA, $^{13}C_7$−PFUnDA, $^{13}C_3$−PFDoDA, $^{13}C_2$−PFTeDA, $^{13}C_3$−PFBS, $^{13}C_3$−PFHxS, $^{13}C_8$−PFOS, $^{13}C_2$−4:2 FTSA, $^{13}C_2$−6:2 FTSA, $^{13}C_2$−8:2 FTSA, $^{13}C_8$−FOSA, D_3−MeFOSAA, and D_5−EtFOSA.

All samples from the soaking experiments were prepared for direct injection analysis by ultraperformance liquid chromatography coupled to tandem mass spectrometry (UPLC-MS/MS) analysis (Sciex Triple Quad 3500 LC-MS/MS, USA) (for details, see Text in S3 and Smith et al).[51] Limits of detection and quantification, as well as method recoveries, are presented in Tables S3 and S4.

Total Oxidizable Precursor (TOP) Assay. To get better estimates of total PFAS concentration in the samples, a TOP assay was performed for samples of the first soaking interval (12 h) on all pipe sections (F, H, and I). Due to the inhibition of PFAS oxidation in the presence of BC, samples containing BC were not included for the TOP assay (for details, see Text S4 and Tables S5−S7). TOP assays were performed in accordance with the originally proposed conditions (60 mM $K_2O_8S_2$/150 mM NaOH).[52] MeOH samples were evaporated to dryness under an N-stream and reconstituted in 1 mL of Milli-Q-water. The volume of sample, oxidant, base, and acid neutralization, as well as pH measurements throughout oxidation, are reported in Tables S8 and S9.

Total Fluorine (TF) Analysis. Due to the inhibition of PFAS precursor oxidation in the TOP assay by BC (see Text S6), total fluorine (TF) analysis was performed to get an insight into how much unrecognized PFAS is present in the samples using a combustion ion chromatography (CIC) system (for details, see Sections S6 and S7) for future experiments. Pipe section I was selected based on the results of the target analysis that showed the highest PFAS concentrations in the first time interval.

Surface Analysis with Time-of-Flight Elastic Recoil Detection Analysis (ToF-ERD). ToF-ERD analysis was used for elemental analysis of surfaces.[53] These data provide accurate measurements for every element that is present on the surface to depths between 100 and 200 nm. The elements of interest for our investigations were carbon (C) and fluorine (F), as these two elements are the predominant elements in PFAS molecules, and iron (Fe), which is the major component of stainless steel (for details, see Section S8 and Figure S2). ToF-ERD measurements were done on pipe section H.

Statistical Analysis. A repeated measures ANOVA was performed using time points (12, 24, 72, and 192 h), temperatures (20 °C, 40 °C, and 70 °C), and treatment solutions (TAP, BC10, and BC20) as fixed factors, including all interactions. MeOH treatment was not considered since it was used only within the 20 °C scenario. Differences were checked for the treatment solutions and temperatures. The statistical analysis was performed in R version 4.3.2.[54]

RESULTS AND DISCUSSION

Kinetics of PFAS Removal and Rebound Effect. PFAS desorption occurred predominantly within the initial soaking interval of 12 h, removing, on average, 68% ± 22% (minimum average: 40% for TAP 20 °C; maximum average: 99% for MeOH 20 °C) with respect to the $\sum_{24}$PFAS after 192 h. Additional desorption of $\sum_{24}$PFAS in the following time intervals was limited to 13% ± 8% (24 h), 11% ± 8% (72 h), and 8% ± 8% (192 h) (see also Figure S3 and Table S10). PFOS was the most abundant single compound measured in the soaking solutions, with an average of 76% ± 22% of $\sum_{24}$PFAS, followed by PFOA (10% ± 14%), 6:2 FTSA (6% ± 8%), PFHxS (5% ± 5%), 8:2 FTSA (3% ± 5%), and PFHxA (2% ± 2%) across all treatment solutions (TAP, MeOH, BC10, and BC20) and temperatures (20 °C, 40 °C, and 70 °C). The high contribution of PFOS indicates that the sprinkler system pipes used in our experiment were predominantly impacted by 3M AFFF formulations (e.g., 3M Light Water).[55] The presence of 6:2 FTSA and unknown precursors suggests that the pipes were also impacted by FT-based AFFF formulations.[26,55] Desorption of PFAS generally followed chain length and headgroup-dependent trends (for details, see Sections S10, S11 and Figures S4 and S5).

The 7-day rebound test using TAP (see Section S12 and Figure S5) showed that in most cases, ∑PFAS concentrations in rebound TAP were higher than in the respective soaking solution after 192 h during the soaking experiment. Furthermore, ∑PFAS concentrations in the rebound test were lower for BC20 solutions and scenarios at 70 °C compared to TAP and BC10 at 20 and 40 °C. In the case of TAP (20 °C), ∑PFAS concentrations in the rebound test were in the same range as they were in the initial soaking interval (12 h). The rebound experiment showed that the continuous

https://doi.org/10.1021/acs.est.4c09474
Environ. Sci. Technol. 2025, 59, 2222−2232

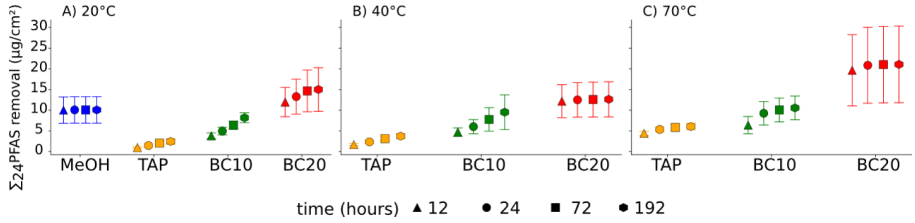

Figure 2. PFAS removal ($\mu g/cm^2$) from stainless steel pipes using methanol (MeOH) (only 20 °C), tap water (TAP), 10 wt % butyl carbitol in TAP (BC10), and 20 wt % BC in TAP (BC20), respectively, during soaking experiments at A) 20 °C, B) 40 °C, and C) 70 °C. Data points represent average concentrations (n = 3), with standard error as error bars.

drop of ∑PFAS concentrations throughout the soaking experiment did not reflect complete PFAS removal from the pipe surfaces and that comparisons between high ∑PFAS concentrations in the initial cleaning step to low(er) ∑PFAS concentrations in following cleaning steps are not a plausible way to demonstrate successful decontamination. Credible rebound tests, in which a previously purified system was exposed to TAP or F3 foam for numerous days, have only been investigated in a few studies. Lang and Devine[46] found PFAS rebound into TAP and F3 foam during a 3-day exposure following a final short-term water flush in which no PFAS were detected. Dahlbom et al.[43] assessed PFAS rebound into TAP after decontamination was performed and found gradually increasing PFAS concentrations over a period of 157 days. Accordingly, Nguyen et al.[47] performed a 6-week rebound experiment using TAP following decontamination and observed steadily increasing PFAS concentrations.

Effect of Temperature on Removal of PFAS. Effects of temperature on PFAS removal are shown in Figure 2 for the average values for three independent pipe sections (for single pipe sections, see Section S12 and Figure S5). Increased temperature generally increased the removal efficiency of PFAS for the same treatment solution steadily. For TAP, the $\sum_{24}$PFAS removal increased by 150% from 2.4 $\mu g/cm^2$ (20 °C) to 6 $\mu g/cm^2$ (70 °C) at 192 h. Statistically significant differences were observed for TAP (20 °C) and TAP (70 °C) at 12 h ($p < 0.05$) and 24 h ($p < 0.05$). For BC10, the $\sum_{24}$PFAS removal increased by 30% from 8.1 $\mu g/cm^2$ (20 °C) to 10.5 $\mu g/cm^2$ (70 °C) at 192 h. For BC20, the $\sum_{24}$PFAS removal increased by 40% from 15 $\mu g/cm^2$ (20 °C) to 21 $\mu g/cm^2$ (70 °C) at 192 h. Accumulated PFAS concentration for BC20 (40 °C) was 16% lower than for BC20 (20 °C) after 192 h, which can be related to measurement uncertainty and heterogeneous distribution of PFAS on pipe sections. For MeOH, only 20 °C was tested showing a $\sum_{24}$PFAS removal of 10 $\mu g/cm^2$ at 192 h. Increased temperature showed increasing solubility of PFAS assemblies from surfaces into solution, which indicates that supramolecular aggregates were solubilized more efficiently into smaller structures and monomers with increasing temperatures. Below the Krafft-point T_K and at sufficiently high surfactant concentrations, surfactants will neither be present as micelles nor as monomers but assemble in various crystalline aggregates, e.g., bilayers.[56] Above T_K, surfactants' solubility increases, and aggregates "melt" into monomers below the critical micelle concentration (CMC) or micelles above CMC. Our results align well with this since higher PFAS concentrations were observed in solutions at elevated temperatures. For Na-PFOS, up to 75 °C and 8.5 mmol/L for T_K and CMC, respectively, have been reported.[57] Temperatures in our experiments ranged within and close to possible T_K for PFOS-based surfactants; however, concentrations measured in our solutions were well below the CMCs (0.02 mmol/L for Na-PFOS),[57] and thus T_K has not been reached and micelle formation in solution did not occur. A similar observation was made previously,[58] where single-chain perfluoroalkyl surfactants formed multilamellar and multilayered vesicles of several hundred nm in size at close to ambient temperature. However, at 40 °C, the structures were broken down into much smaller vesicles between 30−100 nm, and at 70 °C, into globules of 100 nm and fibers of 1−10 nm. Our measurements align to some extent with a previous study,[33] which tested a commercially available and proprietary product for the decontamination of fire suppression systems (Fluoro Fighter, FF) at temperatures of 22 °C, 40 °C, and 80 °C. Their results showed that PFAS were removed from stainless steel pipes into solution using FF and ∑PFAS concentrations increased from ∼4 $\mu g/cm^2$ to ∼6 $\mu g/cm^2$ between 22 and 40 °C, whereas they decreased from 6 $\mu g/cm^2$ to 5 $\mu g/cm^2$ between 40 and 80 °C. Lower removals at 80 °C were attributed to heterogeneity in PFAS distribution on pipe surfaces. Dahlbom et al.[43] compared the removal of PFAS at 22 and 50 °C for a cleaning solution consisting of 44.9% MQ water, 44.9% isopropanol (IPA), and 0.2% sodium hydroxide (25 wt % in MQ water) and found that PFAS removal was slightly higher at 50 °C (∼23 $\mu g/cm^2$) compared to 22 °C (∼19 $\mu g/cm^2$) for galvanized steel but lower at 50 °C (∼195 ng/cm^2) compared to 20 °C (∼220 ng/cm^2) for stainless steel. Nguyen et al.[47] tested TAP, a solution containing TAP, propylene glycol (20%), ethanol (10%), and acetic acid (2%) (CSM solution), and a proprietary cleaning agent at 22 and 50 °C in flow-through experiments on 304 stainless steel pipes. In the flow-through experiments, they found that heating increased PFAS removal from 160 to 240 ng/cm^2, from 250 to 360 ng/cm^2, and from 290 to 450 ng/cm^2 for the proprietary solution, TAP, and CSM solution, respectively. Temperature effects in the present study were smaller between 20 and 40 °C than they are between 40 and 70 °C, which suggests that temperatures near T_K should be pursued for the most optimal conditions for PFAS removal.

Comparison of Cleaning Solutions for Removal of PFAS. In general, the removal of $\sum_{24}$PFAS on the pipe surfaces increased for the solutions in the following order: TAP < BC10 (<MeOH) < BC20. The average increase between TAP and BC10, and between BC10 and BC20, accounted for 154% ± 66% and 71% ± 29%, respectively (Figure 2). We observed statistically significant differences for $\sum_{24}$PFAS between TAP and BC20 at 20 °C (12 h: $p < 0.0005$; 24 h: $p < 0.001$; 72 h: $p < 0.005$; 192 h: $p < 0.005$), at 40 °C (12 h: p

https://doi.org/10.1021/acs.est.4c09474
Environ. Sci. Technol. 2025, 59, 2222−2232

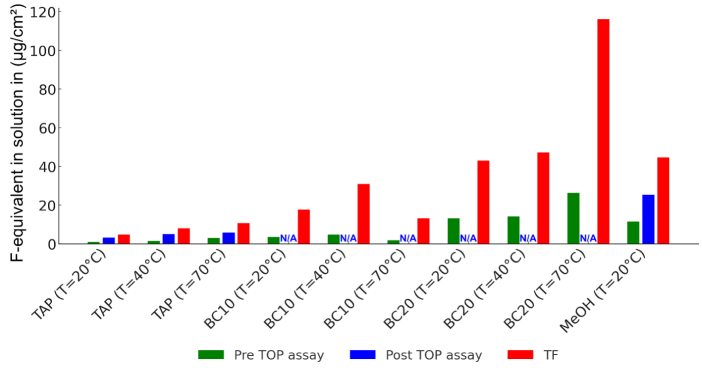

Figure 3. F-equivalent concentrations for target analysis before the TOP assay (green) and after the TOP assay (blue) via LC-MS and total fluorine (TF) analysis via CIC (red). Measurements only for pipe I. NA = not available.

< 0.005; 24 h: $p < 0.05$; 72 h: $p < 0.05$), and at 70 °C (12 h: $p < 0.05$). Further statistically significant differences were observed for TAP and BC10 at 20 °C (12 h: $p < 0.05$; 24 h: $p < 0.05$; 192 h: $p < 0.05$).

The dissolution effects for surfactants in the presence of pure alcohol or due to the addition of alcohol to an aqueous solution are related to the ability of alcohols to increase the surface activity and van der Waals forces between surfactant molecules, thus lowering the CMC of surfactants.[59] The longer the chain length of the alcohol, the larger the decrease of the CMC.[60,61] The decrease of CMC has also been shown to be dependent on the number and type of polar groups associated with the alcohol.[62] Both effects of chain length and polar groups within the alcohol molecule can explain why BC is more effective at 20% concentration than pure MeOH, due to the longer molecular chain and more polar sites within the molecule. Further confirmation of this can be concluded from the log *n*-octanol−water partition coefficient (K_{OW}) which is lower for MeOH ($K_{OW} = -0.77$) compared to BC (log K_{OW} = 0.56), indicating a higher affinity of PFAS with BC. Dong et al.[63] demonstrated a CMC for PFOA in an aqueous solution of 26.5 mM, which was reduced to 14.2 mM and 13 mM with 10% and 20% addition of ethanol, respectively. The large initial reduction of CMC for 10% ethanol in water was attributed to the cosolubilization of ethanol molecules into the PFOA micelle, resulting in reduced surface charge density and lower headgroup repulsion at the micelle surface (cosurfactant effect). On the other hand, the lower reduction of CMC between 10% and 20% addition of ethanol in water was explained by the cosolvent effect, which, in addition to the cosurfactant effect, is influenced by increases in CMC due to disruption of the water structure network, resulting in a reduction in the hydrophobic effect, and thereby the micelle size and intermicellar distance between micelles decrease. As mentioned in the previous chapter, "Effects of temperature on removal of PFAS", it is not suggested that micelle formation is taking place in solution; however, it is suggested that factors leading to the reduction of micelle size will contribute to dissolve formations on surfaces. Dong et al.[63] observed a reduction in micelle size by 34% and 55% in the presence of 10% and 20% ethanol (EtOH) in aqueous solution, respectively, which could promote the disruption of PFAS assemblies on the pipe surfaces and their subsequent dissolution. Giles et al.[64] reported similar effects for 6:2 FT-sulfonamide alkylbetaine (6:2 FTAB), a common constituent in FT-based AFFF formulations, in the presence of up to 0.5 wt % BC. They found 6:2 FTAB micelles to decrease in size in the presence of BC and reasoned that BC was incorporated into the 6:2 FTAB micelles' palisade layer. Similarly, as explained above for MeOH, BC is considered to have a higher potential for preventing PFAS aggregation than EtOH. In fact, BC is a major constituent in most AFFF formulations, serving as a solvent for fluorosurfactants and hydrogen surfactants to allow for storage stability and improved shelf life of AFFF concentrate.[23,25,65]

Comparison of Target PFAS Analysis with TOP Assay and TF. PFAS targeted analysis before the TOP assay was compared to targeted analysis after the TOP assay and TF (Figure 3). The reported F-equivalent concentrations are shown in the following order: targeted analysis before the TOP assay < targeted analysis after the TOP assay < TF. F-equivalent concentrations increased by a factor of 2−4 between targeted analysis before the TOP assay and targeted analysis after the TOP assay and by a factor of 2−8 between targeted analysis before the TOP assay and TF analysis. As shown in previous studies, ∑PFAS concentrations increased during the TOP assay due to the oxidation of unknown precursor PFAS,[52] which is further confirmed by the increased relative contribution of short-chain PFCAs ($<C_8$) between targeted analysis before the TOP assay (2% ± 3%) compared to targeted analysis after the TOP assay (46% ± 13%) (Section S12 and Figure S6).

The observed differences between the TOP assay and TF analysis could be related to factors, such as incomplete oxidation of precursor PFAS during the TOP assay,[66] incomplete recovery of long-chain PFCAs and PFSAs after oxidation[52,67−69] and the formation of ultrashort-chain PFCAs during oxidation.[69−72] For example, Patch et al.[70] have shown that perfluoropropionic acid (PFPrA) could account for up to 19% of ∑PFAS. Previous studies have also shown that the presence of other organic substances, which are present in AFFF, can inhibit PFAS oxidation,[73] as this study has shown for BC (see Table S6 and Text S4). The TOP assay experimental setup in this study does not allow for the correction of incomplete recoveries of long-chain PFCAs and PFSAs or other compounds, since no mass-labeled surrogates

https://doi.org/10.1021/acs.est.4c09474
Environ. Sci. Technol. 2025, 59, 2222−2232

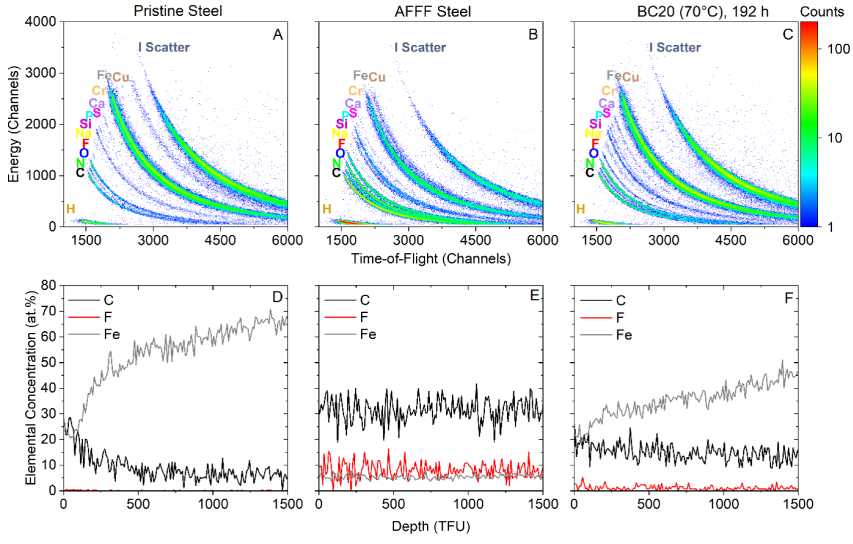

Figure 4. ToF-ERD histograms (top) and depth charts (bottom) for (A) and (D) exterior pipe (hereafter referred to as pristine stainless steel), (B,E) AFFF-impacted stainless steel pipe, and (C,F) pipe treated with BC20 at 70 °C after 192 h. Histograms represent the total elemental composition of the pipe surfaces. Curved plots are derived from velocity (*x*-axis) and energy (*y*-axis) measurements. Depth profiles show a selection of carbon (C), fluorine (F), and iron (Fe). Depth profiles indicate elemental concentrations (*y*-axis) with respect to the analytical depth (*x*-axis) of the ion beam (for details, see Text S13).

were introduced before oxidation.[70] Decomposition/mineralization of PFCAs by sulfate radicals due to decreasing pH[74] can be ruled out as the pH remained high (pH = 14) after oxidation (Table S9).

Surface Analysis of Sprinkler System Pipes by ToF-ERD. Surface analysis with ToF-ERD revealed interesting trends in F, C, and Fe as well as depth profiles between pristine steel, untreated AFFF-impacted pipe sections, and pipe sections after treatment (Figure 4, Section S13,Table S11 and Figures S7−S16). Despite the substantial PFAS removal from pipe sections by the most effective solution tested herein, BC20 70 °C, residual F remained on the pipe sections (Figure 4 C,F). After treatment by BC20 70 °C, F concentration was measured at 1.1 atomic % (hereafter at. %), which represents the lowest residual F concentration measured on pipe sections after treatment. The F concentration was consistently low within the depth profile (Figure 4F), whereas the Fe concentration increased from 20% at the surface (0 thin film units (TFU); representing an aerial unit of 10^{15} atoms per cm^2) to 45% at 1500 TFU. This means that the Fe was no longer covered as much by an AFFF layer compared to the untreated AFFF-impacted pipe. C concentration was relatively constant in the depth profile (on average 15 at. %), decreasing from 20 to 15 at. % at 1500 TFU for the BC20 (70 °C) treated pipes. For pristine stainless steel pipe (Figure 4 A,D), the F concentration ranged around the measurement detection limit of 0.1 atomic %, while Fe and C were measured with average concentrations of 52 at. % and 9.3 at. %, respectively. In the depth profile of the pristine stainless steel pipe, the Fe concentration increased from 20 to 65 at. % (average concentration of 52 at. %) and the C concentration decreased from 25 to 5 at. % (average concentration of 9 at. %) until the analytical depth limit of 1500 TFU. In the AFFF-contaminated untreated pipe sections (n = 5) (Figure 4B,E), the average F concentration was 4.8 at. % (3.4−8.0 at. %), while average concentrations for C and Fe were 28 at. % (25−32 at. %) and 12 at. % (5.5−20.7 at. %), respectively. The depth profile showed consistent detection of all three elements throughout the entire analytical depth. The differences in concentrations and depth profiling between the pristine and AFFF-impacted pipe were a result of a layer composed of PFAS covering the pipe surface. Detection of both F and C indicates the presence of fluorinated carbons on the AFFF-impacted pipe. The lower detection of Fe on the AFFF-impacted pipe compared to that of the pristine stainless steel pipe indicates that the Fe within the pipe was covered and thereby shielded from being detected at a higher intensity as for the pristine stainless steel pipe. Furthermore, the constant detected rates in the histograms and the depth profiles indicate that the AFFF layer is thicker than the analytical depth of the ion beam (1500 TFU).

Further results of F measurements on the treated pipes at 70 °C were consistent with results from the soaking experiment, showing decreasing F concentration remaining on pipe surfaces after 192 h, with 1.8 at. % for TAP (70 °C) and 1.7 at. % for BC10 (70 °C). Regarding the results at 20 and 40 °C, this trend did not strictly uphold for measurements at 40 and 20 °C (Section S13). Despite increasing F removal during soaking, measurements of F, C, and Fe concentrations throughout every treatment interval did not show a consistent stepwise decrease (F and C) or increase (Fe) between the initially measured concentrations on pipe sections and the concentrations in the consecutive time intervals (Table S12). Incoherent behavior in the concentration of all three elements analyzed is related to a nonhomogeneously and nonuniformly distributed AFFF layer on the initial pipe.

https://doi.org/10.1021/acs.est.4c09474
Environ. Sci. Technol. 2025, 59, 2222−2232

However, for all pipe sections after 192 h of treatment, F was detected on the pipe surface with an average of 2.1 at. % for TAP, 2.8 at. % for BC10, 2.2 at. % for MeOH, and 1.8 at. % for BC20, indicating that even after the most efficient treatment (BC20 70 °C), there was still an F-containing layer left beyond the analytical depth of the ion beam. Partial removal of the AFFF-associated layer was indicated not only by decreasing F detection but also from the Fe and C depth profiles comparing treated and untreated pipes (Figure 4). There was a statistically significant decreasing trend for F ($p < 0.0001$) and C ($p < 0.0001$) with increasing Fe concentration (Figure S17). Comparisons of F measurements on surfaces before and after 192 h of treatment allow one to estimate total F removal efficiencies. Based on the average F concentration (4.8 at. %) for five measurements of untreated pipe sections, the highest F removal efficiency was achieved for BC20 (70 °C) with 77 at. % total F removal, followed by 65 and 63 at. % for BC10 (70 °C) and TAP (70 °C). Due to the AFFF-associated layer still being present beyond the analytical depth, the reported F removal efficiencies are likely to be an overestimation.

Previous efforts by Lang et al.[33] identified PFAS assemblies on the pipe surfaces using scanning electron microscopy (SEM) and X-ray photoelectron spectroscopy (XPS) and revealed lower concentrations of elemental F on surfaces after treatment with FF (3 at. %−5 at. %) compared to TAP (7 at. %−17 at. %). However, SEM-XPS is very surface-sensitive, penetrating only the surface to a depth of 7−10 nm, and it cannot detect hydrogen (H). Therefore, the reported elemental concentrations should be seen as indicative. Dahlbom et al.[43] performed surface analysis by SEM electron-dispersive X-ray spectroscopy (EDX) and showed reductions of F-containing structures during treatment without further quantification. SEM-EDX has a penetration depth in the low μm range, which exceeds the AFFF-associated layer deep into the stainless steel. Elemental compositions are therefore skewed toward the elements of steel. Measurements of F are therefore considered semiquantitative.[43,75] ToF-ERD analysis surpasses the limitations regarding analytical depth, depth resolution, and incomplete elemental detection. The measurements by ToF-ERD are highly quantitative across the entire analyzed surface area of 12 mm^2 (Figure S18). The precision is highlighted by the calculation of the number of detected atoms of each element, which allows to draw conclusions about the structural properties of the AFFF-associated layer.

Measurements of PFAS Supramolecular Assemblies. Comparing the SEM image of the pipe exterior to the interior (Figure S1) reveals that the pipe interiors are coated with an amorphous solid mass (AFFF layer), while unexposed pipe surfaces comprise a flat cellular network that is common when imaging stainless steel.[76] Even though the SEM visualization does not reveal any precise depth measurements, differences in both bright and dark areas on the images indicate large differences in layer depth qualitatively, confirming the hypothesis of a nonhomogeneously and nonuniformly distributed AFFF layer across the pipe surfaces. Measurements of F using ToF-ERD provide evidence that these amorphous structures on the pipe interior appear to be supramolecular aggregates of PFAS because ToF-ERD measurements allow a quantitative estimation of the number of F atoms/nm^2 of the pipe surface within the measurement depth of 1500 TFU.

The estimated number of F atoms/nm^2 (see Section S16) for the untreated AFFF-impacted surface is 1200, whereas the number of F atoms/cm^2 for 20% BC (70 °C) is 163. Considering the AFFF layer mainly consists of PFOS, the number of PFOS molecules/cm^2 is 70.6 and 9.6 for the untreated pipe section and BC 20% (70 °C), respectively. The number of PFOS molecules per unit surface area for a monolayer of coverage has been estimated to range from 4 to 20 molecules/nm^2, depending on whether the long axis of the molecule is parallel (4 molecules) or normal (20 molecules) to the surface.[77] Assuming 20 PFOS molecules per cm^2, for a monolayer of PFOS to be present indicates that on the untreated pipe section, PFOS molecules must be present in an arrangement beyond that of a monolayer. Furthermore, the maximum PFOS concentration removed from surfaces in the soaking experiment (Pipe I, BC20 (70 °C), 12 h, Figure S4) was measured at 35 μg/cm^2, which corresponds to 421 PFOS molecules/nm^2. This is yet another indicator of PFOS being stored in multiple layers in supramolecular assemblies. The differences between the number of molecules/nm^2 estimated from the F concentration on the surfaces and the measurement in the soaking solution could be a result of the surface measurements being confined to 1500 TFU. The actual analytical depth goes beyond 1500 TFU; however, thereafter, hydrogen (H) measurements drop unrealistically, and C and oxygen (O) atoms overlap. This would lead to the elemental composition being skewed. The estimated number of F atoms/nm^2, stored in a three-dimensional arrangement, is therefore likely to be higher than the 70 molecules/nm^2 estimated above. Conversion of TFU into a metric scale is theoretically possible; however, it would lead to inaccuracies due to the unknown density of the AFFF layer. The ToF-ERD measurements do not provide information on the actual arrangement and/or orientation of molecules within these assemblies, and it is possible that molecules are not arranged perfectly in monolayers or bilayers but form tilted clusters.

Environmental and Practical Implications. The results from the soaking experiment showed that PFAS removal from surfaces with heated BC (70 °C) was 2- to 8-fold more effective than TAP (70 °C) and 10- to 20-fold more effective than TAP at 20 °C based on single pipe sections. Thus, both the cleaning solution composition and temperature are crucial parameters for the decontamination of infrastructure from PFAS. These data correlate with the surface analysis using ToF-ERD, which revealed the most remaining F on the pipe surfaces after TAP treatments, and even the most effective treatment solution (BC20 (70 °C)) did not remove all PFAS from surfaces, despite the decreasing concentration of removed PFAS into solution during repetitive soaking intervals. The results align with other studies,[43,47] highlighting the challenges of PFAS decontamination in fire suppression systems.

The static desorption experiment conducted herein does not necessarily reflect an actual decontamination scenario since flow-through setups are commonly used. Nguyen et al.[47] compared flow-through conditions to lab-scale batch incubation experiments involving shaking and found that PFAS removal was slightly higher in flow-through experiments as compared to the batch tests. They furthermore showed that surface attrition reduces the PFAS rebound substantially. Thus, in full-scale decontamination, surface attrition (wherever applicable), e.g., pressure washing, in combination with heated BC solution might achieve even higher removal efficiency. An advantage of BC in aqueous solution, compared to other cleaning agents, is that residues of the cleaning solution will not negatively impact the system, since both BC and TAP are

https://doi.org/10.1021/acs.est.4c09474
Environ. Sci. Technol. 2025, 59, 2222−2232

constituents of many AFFF and F3 foam products. Another advantage, compared to other solvents (e.g., MeOH or IPA), is that BC is associated with fewer hazards and precautionary statements under the GHS system,[78] which is relevant for work safety. Decontamination costs are difficult to predict, since they depend on factors, such as the size of the fire suppression system, PFAS composition, and accessibility of the infrastructure, among others. However, decontamination is typically more cost-efficient and sustainable than replacing the infrastructure.

When evaluating PFAS concentrations with respect to AFFF contamination, target PFAS measurements, especially with a limited number of PFAS quantified, are insufficient, and techniques, such as the TOP assay and TF analyses, accounting for precursor PFAS, should be employed.[79−81] The ToF-ERD data identified that the analysis of treatment solutions alone cannot provide evidence for successful decontamination of PFAS from fire suppression systems. Analysis of PFAS remaining on surfaces is required to determine whether decontamination has been successful to reflect the efficacy of treatment. Thus, measuring PFAS concentrations in solution does not reflect the mass of surface-bound PFAS remaining. Remaining PFAS on interior surfaces poses an ongoing risk of PFAS rebounding into F3 foams. PFAS rebound into F3 foams is expected to be greater than into TAP because many F3 foam products contain glycols in their formulations.[82−84] Data describing the PFAS content of F3 foams following different decontamination approaches are scarce. The concentrations of PFAS in F3 foams are likely to rise over the period as the F3 foams are placed into fire suppression systems that held fluorinated foams as a result of slow rebound. Therefore, sampling these foams for PFAS immediately after they are placed in a fire suppression system would be of little value. Regulatory limits concerning PFAS levels in any firefighting foam[34,39,40] could result in F3 foams eventually exceeding these levels as a result of insufficient decontamination, with 1.6 g/L of total PFAS detected in F3 foams one year after a double water rinsing.[41]

The combination of SEM and ToF-ERD data indicates that fluorinated supramolecular aggregates of PFAS exist on the interior pipe surfaces. These stable multilayered supramolecular forms of PFAS may account for the mass of PFAS calculated to be stored on the interior surfaces of the pipes. These multilayered structures represent a reservoir of PFAS that may delaminate over time and could account for the observed rebound effects. Regulators should take this into consideration when evaluating credible methods to prove decontamination.[85] Ultimately, to determine treatment efficiency, it is essential to determine the total PFAS mass on pipe surfaces. Even though ToF-ERD is a valuable method to determine the remaining F on pipe surfaces, further efforts are necessary to facilitate and accelerate the surface analysis of PFAS mass.

■ ASSOCIATED CONTENT

Supporting Information

The Supporting Information is available free of charge at https://pubs.acs.org/doi/10.1021/acs.est.4c09474.

Additional information on experimental setup, analytical methods (SEM, TOP assay, ToF-ERD), statistical analysis, and figures and tables complementing the analysis shown (PDF)

■ AUTHOR INFORMATION

Corresponding Author

Björn Bonnet − *Department of Aquatic Sciences and Assessment, Swedish University of Agricultural Sciences, Uppsala 75651, Sweden;* orcid.org/0009-0008-5427-8637; Email: bjorn.bonnet@slu.se

Authors

Matthew K. Sharpe − *Surrey Ion Beam Centre, University of Surrey, Guildford GU2 7XH, U.K.*

Gulaim Seisenbaeva − *Department of Molecular Sciences, Swedish University of Agricultural Sciences, Uppsala 75651, Sweden*

Leo W. Y. Yeung − *SMTM Research Centre, School of Science and Technology, Örebro University, Örebro 70182, Sweden;* orcid.org/0000-0001-6800-5658

Ian Ross − *CDM Smith, San Francisco, California 94104 USA, United States*

Lutz Ahrens − *Department of Aquatic Sciences and Assessment, Swedish University of Agricultural Sciences, Uppsala 75651, Sweden;* orcid.org/0000-0002-5430-6764

Complete contact information is available at: https://pubs.acs.org/10.1021/acs.est.4c09474

Notes

The authors declare no competing financial interest.

■ ACKNOWLEDGMENTS

This project has received funding from the European Union's Horizon 2020 research and innovation program under Marie Skłodowska-Curie grant agreements No. 860665 (PERFORCE3 Innovative Training Network) and No. 824096 (RADIATE). The authors would further like to thank Claudia van Brömssen for her support in statistical analysis.

■ REFERENCES

(1) Lemal, D. M. Perspective on fluorocarbon chemistry. *J. Org. Chem.* **2004**, *69* (1), 1−11.

(2) Krafft, M. P.; Riess, J. G. Selected physicochemical aspects of poly-and perfluoroalkylated substances relevant to performance, environment and sustainability—Part one. *Chemosphere* **2015**, *129*, 4−19.

(3) Erkoç, Ş.; Erkoç, F. Structural and electronic properties of PFOS and LiPFOS. *J. Mol. Struct.:THEOCHEM* **2001**, *549* (3), 289−293.

(4) Simons, J. H. Fluorocarbons. *Sci. Am.* **1949**, *181* (5), 44−47.

(5) Hale, S. E.; Arp, H. P. H.; Slinde, G. A.; Wade, E. J.; Bjørseth, K.; Breedveld, G. D.; Straith, B. F.; Moe, K. G.; Jartun, M.; Høisæter, Å. Sorbent amendment as a remediation strategy to reduce PFAS mobility and leaching in a contaminated sandy soil from a Norwegian firefighting training facility. *Chemosphere* **2017**, *171*, 9−18.

(6) Høisæter, Å.; Pfaff, A.; Breedveld, G. D. Leaching and transport of PFAS from aqueous film-forming foam (AFFF) in the unsaturated soil at a firefighting training facility under cold climatic conditions. *J. Contam. Hydrol.* **2019**, *222*, 112−122.

(7) Benskin, J. P.; Li, B.; Ikonomou, M. G.; Grace, J. R.; Li, L. Y. Per- and polyfluoroalkyl substances in landfill leachate: patterns, time trends, and sources. *Environ. Sci. Technol.* **2012**, *46* (21), 11532−11540.

(8) Yan, H.; Zhang, C.-J.; Zhou, Q.; Chen, L.; Meng, X.-Z. Short- and long-chain perfluorinated acids in sewage sludge from Shanghai, China. *Chemosphere* **2012**, *88* (11), 1300−1305.

(9) Gallen, C.; Eaglesham, G.; Drage, D.; Nguyen, T. H.; Mueller, J. A mass estimate of perfluoroalkyl substance (PFAS) release from

Australian wastewater treatment plants. *Chemosphere* **2018**, *208*, 975−983.
(10) White, N. D.; Balthis, L.; Kannan, K.; De Silva, A. O.; Wu, Q.; French, K. M.; Daugomah, J.; Spencer, C.; Fair, P. A. Elevated levels of perfluoroalkyl substances in estuarine sediments of Charleston, SC. *Sci. Total Environ.* **2015**, *521*, 79−89.
(11) Martin, J. W.; Mabury, S. A.; Solomon, K. R.; Muir, D. C. Bioconcentration and tissue distribution of perfluorinated acids in rainbow trout (Oncorhynchus mykiss). *Environ. Toxicol. Chem.* **2003**, *22* (1), 196−204.
(12) Kelly, B. C.; Ikonomou, M. G.; Blair, J. D.; Surridge, B.; Hoover, D.; Grace, R.; Gobas, F. A. Perfluoroalkyl contaminants in an Arctic marine food web: trophic magnification and wildlife exposure. *Environ. Sci. Technol.* **2009**, *43* (11), 4037−4043.
(13) Worley, R. R.; Moore, S. M.; Tierney, B. C.; Ye, X.; Calafat, A. M.; Campbell, S.; Woudneh, M. B.; Fisher, J. Per-and polyfluoroalkyl substances in human serum and urine samples from a residentially exposed community. *Environ. Int.* **2017**, *106*, 135−143.
(14) Wang, Z.; Buser, A. M.; Cousins, I. T.; Demattio, S.; Drost, W.; Johansson, O.; Ohno, K.; Patlewicz, G.; Richard, A. M.; Walker, G. W.; et al. A New OECD Definition for Per- and Polyfluoroalkyl Substances. *Environ. Sci. Technol.* **2021**, *55* (23), 15575−15578.
(15) Buck, R. C.; Franklin, J.; Berger, U.; Conder, J. M.; Cousins, I. T.; De Voogt, P.; Jensen, A. A.; Kannan, K.; Mabury, S. A.; van Leeuwen, S. P. Perfluoroalkyl and polyfluoroalkyl substances in the environment: terminology, classification, and origins. *Integr. Environ. Assess. Manage.* **2011**, *7* (4), 513−541.
(16) Hendricks, J. O. Industrial fluorochemicals. *Ind. Eng. Chem. Fundam.* **1953**, *45* (1), 99−105.
(17) Langberg, H. A.; Arp, H. P. H.; Breedveld, G. D.; Slinde, G. A.; Høiseter, Å.; Grønning, H. M.; Jartun, M.; Rundberget, T.; Jenssen, B. M.; Hale, S. E. Paper product production identified as the main source of per-and polyfluoroalkyl substances (PFAS) in a Norwegian lake: Source and historic emission tracking. *Environ. Pollut.* **2021**, *273*, 116259.
(18) Lang, J. R.; Allred, B. M.; Peaslee, G. F.; Field, J. A.; Barlaz, M. A. Release of per-and polyfluoroalkyl substances (PFASs) from carpet and clothing in model anaerobic landfill reactors. *Environ. Sci. Technol.* **2016**, *50* (10), 5024−5032.
(19) Trier, X.; Granby, K.; Christensen, J. H. Polyfluorinated surfactants (PFS) in paper and board coatings for food packaging. *Environ. Sci. Pollut. Res.* **2011**, *18*, 1108−1120.
(20) Lin, A. Y.-C.; Panchangam, S. C.; Lo, C.-C. The impact of semiconductor, electronics and optoelectronic industries on downstream perfluorinated chemical contamination in Taiwanese rivers. *Environ. Pollut.* **2009**, *157* (4), 1365−1372.
(21) Moody, C. A.; Field, J. A. Determination of perfluorocarboxylates in groundwater impacted by fire-fighting activity. *Environ. Sci. Technol.* **1999**, *33* (16), 2800−2806.
(22) Titaley, I. A.; Khattak, J.; Dong, J.; Olivares, C. I.; DiGuiseppi, B.; Lutes, C. C.; Field, J. A. Neutral per-and polyfluoroalkyl substances, butyl carbitol, and organic corrosion inhibitors in aqueous film-forming foams: implications for vapor intrusion and the environment. *Environ. Sci. Technol.* **2022**, *56* (15), 10785−10797.
(23) Upadhayay, H. R.; Joynes, A.; Collins, A. L. 13C dicarboxylic acid signatures indicate temporal shifts in catchment sediment sources in response to extreme winter rainfall. *Environ. Chem. Lett.* **2024**, *22* (2), 499−504.
(24) Rakowska, J. In Best practices for selection and application of firefighting foam. In *MATEC Web of Conferences*, EDP Sciences, 2018, pp 00014.
(25) Peshoria, S.; Nandini, D. Understanding Aqueous Film-forming Foam Components. In *Perfluoroalkyl Substances*. Améduri, B., Ed.; The Royal Society of Chemistry, 2022, pp. 357−387.
(26) Place, B. J.; Field, J. A. Identification of novel fluorochemicals in aqueous film-forming foams used by the US military. *Environ. Sci. Technol.* **2012**, *46* (13), 7120−7127.
(27) D'Agostino, L. A.; Mabury, S. A. Identification of novel fluorinated surfactants in aqueous film forming foams and commercial surfactant concentrates. *Environ. Sci. Technol.* **2014**, *48* (1), 121−129.
(28) Baduel, C.; Mueller, J. F.; Rotander, A.; Corfield, J.; Gomez-Ramos, M.-J. Discovery of novel per-and polyfluoroalkyl substances (PFASs) at a fire fighting training ground and preliminary investigation of their fate and mobility. *Chemosphere* **2017**, *185*, 1030−1038.
(29) Barzen-Hanson, K. A.; Roberts, S. C.; Choyke, S.; Oetjen, K.; McAlees, A.; Riddell, N.; McCrindle, R.; Ferguson, P. L.; Higgins, C. P.; Field, J. A. Discovery of 40 classes of per-and polyfluoroalkyl substances in historical aqueous film-forming foams (AFFFs) and AFFF-impacted groundwater. *Environ. Sci. Technol.* **2017**, *51* (4), 2047−2057.
(30) Peshoria, S.; Nandini, D.; Tanwar, R.; Narang, R. Short-chain and long-chain fluorosurfactants in firefighting foam: a review. *Environ. Chem. Lett.* **2020**, *18*, 1277−1300.
(31) Guelfo, J. L.; Higgins, C. P. Subsurface transport potential of perfluoroalkyl acids at aqueous film-forming foam (AFFF)-impacted sites. *Environ. Sci. Technol.* **2013**, *47* (9), 4164−4171.
(32) Houtz, E. F.; Higgins, C. P.; Field, J. A.; Sedlak, D. L. Persistence of perfluoroalkyl acid precursors in AFFF-impacted groundwater and soil. *Environ. Sci. Technol.* **2013**, *47* (15), 8187−8195.
(33) Lang, J. R.; McDonough, J.; Guillette, T.; Storch, P.; Anderson, J.; Liles, D.; Prigge, R.; Miles, J. A.; Divine, C. Characterization of per-and polyfluoroalkyl substances on fire suppression system piping and optimization of removal methods. *Chemosphere* **2022**, *308*, 136254.
(34) Commission Delegated Regulation (EU)*2020/784. Amending Annex I to Regulation (EU) 2019/1021 of the European Parliament and of the Council as regards the listing of perfluorooctanoic acid (PFOA), ots salts and PFOA-related compounds*European Union2020
(35) European Union. *2021/1297, E., Amening Annex XVII to Regulation (EC) No 1907/2006 of the European Parliament and of the Council as regards perfluorocarboxylic acids containing 9 to 14 carbon atoms in hte chain (C9-C14 PFCAs), their salts and C9-C14 PFCA-related substances*. European Union, 2021.
(36) Senate US. *National Defense Authorization Act for Fiscal Year 2024*. Senate US, 2023.
(37) IPEN. *POPRC-14: White paper, Fluorine-free firefighting foams (3F) - Viable alternatives to fluorinated aqueous film-forming foams (AFFF)*. IPEN, 2018.
(38) IPEN, *Stockholm Convention COP-9 White Paper: The Global PFAS Problem: Fluorine-Free Alternatives As Solutions*. IPEN, 2019.
(39) Commission Regulation (EU). *2017/1000. Amending Annex XVII to Regulation (EC) No 1907/2006 of the European Parliament and of the Council concerning the Registration, Evaluation, Authorisation and Restriction of Chemicals (REACH) as regards perfluorooctanoic acid (PFOA), its salts and PFOA-related substances*. European Union. 2017.
(40) European Union. *Commission Regulation (EU) 2021/1297. Amending Annex XVII to Regulation (EC) No 1907/2006 of the European Parliament and of the Council as regards perfluorocarboxylic acids containing 9 to 14 carbon atoms in the chain (C9-C14 PFCAs), and their salts and C9-C14 PFCA-related substances*. European Union. 2021. 29−32
(41) Ross, I. Foam Transition: Is it as simple as ″Foam out/Foam in?″. *Catalyst* **2020**, *1*, 19.
(42) Cornelsen, M.; Weber, R.; Panglisch, S. Minimizing the environmental impact of PFAS by using specialized coagulants for the treatment of PFAS polluted waters and for the decontamination of firefighting equipment. *Emerging Contam.* **2021**, *7*, 63−76.
(43) Dahlbom, S.; Bjarnemark, F.; Nguyen, B.; Petronis, S.; Mallin, T. Analysis of per-and polyfluoroalkyl substances (PFAS) extraction from contaminated firefighting materials: Effects of cleaning agent, temperature, and chain-length dependencies. *Emerging Contam.* **2024**, *10* (3), 100335.
(44) AECOM. *AFFF Fire Truck and Foam Unit Decontamination Summary Report*. Connecticut Department Energy And Environmental Protection, 2022.

https://doi.org/10.1021/acs.est.4c09474
Environ. Sci. Technol. 2025, 59, 2222−2232

(45) CT. GOV. *Arcadis Trailer Demonstration Project Summary Report*. CT. GOV, 2022.
(46) Lang, J.; Devine, C. *Demonstration and Validation of Environmentally Sustainable Methods to Effectively Remove PFAS from Fire Suppression Systems Final Report*. ESTCP, 2024.
(47) Nguyen, D.; Bellona, C.; Lau, A.; Stults, J.; Andrews, H.; Jones, D.; Megson, D.; Ross, I. Practical Limits of Current Technologies in Removing Per-and Polyfluoroalkyl Substances from Fire Suppression Systems. *J. Hazard. Mater.* **2025**, *481*, 136551.
(48) Bellona, C. *Youtube Remediation of AFFF-Impacted Fire Suppression Systems Using Concentional and Closed-Circuit Desalination*. https://www.youtube.com/watch?v=vQl8qoRfCOs&t=1976s. (Accessed 07 January 2025).
(49) Riess, J. G.; Frézard, F.; Greiner, J.; Krafft, M. P.; Santaella, C.; Vierling, P.; Zarif, L. Membranes, vesicles, and other supramolecular systems made from fluorinated amphiphiles. In *Handbook of nonmedical applications of liposomes*; CRC Press, 2018, pp. 97−142.
(50) Gladysz, J. A.; Curran, D. P.; Horváth, I. T. *Handbook of fluorous chemistry*; John Wiley & Sons, 2006.
(51) Smith, S. J.; Wiberg, K.; McCleaf, P.; Ahrens, L. Pilot-scale continuous foam fractionation for the removal of per-and poly-fluoroalkyl substances (PFAS) from landfill leachate. *ACS Es&t Water* **2022**, *2* (5), 841−851.
(52) Houtz, E. F.; Sedlak, D. L. Oxidative conversion as a means of detecting precursors to perfluoroalkyl acids in urban runoff. *Environ. Sci. Technol.* **2012**, *46* (17), 9342−9349.
(53) Trocellier, P.; Sajavaara, T. Elastic recoil detection analysis. *EAC* **2008**, *1002* (97804), 70027.
(54) R Core Team. *R: A language and environment for statistical computing*. https://www.r-project.org. (Accessed 2025 January 07).
(55) Backe, W. J.; Day, T. C.; Field, J. A. Zwitterionic, cationic, and anionic fluorinated chemicals in aqueous film forming foam formulations and groundwater from US military bases by nonaqueous large-volume injection HPLC-MS/MS. *Environ. Sci. Technol.* **2013**, *47* (10), 5226−5234.
(56) Zhang, B.; Song, J.; Li, D.; Hu, L.; Hill, C. L.; Liu, T. Self-Assembly of Polyoxovanadate-Containing Fluorosurfactants. *Langmuir* **2016**, *32* (48), 12856−12861.
(57) Kissa, E. *Fluorinated surfactants and repellents*; CRC Press, 2001; Vol. *97*.
(58) Krafft, M.-P.; Giulieri, F.; Riess, J. G. Supramolecular assemblies from single-chain perfluoroalkylated phosphorylated amphiphiles. *Colloids Surf., A* **1994**, *84* (1), 113−119.
(59) Schick, M.; Fowkes, F. Foam stabilizing additives for synthetic detergents. Interaction of additives and detergents in mixed micelles. *J. Phys. Chem.* **1957**, *61* (8), 1062−1068.
(60) Ooshika, Y. A theory of critical micelle concentration of colloidal electrolyte solutions. *J. Colloid Sci.* **1954**, *9* (3), 254−262.
(61) Nakayama, H.; Shinoda, K.; Hutchinson, E. The effect of added alcohols on the solubility and the Krafft point of sodium dodecyl sulfate. *J. Phys. Chem.* **1966**, *70* (11), 3502−3504.
(62) Shinoda, K. The effect of alcohols on the critical micelle concentrations of fatty acid soaps and the critical micelle concentration of soap mixtures. *J. Phys. Chem.* **1954**, *58* (12), 1136−1141.
(63) Dong, D.; Kancharla, S.; Hooper, J.; Tsianou, M.; Bedrov, D.; Alexandridis, P. Controlling the self-assembly of perfluorinated surfactants in aqueous environments. *Phys. Chem. Chem. Phys.* **2021**, *23* (16), 10029−10039.
(64) Giles, S. L.; Snow, A. W.; Hinnant, K. M.; Ananth, R. Modulation of fluorocarbon surfactant diffusion with diethylene glycol butyl ether for improved foam characteristics and fire suppression. *Colloids Surf., A* **2019**, *579*, 123660.
(65) Schaefer, T. H. *Fire Fighting Foam Concentrate*. US 20,080,196,908 A1. 2008.
(66) Lange, F. T.; Freeling, F.; Göckener, B. Persulfate based total oxidizable precursor (TOP) assay approaches for advanced PFAS assessment in the environment- a review. *Trends Environ. Anal. Chem.* **2024**, *44*, No. e00242.
(67) Al Amin, M.; Luo, Y.; Nolan, A.; Robinson, F.; Niu, J.; Warner, S.; Liu, Y.; Dharmarajan, R.; Mallavarapu, M.; Naidu, R.; et al. Total oxidisable precursor assay towards selective detection of PFAS in AFFF. *J. Cleaner Prod.* **2021**, *328*, 129568.
(68) Tenorio, R.; Liu, J.; Xiao, X.; Maizel, A.; Higgins, C. P.; Schaefer, C. E.; Strathmann, T. J. Destruction of per-and polyfluoroalkyl substances (PFASs) in aqueous film-forming foam (AFFF) with UV-sulfite photoreductive treatment. *Environ. Sci. Technol.* **2020**, *54* (11), 6957−6967.
(69) Zhang, Y.; Liu, J.; Ghoshal, S.; Moores, A. Density functional theory calculations decipher complex reaction pathways of 6: 2 fluorotelomer sulfonate to perfluoroalkyl carboxylates initiated by hydroxyl radical. *Environ. Sci. Technol.* **2021**, *55* (24), 16655−16664.
(70) Patch, D.; O'Connor, N.; Vereecken, T.; Murphy, D.; Munoz, G.; Ross, I.; Glover, C.; Scott, J.; Koch, I.; Sauvé, S.; et al. Advancing PFAS characterization: Enhancing the total oxidizable precursor assay with improved sample processing and UV activation. *Sci. Total Environ.* **2024**, *909*, 168145.
(71) Martin, D.; Munoz, G.; Mejia-Avendaño, S.; Duy, S. V.; Yao, Y.; Volchek, K.; Brown, C. E.; Liu, J.; Sauvé, S. Zwitterionic, cationic, and anionic perfluoroalkyl and polyfluoroalkyl substances integrated into total oxidizable precursor assay of contaminated groundwater. *Talanta* **2019**, *195*, 533−542.
(72) Tsou, K.; Antell, E.; Duan, Y.; Olivares, C. I.; Yi, S.; Alvarez-Cohen, L.; Sedlak, D. L. Improved total oxidizable precursor assay for quantifying polyfluorinated compounds amenable to oxidative conversion to perfluoroalkyl carboxylic acids. *ACS Es&t Water* **2023**, *3* (9), 2996−3003.
(73) Hutchinson, S.; Rieck, T.; Wu, X. Advanced PFAS precursor digestion methods for biosolids. *Environ. Chem.* **2020**, *17* (8), 558−567.
(74) Bruton, T. A.; Sedlak, D. L. Treatment of aqueous film-forming foam by heat-activated persulfate under conditions representative of in situ chemical oxidation. *Environ. Sci. Technol.* **2017**, *51* (23), 13878−13885.
(75) Prencipe, I.; Dellasega, D.; Zani, A.; Rizzo, D.; Passoni, M. Energy dispersive x-ray spectroscopy for nanostructured thin film density evaluation. *Sci. Technol. Adv. Mater.* **2015**, *16* (2), 025007.
(76) Latifi, A.; Imani, M.; Khorasani, M. T.; Joupari, M. D. Electrochemical and chemical methods for improving surface characteristics of 316L stainless steel for biomedical applications. *Surf. Coat. Technol.* **2013**, *221*, 1−12.
(77) Johnson, R. L.; Anschutz, A. J.; Smolen, J. M.; Simcik, M. F.; Penn, R. L. The adsorption of perfluorooctane sulfonate onto sand, clay, and iron oxide surfaces. *J. Chem. Eng. Data* **2007**, *52* (4), 1165−1170.
(78) European Union. *Regulation (EC) No 1272/2008 of the European Parliament and the Council of 16 December 2008 on classification, labelling and packaging of substances and mixtures, amening and repealing Directives 67/548/EEC and 1999/45/EC, and amening Regulation (EC) No 1907/2006*. European Union. 2008.
(79) Weiner, B.; Yeung, L. W.; Marchington, E. B.; D'Agostino, L. A.; Mabury, S. A. Organic fluorine content in aqueous film forming foams (AFFFs) and biodegradation of the foam component 6: 2 fluorotelomermercaptoalkylamido sulfonate (6: 2 FTSAS). *Environ. Chem.* **2013**, *10* (6), 486−493.
(80) Smith, S. J.; Lauria, M.; Higgins, C. P.; Pennell, K. D.; Blotevogel, J.; Arp, H. P. H. The need to include a fluorine mass balance in the development of effective technologies for PFAS destruction. *Environ. Sci. Technol.* **2024**, *58* (6), 2587−2590.
(81) Gonda, N.; Zhang, C.; Tepedelen, D.; Smith, A.; Schaefer, C.; Higgins, C. P. Quantitative assessment of poly-and perfluoroalkyl substances (PFASs) in aqueous film forming foam (AFFF)−impacted soils: a comparison of analytical protocols. *Anal. Bioanal. Chem.* **2024**, *416*, 6879−6892.
(82) Fomtec. *Safety Data Sheet: Fomtec Enviro USP*. 2024.
(83) National Foam. *Safety Data Sheet - NMS#S15 AvioF3 Green KHC 3% Fluorine Free Foam Concentrate*. National Foam, 2023.

(84) Perimeter Solutions, *Satefy Data Sheet: SOLBERG(R) Re-Healing RF3*; Perimeter Solutions, 2022.
(85) Vatankhah, H.; Anderson, R. H.; Ghosh, R.; Willey, J.; Leeson, A. Making Waves: The Progress of Management Strategies for Cleaning and Rinsing of PFAS-Impacted Fire Suppression Systems. *Water Res.* **2025**, *268*, 122661.

https://doi.org/10.1021/acs.est.4c09474
Environ. Sci. Technol. 2025, 59, 2222−2232

Supplementary Information

Decontamination and surface analysis of PFAS-contaminated fire suppression system pipes: effects of cleaning agents and temperature

Björn Bonnet[a*], Matthew K. Sharpe[b], Gulaim Seisenbaeva[c], Leo W. Y. Yeung [d], Ian Ross[e] and Lutz Ahrens[a]

[a]Department of Aquatic Sciences and Assessment, Swedish University of Agricultural Sciences, 75651 Uppsala, Sweden

[b]Surrey Ion Beam Centre, University of Surrey, Guildford, Surrey, GU2 7XH, UK

[c]Department of Molecular Sciences, Swedish University of Agricultural Sciences, 75651 Uppsala, Sweden

[d]SMTM Research Centre, School of Science and Technology, Örebro University, 70182 Örebro, Sweden

[e]CDM Smith, 220 Montgomery Street. Suite 1418. San Francisco, CA 94104 USA, USA

*Email: bjorn.bonnet@slu.se

This document contains 31 pages, 18 figures and 11 tables.

S1: Pre-investigation of decommissioned stainless steel sprinkler system pipes

Two pre-investigations were undertaken to reduce the number of eligible pipes used for the experiment, with the goal of selecting the most contaminated pipes.

Pre-investigation 1: Ultrasonication supported methanol extraction.

Approximately 1 cm wide sections (diameter see Table S1) were cut off each pipe (n = 9). The cut outs were put into differently sized glass beakers (150-250 mL capacity) individually. Beakers were filled with methanol until the pipe section was completely covered (Table S1). Containers were placed into an ultrasonication bath for 1 hour. After sonication, methanol was analyzed for PFAS using 0.9 mL sample and 100 µL internal standard (IS) solution (for details see section 'PFAS analysis').

Table S1: Methanol extraction of stainless-steel pipe sections

ID/Label	Inner Diameter of pipe (cm)	Volume of methanol (mL)	Measured ∑PFAS (ng/mL)
A_MeOH	3.86	50	0.50
B_MeOH	3.86	50	0.40
D_MeOH	4.40	50	0.60
E_MeOH	3.00	40	168
F_MeOH	4.50	50	1760
G_MeOH	3.86	50	0.10
H_MeOH	3.85	50	1220
I_MeoH	5.70	70	1250
J_MeoH	3.00	40	36.8

The analysis showed that pipes F, H and I were the most PFAS-contaminated pipes and thus these pipe sections were selected for further experiments.

Pre-investigation 2: Scanning electron microscopy (SEM)

Approximately 1 cm x 1 cm pieces were cut out from pipes F, H and I for investigation using a scanning electron microscope (SEM). The goal behind this investigation was to visualize the structures of the AFFF-contaminated surfaces (Figure S1). Additionally, the outside of a stainless steel pipe was investigated as well. Multi-layered PFAS structures were previously identified on surfaces of sprinkler system pipes using SEM-EDX by Lang et al. (2022). Figure S1 showed that for all three pipes sections (F, H, I) the steel surface was completely covered compared to the the outside of a pipe section. SEM did not provide any precise resolution regarding the thickness of the layer, however, cracks in Figure S1 indicate a considerable depth of several. Figure S1 furthermore shows structures that could be associated with PFAS.

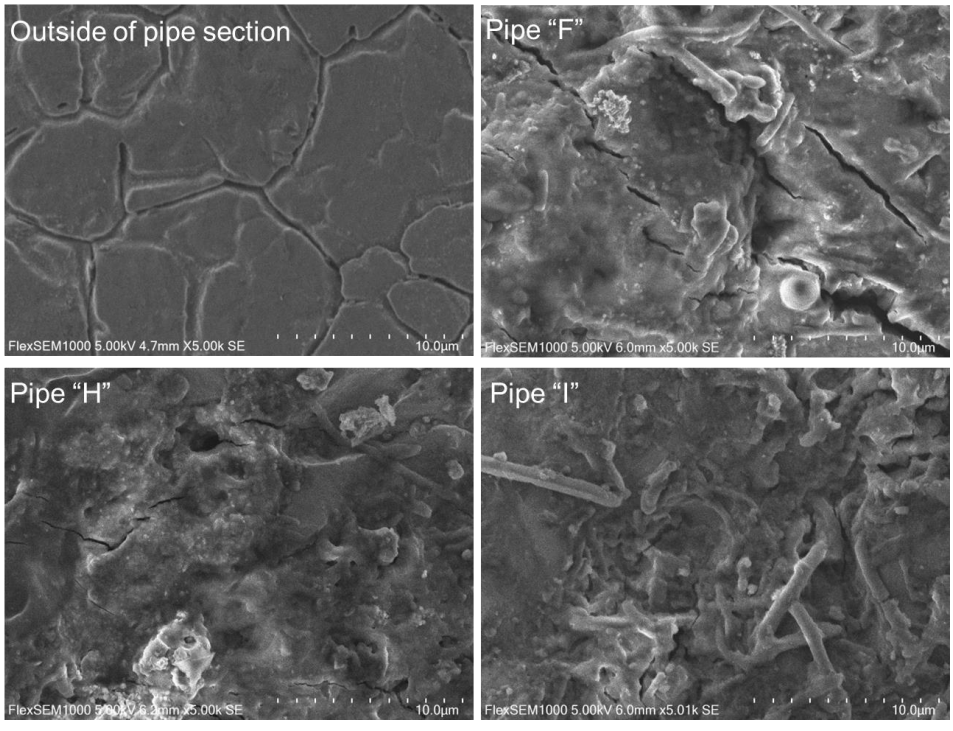

Figure S1: SEM images at 5000-fold magnification produced using Hitachi FlexSEM-1000 II microscope operating at 5 kV accelerating tension, working distance ca. 6 mm.

S2: Experimental Design – Soaking experiment

Multiple pipe sections (Table S2) were put into a PP-container to increase surface area. When placing the pipe sections into the container, it was ensured that the contaminated surface of each pipe section was always in full contact with the soaking solution and was not covered up by the other pipe sections. Pipe sections were completely covered within the soaking solution and volumes of soaking solutions were adjusted accordingly.

Table S2: Parameters of pipe sections and conditions for soaking experiment

Temperature [°C]	Cleaning solution	Pipe section	Number of pipe sections	Surface area at T1 [cm²]	Soaking Volume [mL]
20	MeOH	F	2	38.4	100
		H	4	64.3	150
		I	2	67.2	200
	TAP	F	2	39.0	100
		H	4	67.1	150
		I	2	68.0	200
	BC10	F	2	37.8	100
		H	4	66.2	150
		I	2	66.4	200
	BC20	F	2	38.4	100
		H	4	68.3	150
		I	2	67.2	200
40	TAP	F	2	39.6	100
		H	4	67.5	150
		I	2	64.8	200
	BC10	F	2	38.7	100
		H	4	62.8	150
		I	2	67.2	200
	BC20	F	2	37.8	100
		H	4	66.1	150
		I	2	65.6	200
70	TAP	F	2	38.4	100
		H	4	65.9	150
		I	2	67.2	200
	BC10	F	2	38.4	100
		H	4	66.5	150
		I	2	66.4	200
	BC20	F	2	38.9	100
		H	4	64.7	150
		I	2	68.1	200

The soaking experiment was performed at three different temperatures: Room temperature (20°C), 40°C and 70°C. Experiments at room temperature were performed under a fume hood at laboratory conditions and elevated temperatures were conducted within temperature-controlled ovens (40°C: Nabertherm, N-54E; 70°C: VWR, Dry-Line 56 Prime) set to the respective temperature. Temperature was measured throughout the whole experimental runtime.

Pipe sections of pipe H were used for a follow-up experiment using time-of-flight elastic recoil detection (ToF-ERD) (see section 'S8 Surface analysis with ToF-ERD'). To enable a surface analysis of each time point without interrupting the soaking experiment, it was necessary to remove one pipe section of pipe H from the container after each time point. Therefore, the total surface area interacting with the soaking solution was reduced by the area of the removed pipe section. Calculated concentrations were adjusted for this change in surface area.

S3: PFAS target compounds and target analysis

A total of 24 PFAS were analyzed including 11 perfluoroalkyl carboxylic acids (PFCAs) (perfluorobutanoic acid (PFBA), perfluoropentanoic acid (PFPeA), perfluorohexanoic acid (PFHxA), perfluorohepanoic acid (PFHpA), perfluorooctanoic acid (PFOA), perfluorononanoic acid (PFNA), perfluorodecanoic acid (PFDA), perfluoroundecanoic acid (PFUnDA), perfluorododecanoic acid (PFDoDA), perfluorotridecanoic acid (PFTriDa) and perfluorotetradecanoic acid (PFTeDA)), 7 perfluorosulfonic acids (PFSAs) (perfluorobutanesulfonic acid PFBS, perfluoropentanesulfonic acid (PFPeS), perfluorohexanesulfonic acid (PFHxS), perfluorohepanesulfonic acid (PFHpS), perfluorooctanesulfonic acid (PFOS), perfluorononanesulfonic acid (PFNS) and perfluorodecanesulfonic acid (PFDS)), 3 fluorotelomer sulfonates (4:2 FTSA, 6:2 FTSA and 8:2 FTSA), N-methyl-perfluorooctane sulfonamido acetic acid (Me-FOSAA), N-ethyl-perfluorooctane sulfonamido acetic acid (Et-FOSAA) and perfluorooctane sulfonamide (FOSA).

All samples from the soaking experiments were prepared for direct injection analysis by ultraperformance liquid chromatography coupled to tandem mass-spectrometry (UPLC-MS/MS) analysis (Sciex Triple Quad™ 3500 LC-MS/MS, USA) (for details see Smith et al., 2022). For aqueous samples (TAP, BC10, BC20), 250 µL sample, 250 µL MilliQ, 400 µL methanol and 100 µL IS-solution in methanol were used, while for methanol-based samples, 250 µL sample, 150 µL methanol, 500 µL MilliQ and 100 µL IS-solution in methanol were added to a 1.7 mL PP autoinjector vial and vortexed. Due to exceeding the linear range of the calibration curve for PFOA, PFHxS and PFOS in for some samples, a diluted series with 25 µL sample was prepared.

Table S3: Limits of detection (LOD) and limits of quantification (LOQ) in (ng/mL)

	TAP		BC10		BC20		MeOH	
	LOD	LOQ	LOD	LOQ	LOD	LOQ	LOD	LOQ
PFBA	0.01	0.03	0.01	0.03	0.01	0.03	0.01	0.03
PFPeA	0.01	0.03	0.01	0.03	0.01	0.03	0.01	0.03
PFHxA	0.01	0.03	0.01	0.03	0.01	0.03	0.01	0.03
PFHpA	0.01	0.03	0.01	0.03	0.01	0.03	0.01	0.03
PFOA	0.01	0.03	0.01	0.03	0.01	0.03	0.01	0.03
PFNA	0.25	0.72	0.01	0.03	0.22	0.63	0.01	0.03
PFDA	0.01	0.03	0.22	0.57	0.04	0.10	0.67	1.95
PFUnDA	0.05	0.12	0.01	0.03	0.18	0.52	0.18	0.45
PFDoDA	0.10	0.25	0.08	0.22	0.07	0.19	0.12	0.34
PFTriDA	0.01	0.03	0.01	0.03	0.01	0.03	0.01	0.03
PFTeDA	0.06	0.15	0.01	0.03	0.01	0.03	0.08	0.23
PFBS	0.03	0.08	0.06	0.15	0.02	0.03	0.07	0.15
PFPeS	0.07	0.18	0.02	0.04	0.04	0.08	0.14	0.36
PFHxS	0.02	0.05	0.01	0.03	0.01	0.03	0.12	0.33
PFHpS	0.10	0.28	0.01	0.03	0.01	0.03	0.11	0.31
PFOS	0.05	0.14	0.02	0.03	0.03	0.07	0.39	1.07
PFNS	0.06	0.14	0.01	0.02	0.04	0.09	0.08	0.20
PFDS	0.07	0.16	0.03	0.05	0.07	0.17	0.09	0.15
4:2 FTSA	0.01	0.03	0.01	0.03	0.01	0.03	0.01	0.03
6:2 FTSA	0.24	0.68	0.33	0.75	0.43	1.19	0.12	0.17
8:2 FTSA	0.01	0.03	0.01	0.03	0.01	0.03	0.16	0.46
FOSA	0.04	0.10	0.01	0.03	0.01	0.03	0.04	0.09
Me-FOSAA	0.01	0.03	0.01	0.03	0.01	0.03	0.07	0.19
Et-FOSAA	0.04	0.10	0.01	0.03	0.05	0.14	0.19	0.55

Table S4: Method relative recoveries in (%)

	Soaking experiment	TOP assay		Soaking experiment	TOP assay
PFBA	77%	95%	PFOS	103%	89%
PFPeA	145%	90%	PFNS	103%	89%
PFHxA	78%	88%	PFDS	103%	89%
PFHpA	80%	85%	4-2FTSA	86%	90%
PFOA	81%	93%	6-2 FTSA	74%	87%
PFNA	98%	89%	8-2 FTSA	70%	79%
PFDA	73%	83%	FOSA	73%	88%
PFUnDA	71%	86%	Me-FOSAA	85%	84%
PFDoDA	78%	90%	Et-FOSAA	75%	85%
PFTriDA	74%	95%			
PFTeDA	74%	95%			
PFBS	77%	88%			
PFPeS	82%	85%			
PFHxS	82%	85%			
PFHpS	103%	89%			

S4: Total oxidizable precursor assay – spiking test

A total oxidizable precursor (TOP) assay was performed to estimate contribution of precursor PFAS not identified in the targeted analysis (for details see Houtz&Sedlak, 2012). Due to the addition of BC, an organic compound, interferences during oxidation in the TOP assay inhibiting oxidation of PFAS precursors were expected. Hence, a spiking experiment with a known concentration of an oxidizable PFAS precursor (6:2 FTSA) was performed in MilliQ water and in an aqueous solution containing 20% BC as in the soaking experiment. 100 µL of 6:2 FTSA in methanol (c = 32 µg/mL) was spiked into a 15 mL PP-tube and brought to dryness under N-stream. One set of duplicates was reconstituted in 100 µL MQ-water and another set in 100 µL MilliQ-water containing 20% BC. TOP assay was performed for three different dosages of oxidant potassium persulphate ($K_2O_8S_2$) and base sodium hydroxide solution (NaOH) (Table S5). The lowest dosage (60 mM $K_2O_8S_2$/150mM NaOH) used according to the TOP assay originally proposed by Houtz&Sedlak (2012). Additionally, dosages of 120 mM $K_2O_8S_2$/300 mM NaOH and 180 mM $K_2O_8S_2$/450 mM NaOH were prepared. Oxidant and base were added from prepared stock solution of 200 mM $K_2O_8S_2$ and 9 M NaOH, MQ water was added to a final volume of 2 mL. Blanks were prepared consisting of 100 µL MQ water instead of sample. Control samples of 6:2 FTSA without oxidant and base in only MilliQ-water were prepared in triplicates. All samples were put into a temperature-controlled water bath at 85 °C and removed after 6 hours. After reaching room temperature, pH was estimated using indicator paper (ROTA®, pH 1-14, VWR, Belgium), 50 µL of methanol and different volumes of 6 M HCL were added to obtain a target pH between 4-7 (Table S5).

Table S5: TOP Assay – spiking test

200 mM $K_2O_8S_2$ (µL)	9 mM NaOH (µL)	Sample (µL)	MilliQ (µL)	Final Volume (µL)
600	34	100	1266	2000
1200	67	100	633	2000
1800	100	100	-	2000

The spiking test with 6:2 FTSA in MilliQ water and MilliQ water containing 20% BC (BC20) was performed to test if oxidation of 6:2 FTSA will be inhibited due to the presence of BC. The tests indicate that oxidation was not only inhibited but completely prevented if BC was present in the solution (Table S6). The concentrations of the spiked substance 6:2 FTSA as well as their predominantly found product PFCAs after oxidation during the TOP assay for three different dosages (i.e. 60/150, 120/300 and 180/450) of oxidant ($K_2S_2O_8$) and base (NaOH) are presented in Table S6. For spiking tests in MilliQ water, initially spiked 6:2 FTSA concentration (32000 ng/mL) was reduced to an average concentration of 458 ng/mL, 148 ng/mL and 161 ng/mL for 60/150, 120/300 and 180/450 ($K_2S_2O_8$/NaOH), respectively. For BC20, concentrations of initially spiked 6:2 FTSA remained at the initially spiked level and did not produce any PFCA product above the LOD. Increasing dosages of oxidant and base did not have any effect on successful oxidation during the TOP assay either. We conclude from these spiking tests that PFAS present in samples from the soaking experiment including BC are not going to be successfully oxidized during the TOP assay. Therefore, we decided to include only TAP samples and MeOH samples for TOP assays. To account for contribution of precursors in samples containing BC, we decided to determine total fluorine (TF) content by combustion-ion-chromatography (CIC).

Table S6: Concentration of spiked 6:2 FTSA and its products after oxidation in TOP assay

	60/150		120/300		180/450	
ng/mL	BC20	MilliQ	BC20	MilliQ	BC20	MilliQ
6:2-FTSA	31655	458	31456	148	31834	161
PFBA	<LOD	3136	<LOD	3002	<LOD	2829
PFPeA	<LOD	5486	<LOD	4887	<LOD	4717
PFHxA	<LOD	3884	<LOD	3797	<LOD	3801
PFHpA	<LOD	627	<LOD	695	<LOD	594

Table S7: pH and neutralization after oxidation for TOP assay spiking test with 6M HCL

	60/150				120/300				180/450			
Replicate	1		2		1		2		1		2	
	Vol.HCL (µL)	pH	Vol. HCL (µL)	pH	Vol. HCL (µL)	pH	Vol. HCL (µL)	pH	Vol. HCL (µL)	pH	Vol. HCL (µL)	pH
MilliQ before neutralization	0	14	0	14	0	14	0	14	0	14	-	14
MilliQ after neutralization	10	6-7	10	6-7	25	6-7	20	6-7	30	6	30	6
BC20 before neutralization	0	14	0	14	0	14	0	14	0	14	0	14
BC20 after neutralization	5	6-7	5	6-7	10	7	10	7	10	6	10	6

S5: Total oxidizable precursor assay – real samples

Table S8: TOP assay on 12 h samples – volumes and concentrations of TOP assay constituents

200 mM K2O8S2 (µL)	9 mM NaOH (µL)	Sample (µL)	MilliQ (µL)	Final Volume (µL)
600	34	1000	366	2000

Table S9: pH and neutralization of TOP assay for T1 samples with 6M HCL

Sample ID	F		H		I	
Replicate	1	2	1	2	1	2
	Vol. HCL (µL)	pH	Vol. HCL (µL)	pH	Vol. HCL (µL)	pH
TAP before neutralization	0	14	0	14	0	14
TAP after neutralization	10	7	10	7	10	6-7
TAP40 before neutralization	0	14	0	14	0	14
TAP40 after neutralization	10	7	10	7	10	7
TAP70 before neutralization	0	14	0	14	0	14
TAP70 after neutralization	10	7	10	7	10	7
MeOH before neutralization	0	14	0	14	0	14
MeOH after neutralization	10	2	5	6	5	7
Blank before neutralization	0	14	0	14	0	14
Blank after neutralization	5	7	10	7	10	7

S6: Total fluorine (TF) analysis

The system is consisted of a combustion module (Analytikjena, Germany), a 920 absorbent module, and a 930 Compact IC flex (Metrohm, Switzerland). The separation of anions was performed on an ion-exchange column (Metrosep A Supp5, 4 mm x 150 mm) with isocratic elution using the following eluent (64 mM sodium carbonate and 20 mM sodium bicarbonate). In brief, 100 µL of the liquid samples was placed on a quartz glass boat and combusted with hydropyrolysis at 1050 °C. During combustion, all fluorine was converted into hydrogen fluoride (HF) and were absorbed into ultrapure water (18.2 MΩ). The levels of fluoride ions in the solution were analyzed using the ion chromatograph with conductivity detector. Since background fluoride contamination was noted in daily measurement, the measurement of TF started until low variation (RSD < 10%) of background combustion blanks (empty quartz glass boat) were obtained. The TF results were obtained using a five-point external calibration curve (50 to 1000 ng/mL F) prepared from solid PFOA potassium salt (Fluka, Hampton, United States). Quantification of fluoride was performed by subtracting the peak area of fluoride in the combustion blanks between samples and then using a five-point external calibration curve for calculation. The peak areas of the calibration curve had been also subtracted from that of the combustion blank. Quality control standard using 250 ng F/mL PFOA standard was used in between 10 samples to evaluate the stability of the instrument; the reported concentrations of the QC standard was 236 ng F/mL with the relative standard deviation of 24%. Blank samples of TAP, BC10 and BC20 were evaluated and subtracted, and their levels were found to be 1.4, 0,63 and 0,53 ng F/L, respectively.

S7: Data conversion for F-equivalent

Since CIC only measures the F content (both organic bound or inorganic fluoride) of a sample, to compare the results from target PFAS and TOP assay analyses, concentrations of PFAS have to be converted into F-equivalent concentration using the following formula:

$$c_F = \frac{n_F MW_F}{MW_{PFAS}} \times c_{PFAS}$$

where C_F is the corresponding fluoride level (ng/mL F), n_F stands for the numbers of fluorine in the PFAS, MW_F is the molecular weight of fluorine, MW_{PFAS} stands for the molecular weight of PFAS and C_{PFAS} is the quantifiable PFAS concentration in target PFAS or TOP assay analyses.

S8: Surface analysis with ToF-ERD:

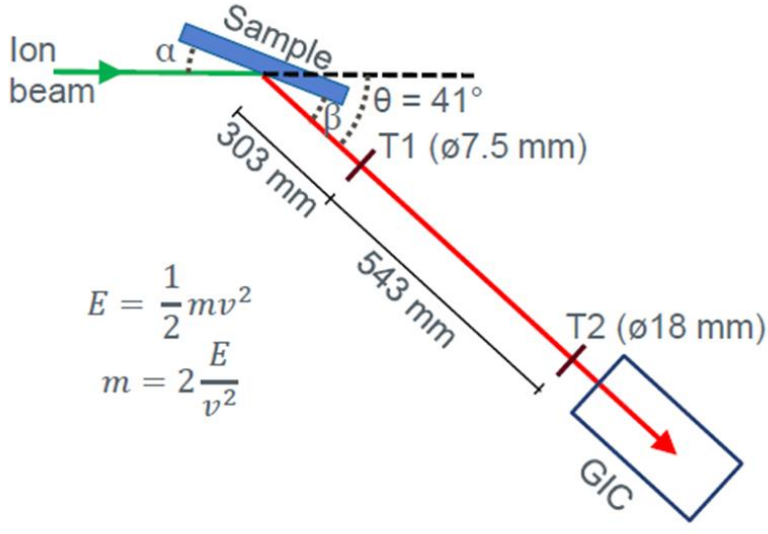

Figure S2: Schematic of ToF-ERD setup. Incident angle (α) and exit angle (β) equal to 69.5° from sample normal. Timing gates, T1 and T2, used for detecting time-of-flight of recoiled atoms, with Gas Ionisation Chamber (GIC) used for detecting energy of recoiled atoms.

Figure S2 in SI illustrates the time-of-flight elastic recoil detection (ToF-ERD) configuration at the Ion Beam Center at Surrey University[1]. This setup features two timing foils for time-of-flight measurements and a gas ionization chamber (GIC) for assessing energy. For this study, the scattering angle was set at 41°, with the incident and exit angle at 69.5° to maximize sensitivity, mass, and depth resolution throughout the whole sample[2]. A HVE 860 negative sputter ion source generates negatively charged ions that an injector magnet then leads into a 2 MV tandem accelerator, accelerating the ions to a designated energy and converting them to a positive charge. The experiment utilized 16 MeV $^{127}I^{8+}$ ion beams with an energy dispersion under 10 keV, chosen for optimal cross-sections, count rate, and mass differentiation. The ToF-ERD experiment ran for 20 min for each sample with a 3 x 4 mm² beam spot, adjustable by slits prior to entering the sample chamber. Coincidence counts between the second timing foil and the GIC were approximately 900 counts/s, against a background of less than 20 counts/s. The ToF-ERD histograms were processed with Potku software (Build 2.2.4)[3] to remove any spurious coincidences caused by incorrect ToF readings, producing elemental depth profiles. Pristine stainless steel which never was in contact with AFFF was analyzed as a blank.

S9: Results Soaking experiment

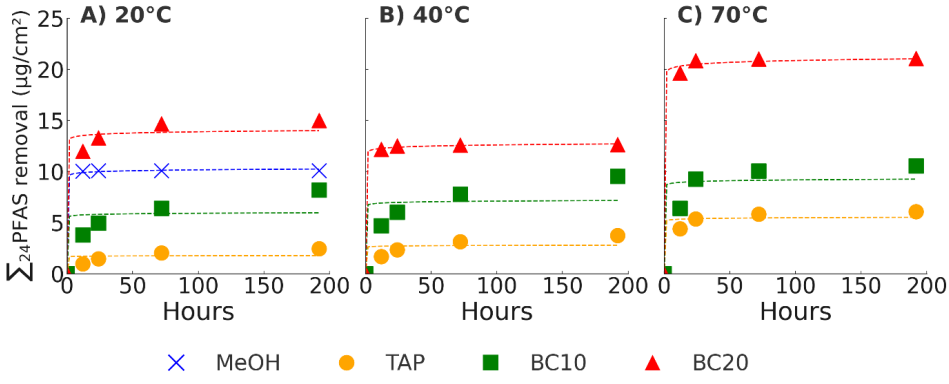

Figure S3: Accumulated PFAS removal (µg/cm²) from stainless steel pipes using methanol (MeOH) (only 20°C), tap water (TAP), 10 wt% butyl carbitol in TAP (BC10) and 20 wt% BC in TAP (BC20), respectively, during soaking experiments at A) 20°C, B) 40°C and C) 70°C. Data points represent average concentrations (n=3). Fitted logarithmic functions are presented in table S11.

Table S10: Fitted logarithmic functions and R^2 values for soaking experiment

Treatment	Temperature	Equation	R^2
MeOH	20	343.3ln(x)+8745.19	0.9941
TAP	20	62.35ln(x)+1508.09	0.7297
BC10	20	209ln(x)+5088.93	0.7873
BC20	20	475.68ln(x)+11953.36	0.9863
TAP	40	97.65ln(x)+2376.4	0.7823
BC10	40	250.19ln(x)+6112.13	0.8155
BC20	40	426.37ln(x)+10842	0.9970
TAP	70	188.33ln(x)+4712.9	0.9668
BC10	70	318.14ln(x)+7899.16	0.9076
BC20	70	707.26ln(x)+17954.01	0.9977

S10: Trend for chain length and head group dependent desorption of PFAS

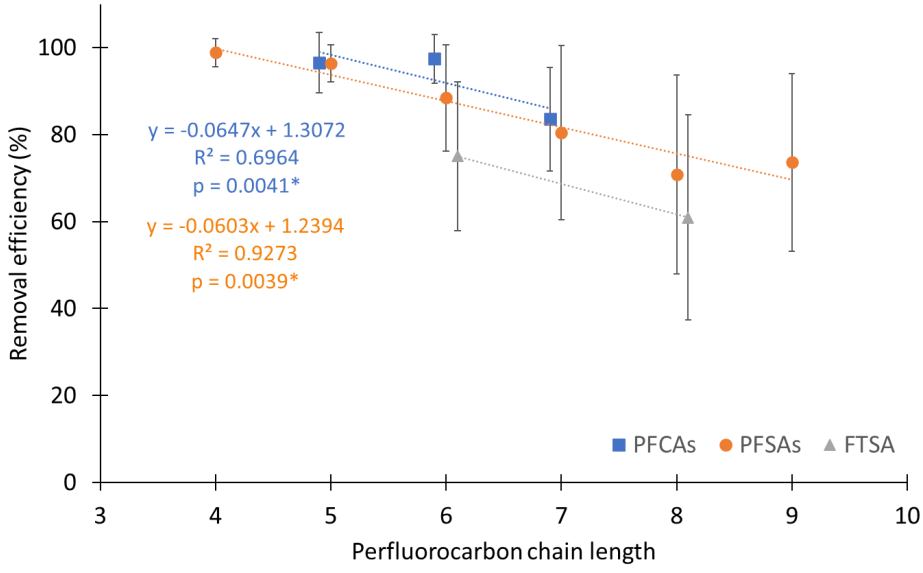

Figure S4: Removal efficiency (%) (∑PFAS 12h/∑PFAS 192h * 100) as a function of perfluorocarbon chain length. Data points represent subgroup averages of values across all treatments. Only compounds with 100% detection frequency (n = 10 per data point) are presented. *p-values are calculated based upon all available data points.

The removal of PFAS was dependent on the perfluorocarbon chain length and functional group comparing TAP, BC10, BC20 and MeOH after 192 h (Figure S4 in SI). After 192 h, the average removal decreased by 6.6 ± 7.6% for each CF_2 moiety for C_5-C_7 PFCAs and 5.6 ± 2.9% for C_4-C_9 PFSA. This indicates that shorter chain compounds are released into solution more easily than longer chain compounds under the same experimental conditions. Krafft Point (T_K) is the temperature at which the solubility of a surfactant is equal to the critical micelle concentration (CMC)[4, 5]. T_K increases with increasing number of carbons in alkyl chain[4]. In addition, each additional CH_2 moiety increases the hydrophobicity and surface activity of the surfactant[4] and thus longer chain PFAS show a stronger interaction with surfaces. When comparing the functional groups, we generally observed the trend with increasing removal efficiency for PFCAs > PFSAs > FTSA. The removal efficiency was 4.7 ± 2.9% higher for PFCAs compared to PFSAs and 17 ± 0.87% higher for PFSAs compared to FTSAs. Removal efficiency was 22% higher for PFHxA than for 6:2 FTSA and 10% higher for PFOS than for 8:2 FTSA Dahlblom et al. found decreasing PFAS removal for compounds with increasing chain length from contaminated fire suppression materials, however, the assessment of removal

efficiency differed between the present study. This is in accordance with previous studies which investigated the (de)sorption kinetics of PFAS on soils[6, 7].

S11: Observations on single pipe sections and rebound experiment

Figure S5 presents the PFAS concentration in solution expressed in terms of surface area of pipe that they evolved from for all individual pipe sections (F, H and I; not averaged). The four fading green bars indicate the different soaking intervals (12 h, 24 h, 72 h and 192 h). We observed the highest PFAS removal into solution within the first soaking interval (12 h) and generally saw a decreasing removal in the following time intervals. We furthermore observed that the amount of PFAS removed from surfaces differed between the individual pipe sections. The PFAS removal from pipe section I was generally higher than for pipe sections F and H. The differences became most rigorous in the BC20 scenarios. The three maximum concentrations removed into solution in the entire soaking experiment were observed for pipe I in BC20 (20°C), BC20 (40°C) and BC20 (70°C) with 20400 ng/cm², 21800 ng/cm² an 40000 ng/cm² respectively. The factor by which the total removed PFAS increased between pipe F and H to pipe I were 2-3 (BC20 (20°C) and BC20 (40°C)) and 4-5 in BC20 (70°C). Reasons for why there were more PFAS removed from pipe I could be either that pipe I was more contaminated in the first place, or that the experimental conditions were more effective for pipe I, in the sense that the conditions were more closely to the overall T_K of PFAS assemblies on pipe I.

The red bars in Figure S5 represent the PFAS removed from surfaces during the rebound experiment (rebound experiment was not performed for pipe F). The highest concentrations were found for pipe I previously soaked in BC10 (20°C), TAP (20°C) and TAP (40°C) with 1990 ng/cm², 1350 ng/cm² and 1077 ng/cm² respectively. We observe that PFAS rebound was generally higher for pipe sections which received a less efficient treatment in the first place. For pipe I treated with TAP (20°C), PFAS rebound was almost as high as the initial soak (1490 ng/cm²). PFAS rebound was less pronounced for treatments at 70°C and with BC20 (all temperatures). The rebound experiment was only performed in TAP and only for 7 days. In the future it would be necessary to perform rebound experiment over a longer period (Dahlbom et al. 2024) and into actual F3 foam to represent a more realistic scenario. However, we can conclude from our soaking experiments that PFAS dissolved more efficiently into solutions containing BC. Since BC is a major constituent of F3 foams, we expect higher rebound into F3 foams. Considering long residence time within the system, PFAS rebound might happen over several years.

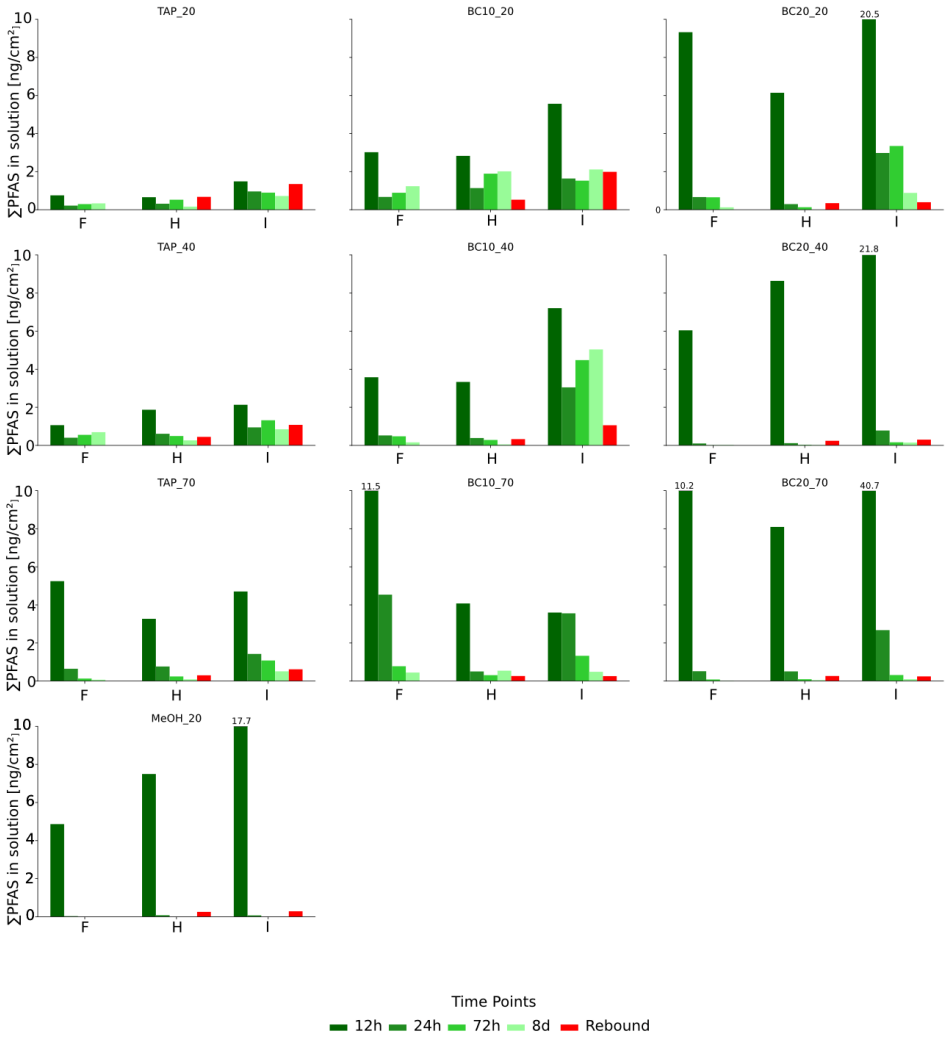

Figure S5: PFAS concentrations from soaking experiment expressed for single pipe sections including rebound test. Rebound test concentrations were measured after 1 week of incubation in tap water.

S12: TOP assay:

Comparison of PFAS concentration before and after TOP assay:

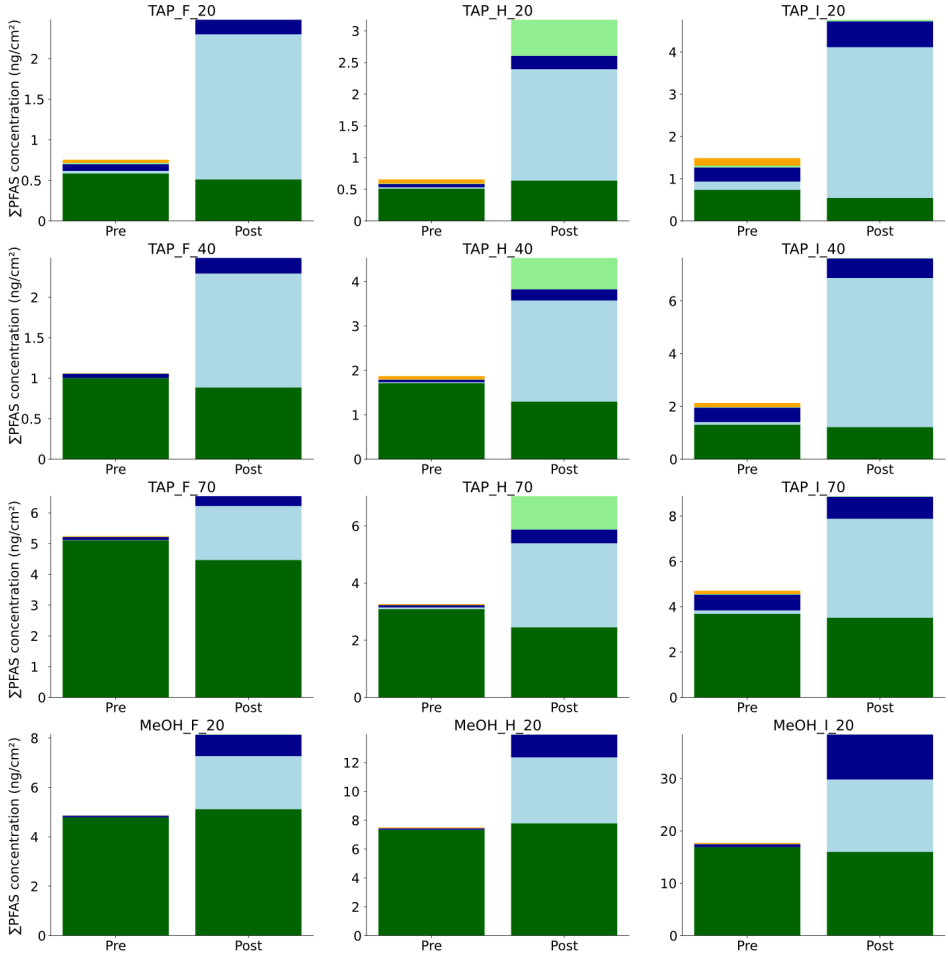

Figure S6: Comparison of ∑PFAS concentration before (pre) and after (post) oxidation in TOP assay. Y-axis in ng/cm^2.

For targeted analysis, the overall dominant fraction of PFAS were long chain PFSAs (i.e. PFOS, PFHxS, PFHpS), which contributed 68% (TAP (20°C)) to 97% (MeOH (20°C)) of total PFAS (Figure S6 in SI). After oxidation the ratio shifted and overall contribution of PFSAs decreased to 17% (TAP (20°C)) to 53% (MeOH (20°C)). Short chain PFSAs (i.e. PFBS, PFPeS) in targeted analysis contributed to a maximum of 2% in TAP (20°C). After oxidation, contribution of short chain PFSAs increased to a maximum contribution of 6.2% (TAP (20°C)). The highest contribution of short chain PFCAs accounted for 6.8% (TAP (20°C)) in targeted analysis and increased to an overall contribution of 32% (MeOH (20°C)) up to 67% (TAP

(20°C)) using TOP assay. Long chain PFCAs ranged between 2.1% (MeOH (20°C)) and 14% (TAP (20°C)) in targeted analysis and ranged between 6.1% (TAP (40°C)) and 15% (MeOH (20°C)) after oxidation. Other PFAS (i.e. detected 6:2 and 8:2 FTSA) contributed between 0.68% and 9.1% in targeted analysis and were not detected after oxidation which is expected since PFAS precursors have shown to break down during TOP assay[8].

S13: ToF-ERD measurements:

General information of histograms and depth profiles

Histograms and depth profiles of ToF-ERD measurements for all samples are presented in Figures S7 to S16. The histograms display both the composition as well as the intensity (counts/s) (referring to the color scale) of elements detected on the surface of each sample. Elements represented in the plot are the measurements of velocity (x-axis) and energy (y-axis). The curved shape of the plot for each element results from differences in velocity and energy for detected atoms (relating to the atoms mass from the kinetic energy $E = \frac{1}{2}mv^2$). A detection at the tip (top left) of the curve indicates a measurement with both high velocity and energy, whereas atoms detected towards the bottom of the curve (bottom right) are lower in both velocity and energy. Differences in velocity and energy for the same element result from interferences with the electron clouds of other elements after they have been recoiled by the ion beam. Interferences with electron clouds of other elements are less pronounced for atoms sitting at the very surface of the sample compared to atoms further in. Hence, we obtained depth position information of the atom within the sample. This information is further specified within the depth profiles. Depth profiles display the elemental concentration (y-axis) at a particular depth within the sample (x-axis).

Remaining F, C and Fe during soaking experiment

At 20°C remaining F concentration after 192 h were measured with 2.6 at.%, 4.7 at.%, 2.2 at.% and 2.1 at.% for TAP (20°C), BC10 (20°C), MeOH (20°C) and BC20 (20°C). At 40°C remaining F on pipe surfaces was highest for BC20 (40°) with 2.3 at.%, whereas TAP (40°C) and BC10 (40°C) showed 1.9 at.% remaining F after 192 h of treatment (Table S12).

For C, we generally observed a decrease between the initial concentration (untreated) and the concentration after 8 days of treatment. The three highest remaining C concentration on the pipe sections after treatment were observed for TAP (40°C), TAP (20°C) and BC (20°C) with 28% (50 counts/s), 27% (50 counts/s) and 26% (50 counts/s) respectively. The lowest C concentrations remaining on pipe surfaces besides treatment BC20 (70°C) were observed for MeOH (20°C) with 19% (30 counts/s) and BC10 (70°C) with 18% (30 counts/s).

For Fe, we generally observed an increase between the initial (untreated) concentration and the concentration after 8 days of treatment. Highest Fe concentration after 8 days of treatment were measured for BC20 (20°C) with 35% (50 counts/s), MeOH_20 with 28% (30 counts/s) and BC10 (70°C) with 25.9% (30 counts/s). The lowest Fe concentration after 8 days of treatment were measured for TAP (40°C), TAP (20°C) and BC10 (20°C) with 9.4% (10 counts/s), 12% (10 counts/s) and 16% (20 counts/s) respectively.

For TAP treatment at all temperatures as well as for BC10 (20°C), BC10 (40°C) and BC20 (40°C), we observed constant detection of all elements throughout the entire analytical depth, especially for Fe we did not observe a significant increase in detection, indicating it is covered up by the AFFF associated layer.

For MeOH (20°C), we observed concentration of Fe starting to increase and of C starting to decrease at a depth of around 500 TFU and 250 TFU after 24 h and 192 h of treatment respectively. F was detected constantly.

For BC10 (70°C), Fe concentration was starting to increase after 72 h of treatment at a depth of around 1000 TFU and yielding 25% at a depth of 1500 TFU. After 192 h of treatment, Fe started to increase at 750 TFU and reaches 30% at 1500 TFU. C concentrations began to decrease at the same depth, whereas F concentrations are measured constantly throughout all treatments with decreasing intensity after 192 h of treatment.

In BC20 treatments, we observed an increasing Fe and decreasing C concentration for BC20 (20°C) starting after 24 h of treatment at a depth of about 750 TFU and even earlier in after 192 h. F was measured constantly throughout the entire analytical depth with lower intensity after 192h of treatment. For BC20 (70°C) this trend was most distinct. Fe started to increase at a depth between 100 TFU to 250 TFU after 24 h of treatment and thereafter. For BC20 (70°C) after 192 h of treatment the Fe increased is most significant and reaches an elemental concentration of 45% at a depth of 1500 TFU. C showed decreasing concentration at similar analytical depths and F concentration decreases with increasing treatment time.

Discussion about the extent of the analyzed surface area

Five measurements of untreated pipe sections by ToF-ERD showed that the initial concentration of F, C and Fe may varied between 3.4 at.% - 8.0 at.%, 26 at.% - 32 at.% and 5.4 at.% - 21 at.% respectively, confirming variation of elemental concentration. Furthermore, ToF-ERD measurements throughout the treatments were performed on a ca. 10 mm x 10 mm piece cut off from a larger subsection (ca. 3 cm x 6 cm) of the initial pipe (see Figure S7 in SI). Therefore, pieces analyzed by ToF-ERD did have several cm between them. The actual area analyzed by ToF-ERD is approximately 3 mm x 4 mm (Figure S8 in SI). Despite the high

accuracy of ToF-ERD measurements themselves, the fact that only a 3 mm x 4 mm area is analyzed will lead to higher measurement uncertainties with respect to the soaking experiment, where there are substantially larger surface areas interacting with the soaking solution. It could have been more representative to cut out 10 mm x 10 mm pieces right next to each other. This would, however, have been less practical during the soaking experiment. It is recommended to take these factors into account for future analysis

Table S11: Elemental concentration of F, C and Fe on pipe sections measured by ToF-ERD presented in atomic % during the time points T1 (12 h), T2 (24 h), T3 (72 h) and T4 (192 h)

pristine steel (blank)			**Untreated (T0)**				**MeOH_20**		
F	C	Fe	F	C	Fe		F	C	Fe
0.1	9.3	52.4	5.7 ± 2.3	28.7 ± 2.9	13.1 ± 7.7	T1	2.5	23.2	9.8
						T2	1.5	18.8	25.4
						T3	2.2	20.5	19.9
						T4	2.2	18.5	28.3
	TAP_20			**BC10_20**			**BC20_20**		
	F	C	Fe	F	C	Fe	F	C	Fe
T1	4.5	25.5	13.6	7.7	27.8	9.0	3.5	25.8	13.6
T2	2.3	25.1	12.1	7.3	29.7	7.2	2.2	19.5	34.0
T3	1.5	24.1	14.9	5.0	30.4	7.0	1.8	18.1	25.6
T4	2.6	26.9	12.0	4.7	26.1	15.8	2.1	19.7	35.4
	TAP_40			**BC10_40**			**BC20_40**		
	F	C	Fe	F	C	Fe	F	C	Fe
T1	2.5	22.7	18.9	1.7	19.9	26.0	1.9	20.8	22.9
T2	3.1	26.3	13.2	3.0	27.0	11.1	2.5	23.2	18.3
T3	2.0	22.2	21.0	2.1	23.0	19.6	3.8	23.2	17.5
T4	1.9	27.5	9.4	1.9	23.2	21.2	2.3	21.4	21.5
	TAP_70			**BC10_70**			**BC20_70**		
	F	C	Fe	F	C	Fe	F	C	Fe
T1	3.2	27.4	10.0	2.3	27.3	8.6	2.5	24.6	13.1
T2	1.8	20.8	23.8	1.8	20.4	26.0	1.5	16.4	30.7
T3	2.3	21.5	21.9	2.3	20.1	22.1	1.3	17.7	27.5
T4	1.8	22.2	16.5	1.7	18.1	25.9	1.1	15.0	35.4

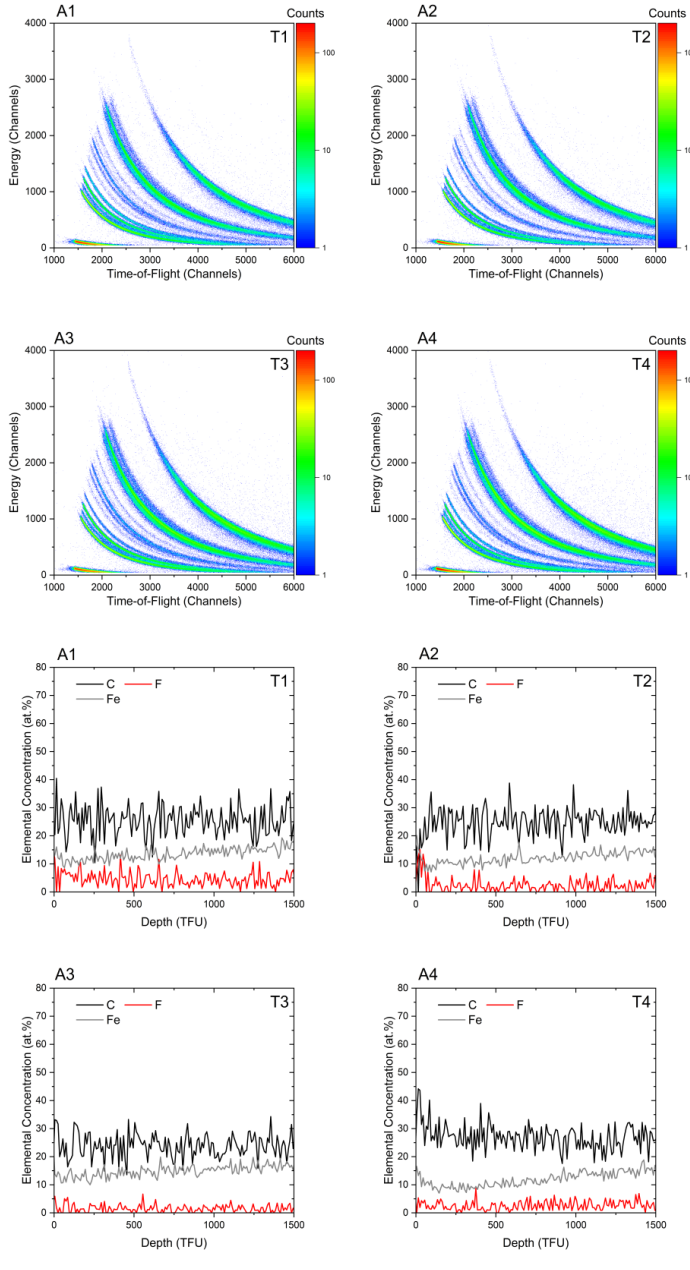

Figure S7: Histograms and depth profiles of TAP at 20°C.

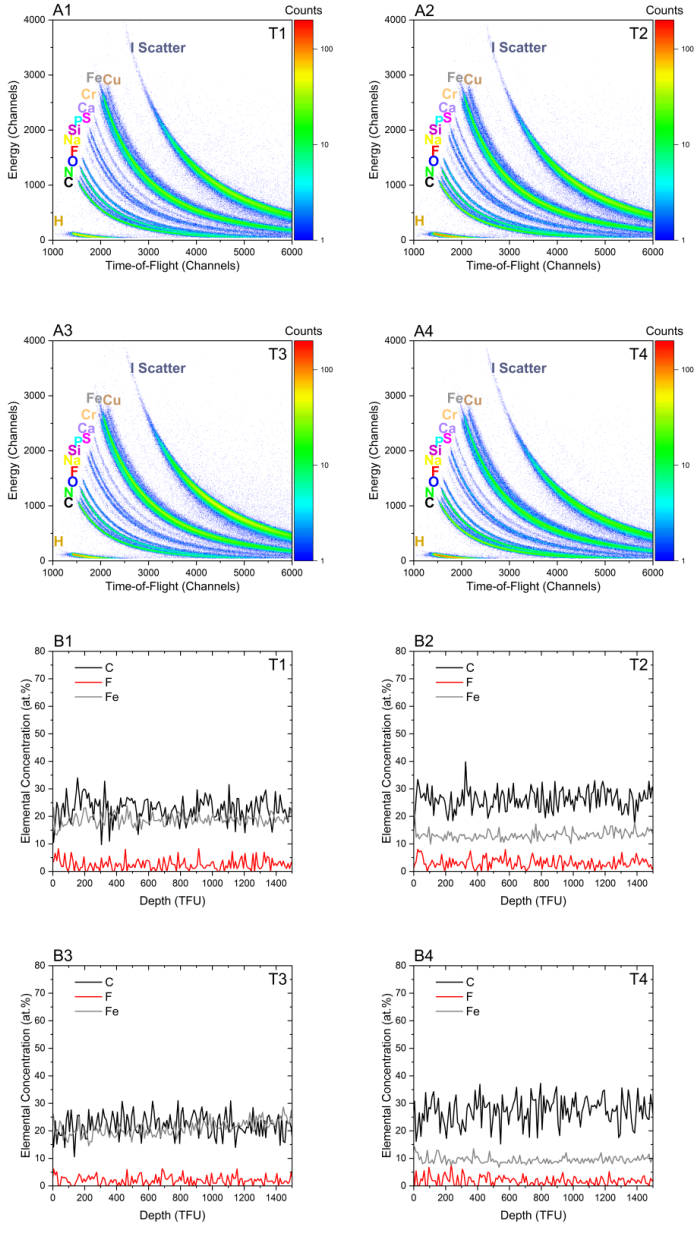

Figure S8: Histograms and depth profiles of TAP at 40°C.

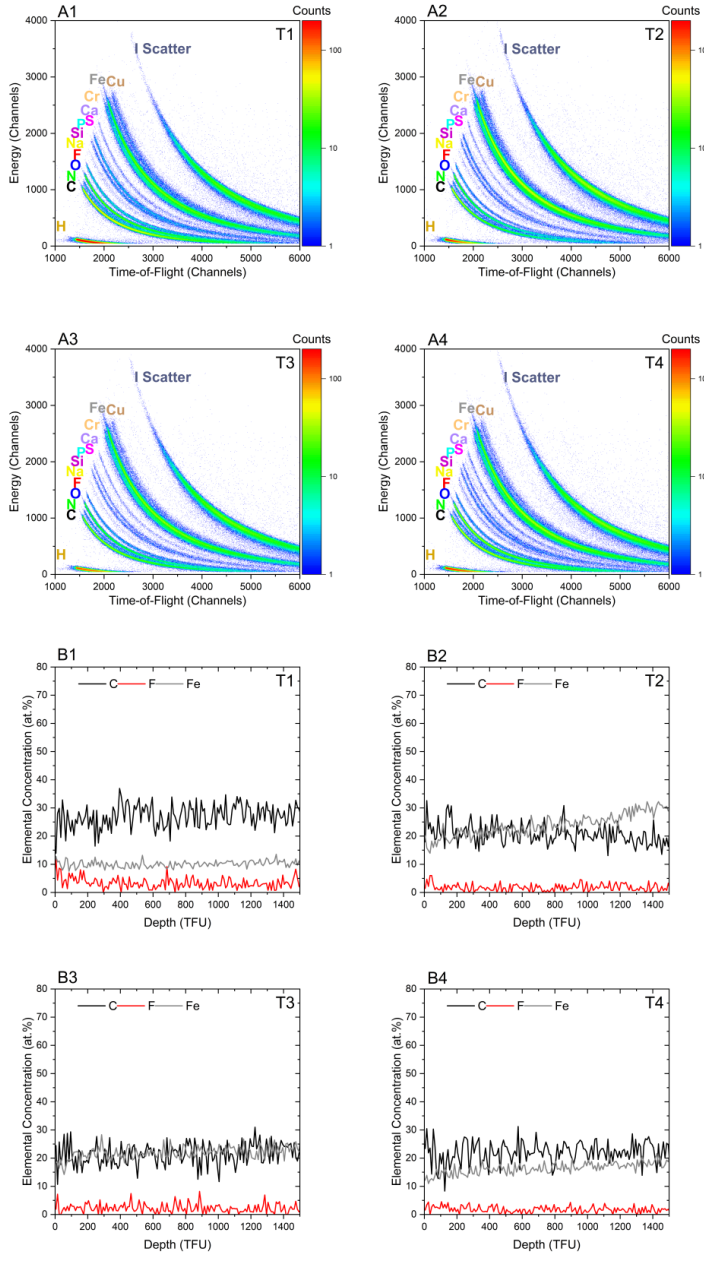

Figure S9: Histograms and depth profiles of TAP at 70°C.

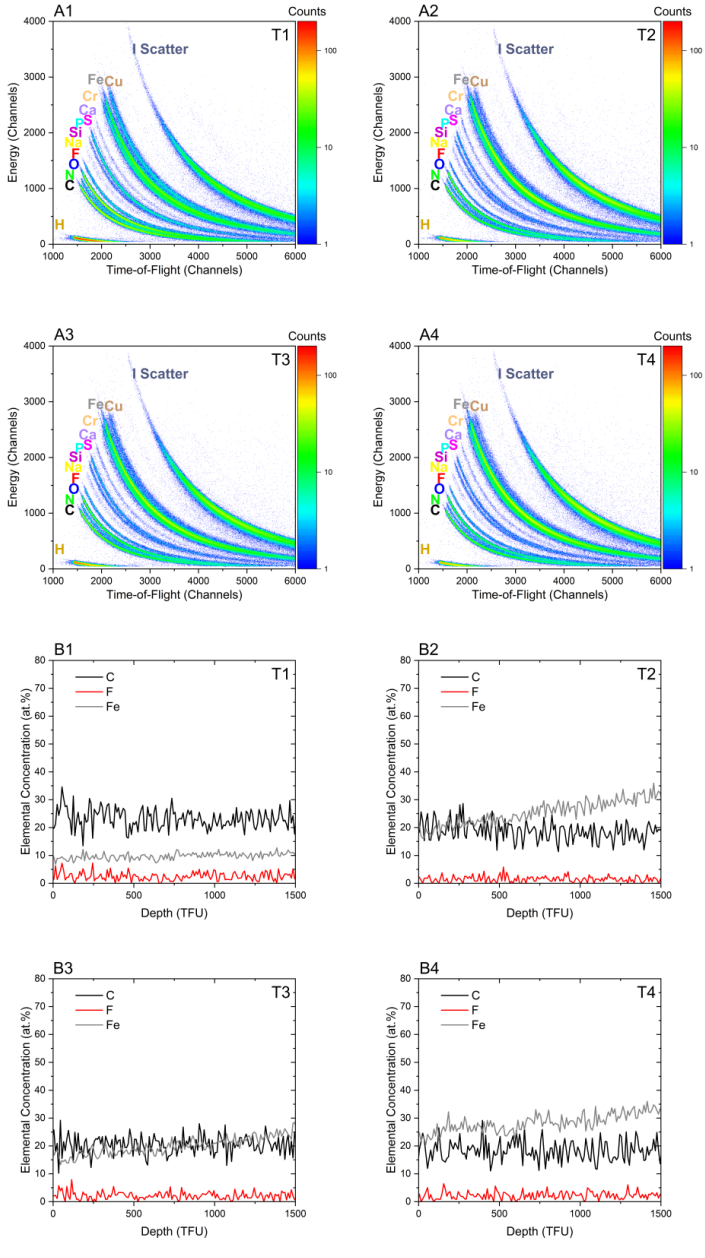

Figure S10: Histograms and depth profiles of MeOH at 20°C.

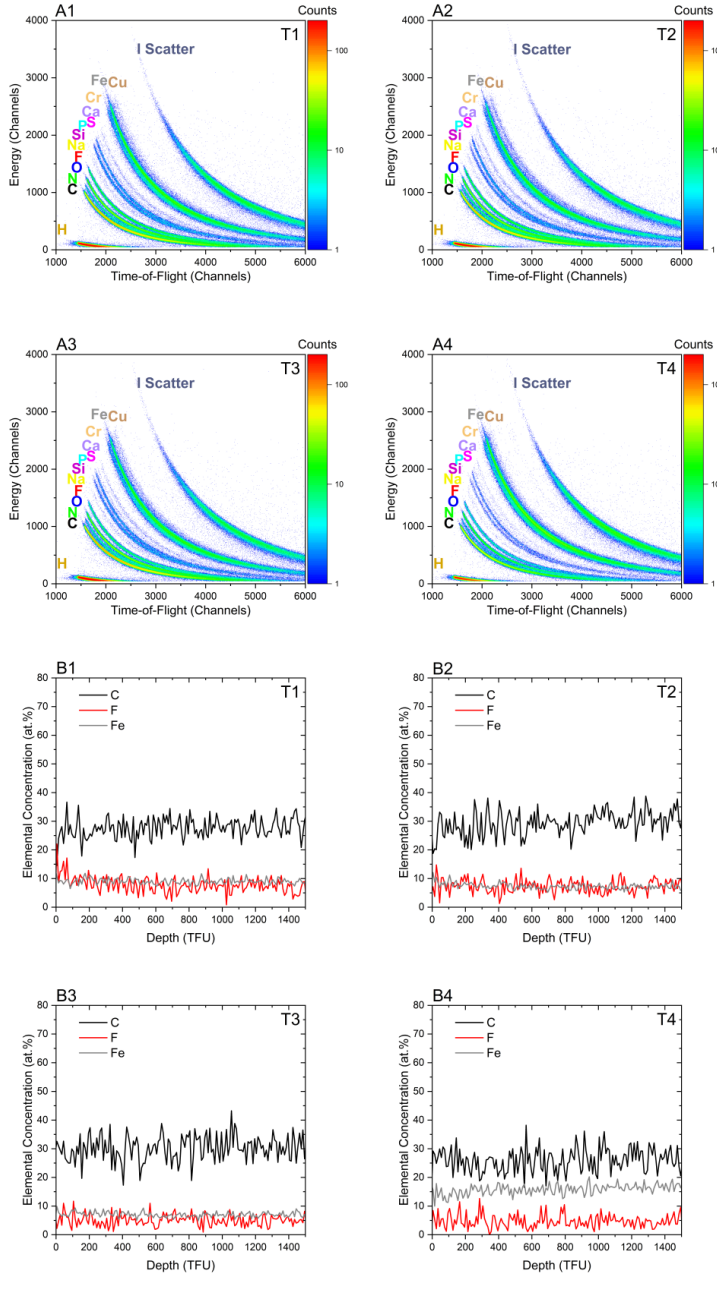
A1
T1
I Scatter
Counts
Energy (Channels)
Time-of-Flight (Channels)
A2
T2
A3
T3
A4
T4
B1
T1
C
F
Fe
Elemental Concentration (at.%)
Depth (TFU)
B2
T2
B3
T3
B4
T4

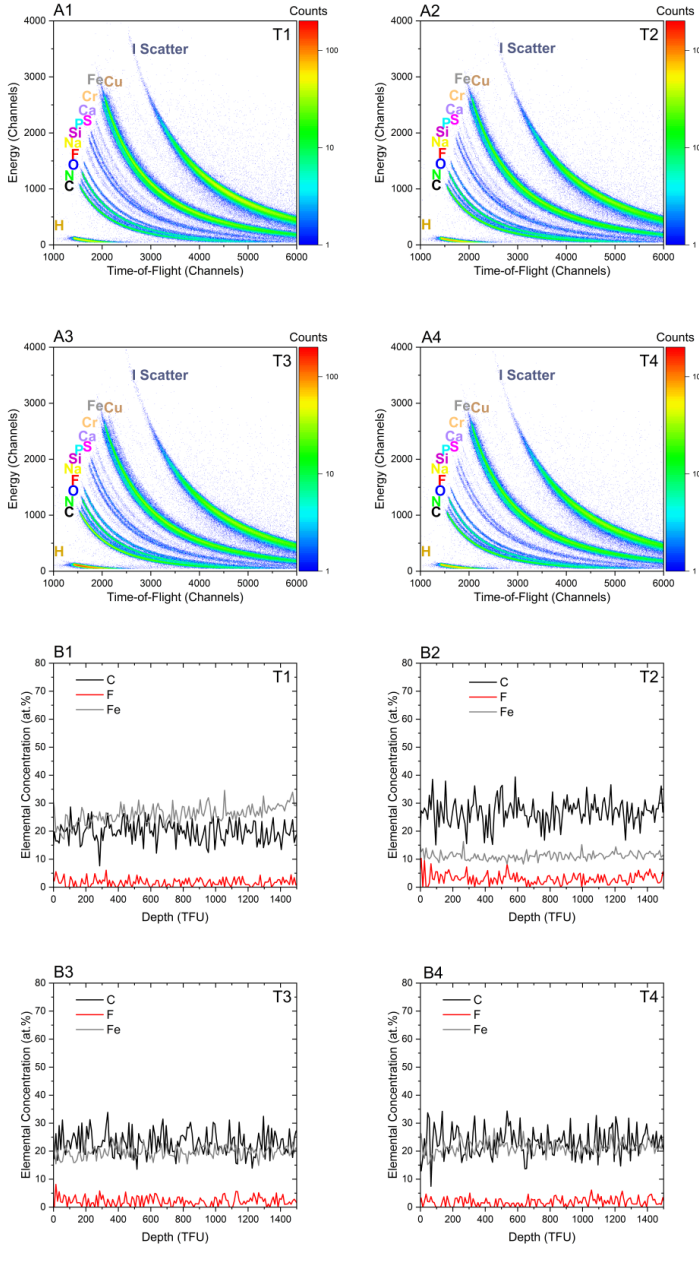

Figure S12: Histograms and depth profiles of BC10 at 40°C.

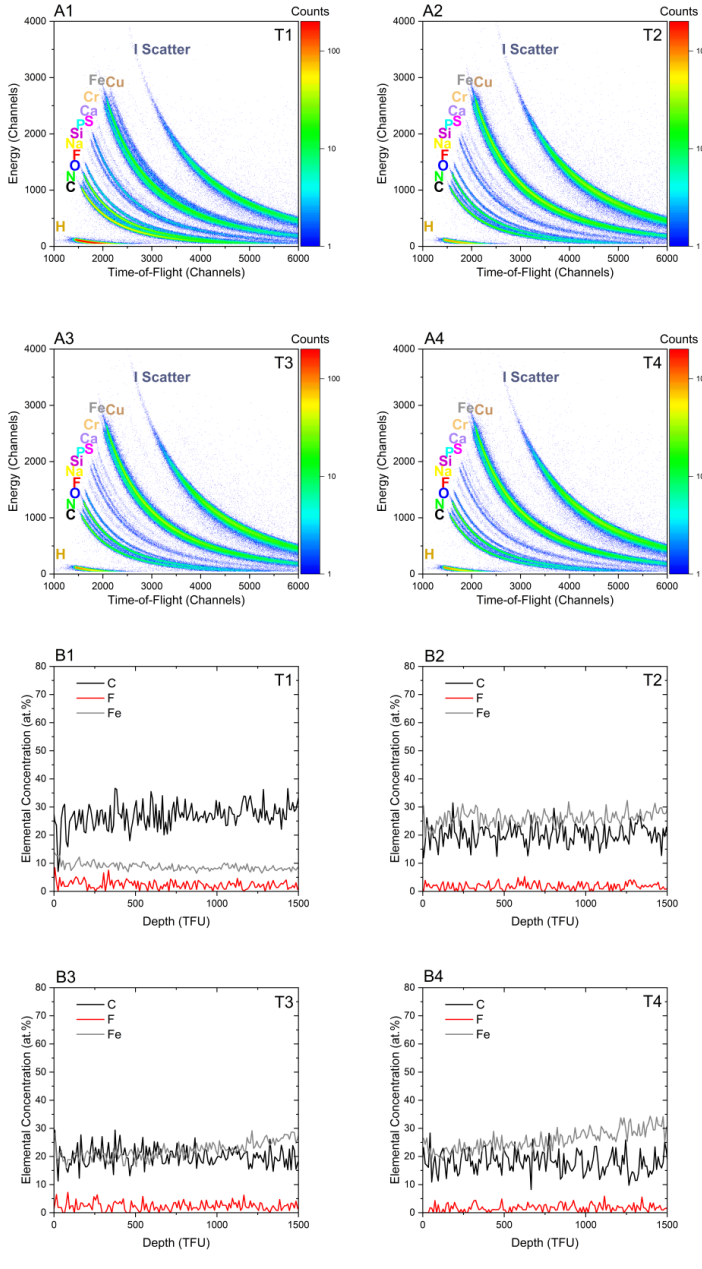

Figure S13: Histograms and depth profiles of BC10 at 70°C.

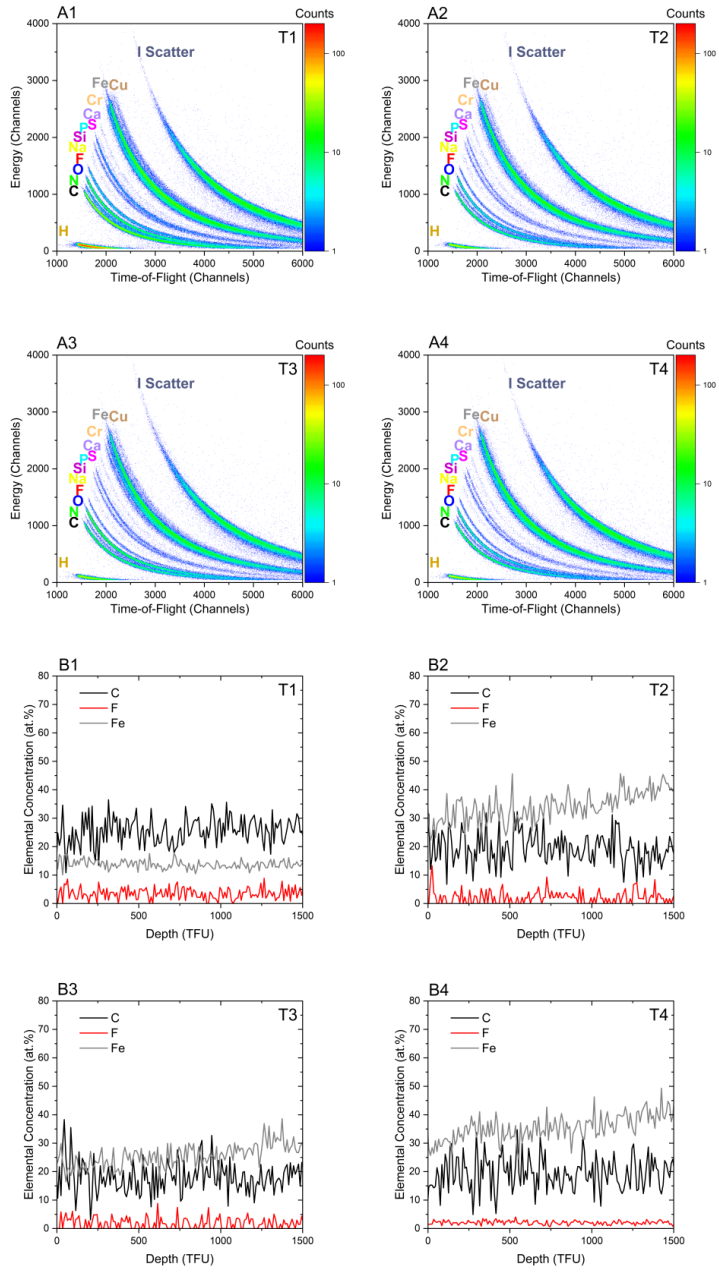

Figure S14: Histograms and depth profiles of BC20 at 20°C.

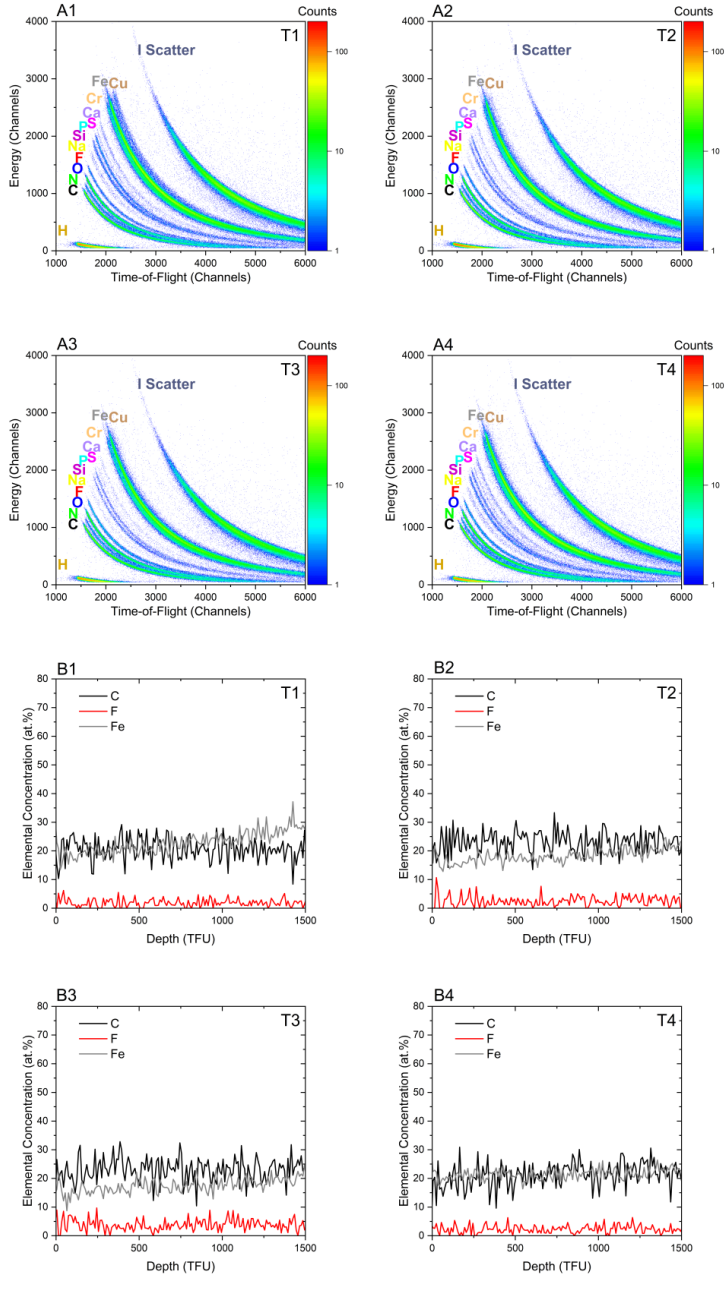

Figure S15: Histograms and depth profiles of BC20 at 40°C.

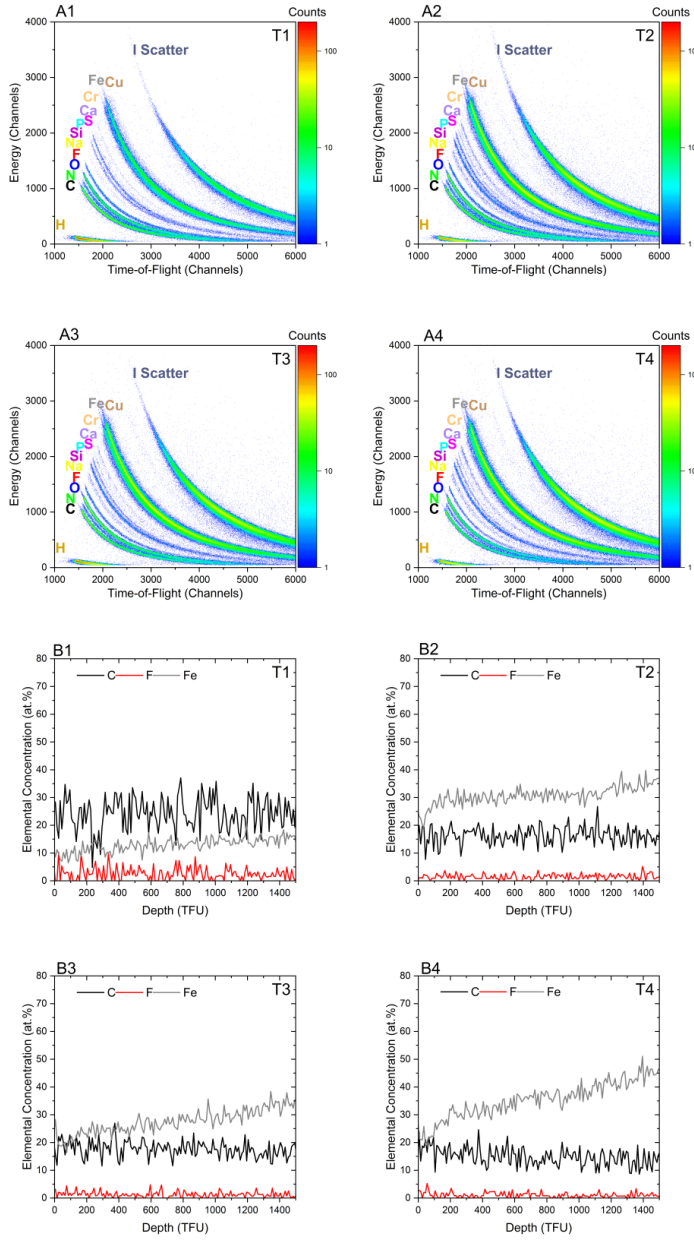

Figure S16: Histograms and depth profiles of BC20 at 70°C.

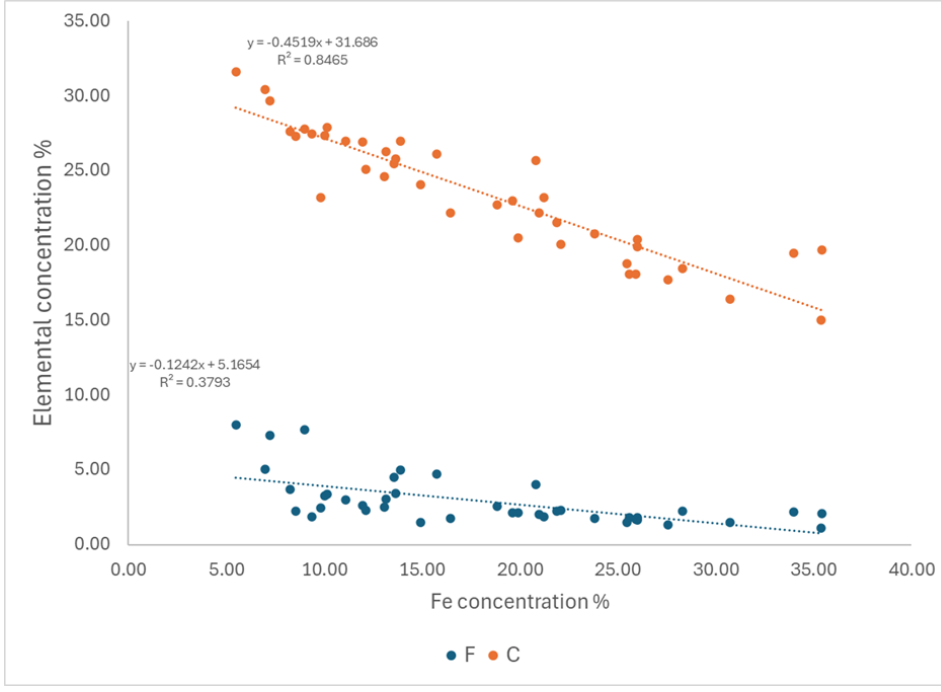

Figure S17: Relationship between surface concentrations of fluorine (F), carbon (C) (y-axis) and iron (Fe) from ToF-ERD measurements. All samples measured with ToF-ERD, including every time step and every soaking solution are included in the Figure.

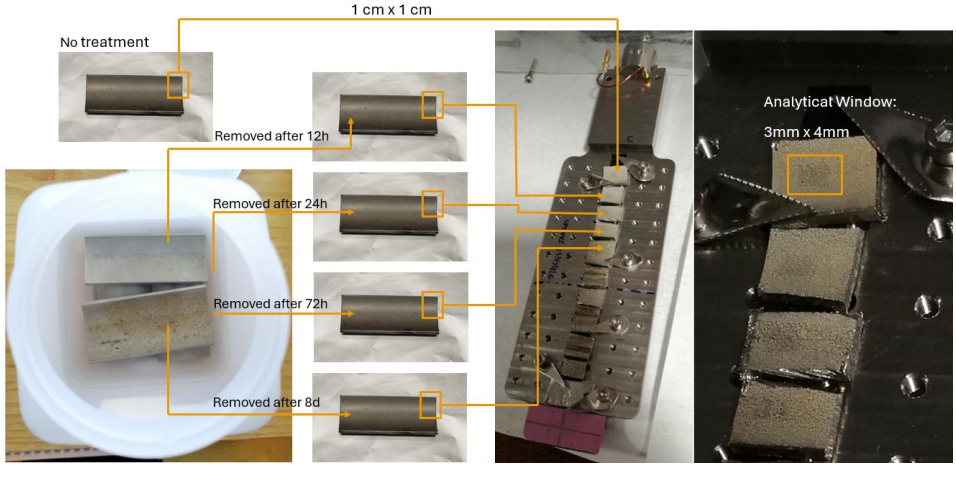

Figure S18: Workflow of preparations for ToF-ERD analysis

S16: Calculation of number of atoms per cm²

The equation for calculating the number of atoms per cm² is given below,

$$n = \left(\frac{elemental\ concentration\ (at.\%) * TFU}{100} \right) * 10^{15}$$

References

1. Shi, Y.; Wright, M.; Sharpe, M. K.; McAleese, C. D.; Polzin, J.-I.; Niu, X.; Zhao, Z.; Morris, S. M.; Bonilla, R. S., Characterization of solar cell passivating contacts using time-of-flight elastic recoil detection analysis. *Applied Physics Letters* **2023,** *123* (26).
2. Julin, J.; Sajavaara, T., Conceptual study of a heavy-ion-ERDA spectrometer for energies below 6 MeV. *Nuclear Instruments and Methods in Physics Research Section B: Beam Interactions with Materials and Atoms* **2017,** *406*, 61-65.
3. Arstila, K.; Julin, J.; Laitinen, M.; Aalto, J.; Konu, T.; Kärkkäinen, S.; Rahkonen, S.; Raunio, M.; Itkonen, J.; Santanen, J.-P., Potku–New analysis software for heavy ion elastic recoil detection analysis. *Nuclear Instruments and Methods in Physics Research Section B: Beam Interactions with Materials and Atoms* **2014,** *331*, 34-41.
4. Kissa, E., *Fluorinated surfactants and repellents*. CRC Press: 2001; Vol. 97.
5. Chang, Q., *Colloid and interface chemistry for water quality control*. Academic Press: 2016.
6. Hubert, M.; Meyn, T.; Hansen, M. C.; Hale, S. E.; Arp, H. P. H., Per-and polyfluoroalkyl substance (PFAS) removal from soil washing water by coagulation and flocculation. *Water Research* **2024,** *249*, 120888.
7. Nguyen, T. M. H.; Bräunig, J.; Thompson, K.; Thompson, J.; Kabiri, S.; Navarro, D. A.; Kookana, R. S.; Grimison, C.; Barnes, C. M.; Higgins, C. P., Influences of chemical properties, soil properties, and solution pH on soil–water partitioning coefficients of per-and polyfluoroalkyl substances (PFASs). *Environmental science & technology* **2020,** *54* (24), 15883-15892.
8. Houtz, E. F.; Sedlak, D. L., Oxidative conversion as a means of detecting precursors to perfluoroalkyl acids in urban runoff. *Environmental science & technology* **2012,** *46* (17), 9342-9349.

Acta Universitatis Agriculturae Sueciae

Doctoral Thesis No. 2025:22

Per- and polyfluoroalkyl substances (PFAS) are persistent chemicals used in aqueous film-forming foam (AFFF), contaminating soil and fire suppression systems. This thesis explores PFAS immobilization in soil using biochar and decontamination of fire suppression systems with heated glycol-based cleaning solutions. Biochar effectively immobilized PFAS in soil, while glycol-based solutions outperformed water but left residual PFAS. Further research is needed to develop more effective treatment methods.

Björn Bonnet received his doctoral education at the Department of Aquatic Sciences and Assessment of the Swedish University of Agricultural Sciences (SLU). He received master's degrees in agriculture from the University of Copenhagen and in environmental sciences from SLU and his bachelor degree in geography from the University of Tübingen.

Acta Universitatis Agriculturae Sueciae presents doctoral theses from the Swedish University of Agricultural Sciences (SLU).

SLU generates knowledge for the sustainable use of biological natural resources. Research, education, extension, as well as environmental monitoring and assessment are used to achieve this goal.

ISSN 1652-6880
ISBN (print version) 978-91-8046-457-4
ISBN (electronic version) 978-91-8046-507-6